PRACE
INSTYTUTU AERODYNAMICZNEGO
W WARSZAWIE

Prowadzone pod kierunkiem prof. C. Witoszyńskiego.

Zeszyt IV.

TRAVAUX
DE L'INSTITUT AÉRODYNAMIQUE
DE VARSOVIE

Exécutés sous la direction du prof. C. Witoszyński.

Fascicule IV.

WARSZAWA — 1930.

PRACE
INSTYTUTU AERODYNAMICZNEGO
W WARSZAWIE

Prowadzone pod kierunkiem prof. C. Witoszyńskiego.

Zeszyt IV.

TRAVAUX
DE L'INSTITUT AÉRODYNAMIQUE
DE VARSOVIE

Exécutés sous la direction du prof. C. Witoszyński.

Fascicule IV.

WARSZAWA — 1930.

TREŚĆ:

CONTENTS:

ERRATA:

Page 7, line 3 reading down, instead of "$Z\ \infty$," read "$Z \rightarrow \infty$".

„ 7, „ 13 „ up, „ „ "convenien", read "convenient".

„ 9, „ 11 „ „ „ „ $-4\, a e^{i(\varphi + \frac{\beta}{\pi}\Theta)}$, read $-4\, ie^{-i(\varphi + \frac{\beta}{\pi}\Theta)}$.

„ 10, „ 5 „ up, „ „ "$\beta = \Theta$", read "$\beta = 0$".

„ 13, Note 1, instead of "page 16", read "page 167".

„ 18, formula (20), instead of "$8\, iua^{1/2} \sin\alpha$", read "$8\, iua^{3/2} \sin\alpha$".

„ 21, last formula, in denominator, instead of "$\rho_2 + e^{-2i\varphi}$", read "$\rho^2 + e^{-2i\varphi}$".

„ 23, formula (25), instead of "P_x", read "P_{x_1}".

„ 24, „ (26), „ „ $\sum_{n=}^{\infty}$, read $\sum_{n=1}^{\infty}$.

„ 59, Table IX-b, for $\beta = 30^0$, $\alpha = 10^0$, instead of "$C_m = 49{,}090$", read "$C_m = 46{,}090$".

„ 61, „ IX-d, for $\beta = 5^0$, $\alpha = 10^0$, „ „ "$C_{mf} = 0{,}93631$", read "$C_{mf} = 0{,}43631$".

„ 64, line 11 reading up, in formula for C_{H}, instead of "α'_3", read "α'_s".

„ 64, „ 7 „ „ instead of "$\frac{C_m}{\beta}$", read "$\frac{\alpha'_{s_0}}{\beta}$".

„ 65, „ 3 reading down, instead of "avarage", read "average".

„ 80, „ 20 „ „ „ „ "oscilation", read "oscillation".

„ 81, „ 12 „ „ „ „ "are", read "is".

„ 92, „ 1 „ „ „ „ "mentoned", read mentioned".

„ 95, in Figure 15, the polar curve without a number should read "$\beta = -5^0$"; instead of "$\beta = -5^0, -10^0, -15^0$", read "$\beta = -10^0, -15^0, -20^0$", respectively.

Druk. Koop. Prac. Druk., Warszawa, Zielna 47 Tel. 19-57

MILTON J. THOMPSON, M. S. E.

THE EFFECT OF A HINGED FLAP ON THE AERODYNAMIC CHARACTERISTICS OF AN AIRFOIL.

The work presented in this paper is an approximate solution of the problem of the determination of the effect of a hinged flap on the aerodynamic characteristics of an airfoil, the theory being applicable to the study of the properties of the control surfaces of an airplane or dirigible. The fluid through which the airfoil is moving is assumed to be non-viscous and incompressible and the wing itself as being of infinite length so that the problem becomes a two-dimensional one and the usual methods based on the theory of functions of a complex variable may be employed. The case of a wing of finite aspect ratio is not considered in the theoretical work. Results are obtained for the lift, drag, total moment, and hinge moment coefficients of a bi-linear profile consisting of two straight line segments set at an angle to one another, as functions of the angle of attack, the angle between the flap and the fixed part of the profile, or flap angle, and the flap-chord ratio. Finally these results are compared with experimental data and an attempt is made to obtain some general conclusions as to the effect of a flap on the characteristics of any profile.

In the first part of this paper the fundamental theoretical assumptions are given in detail and a transformation function is developed which transforms a circle into the desired bi-linear profile, whose various geometric properties are then studied. Then the lift, total moment, and hinge moment acting on a unit length of an infinitely long wing having such a profile are calculated using the well-known Joukovsky potential function to represent the flow. In the third section, the drag, as well as these other values, is calculated by means of the so-called "discontinuous potential" first proposed by Witoszyński. In the case of the lift and drag, the results obtained by means of this potential are of an extremely complicated nature and not readily suited to computations, consequently an approximate method is developed for profiles having flap angles and flap-chord ratios such as are used in practice by means of which the necessary numerical calculations may be made with considerably less effort. The last section of the paper contains the numerical values of these characteristics for a large number of profiles calculated by the formulas obtained with the Joukovsky potential and the discontinous potential. By comparing these results with experimental data, an attempt is made to obtain an idea as to the relative merits of the two theories and also to determine whether or not the theoretical results obtained can be used as an indication of the effect of a flap on any profile.

This problem has already been attacked by several other writers who have obtained approximate results for thin airfoils based in every case on the Joukovsky potential and the theory of Prandtl for wings of finite length. Two different methods of attacking this problem have been employed, leading to the same results in the case of infinite aspect

ratio, one based on a method developed by Birnbaum [1]) and applied to this problem by Glauert [2]), Wieselsberger [3]), and Carafoli [4]), while the second method, due to Munk [5]), has been employed also by Glauert [6]) and by Toussaint and Carafoli [7]). In both cases the profile is replaced by its mean camber line which is in turn obtained by approximate methods, Birnbaum's theory being based on the assumption that this line may be replaced by a distribution of constrained vortices, while the fundamental idea of Munk's method is that the desired mean camber line may be obtained by combining a transformation function which transforms the bi-linear profile into a curve that differs but little from a circle with one that transforms this curve into the circle. The work of Carafoli (reference 4), is perhaps the most complete treatise on the subject, for there the problem is studied in the cases of both infinite and finite aspect ratio and the case of a wing with two flaps set in the same or in opposite directions is also considered. In all this work, however, the mean camber line, as mentioned above, is obtained by approximate methods so that the transformation function presented here is therefore believed to be an original contribution, as well as the application of the discontinuous potential to the problem. It is hoped that the results thus obtained will be in closer agreement with experimental data than those based on the methods referred to above.

I. Transformation Function for the Bi-linear Profile.

Before proceeding to the details of the development of the transformation function for the bi-linear profile, it will be necessary to state the basic assumptions on which this solution of the problem is based. In the first place the wing is assumed to be an infinitely long cylinder of uniform cross-section moving along a straight line perpendicular to any one of its generators and with a constant velocity through a non-viscous, incompressible fluid which fills all space. If the component of the velocity parallel to the axis of the cylinder is zero at every point in the fluid, and the motion in every plane perpendicular to a generator of the cylinder is identical, then the flow is said to be two-dimensional. Now it is pointed out in most text books on classical hydrodynamics that if such a motion possesses a velocity potential, then the motion around a cylinder of different cross-section may be obtained from this original one if a function of a complex variable can be found which will conformally transform the region external to the first cylinder into that outside of the second, at the same time keeping unchanged the regions infinitely far away from the cylinders. The general method employed by both Joukovsky and Witoszyński in the study of the two-dimensional motion of an airplane wing in a perfect fluid is to assume a certain motion around a circular cylinder and then transform this flow into that around a cylinder having a different cross-section, namely, that of the profile which it is desired to study. Consequently, assuming that the motion around the wing

---

[1]) *W. Birnbaum:* "Die tragende Wirbelfläche als Hilfsmittel zur Behandlung des ebenen Problems der Tragflügeltheorie", (Zeitschrift für angewandte Mathematik und Mechanik, 1923).

[2]) *H. Glauert:* "The Elements of Airfoil and Airscrew Theory", (Cambridge University Press, 1926), pgs. 87—93.

"Theoretical Relationships for an Airfoil with Hinged Flap", (Reports and Memoranda No. 1095, Aeronautical Research Committee, London, April, 1927).

[3]) *C. Wieselsberger:* "Theoretische Untersuchungen über die Querruderwirkung beim Tragflügel", (Report of the Aeronautical Research Committee, Tokyo Imperial University, No. 30, December, 1927).

[4]) *E. Carafoli:* "Influence des Ailerons sur les Propriétés Aérodynamiques des Surfaces Sustentatrices", (Aéro-Club de France, Travaux du Cercle d'Études Aérotechniques, Fascicule II, 1929).

[5]) *M. Munk:* "General Theory of Thin Wing Sections", (Report No. 142, U. S. National Advisory Committee for Aeronautics, Washington, 1922). See also

A. Toussaint et E. Carafoli: "Théorie et Tracés des Profils d'Ailes Sustentatrices" (E. Chiron, Paris, 1928), pgs. 107 — 113.

[6]) *H. Glauert:* "A Theory of Thin Airfoils", (Reports and Memoranda No. 910, Aeronautical Research Committee, London, 1924).

[7]) *A. Toussaint et E. Carafoli:* loc. cit. (reference 5), pgs. 113 — 121.

whose cross-section is the bi-linear profile is two-dimensional and that the fluid is perfect, the first step in the determination of its aerodynamic characteristics will be to find a complex function which will transform the so-called primitive circle into the required broken line consisting of two finite segments.

It is most desirable, of course, to develop such a function by a rational method and in the following such a procedure will be adhered to as closely as possible although at certain points it will be necessary to resort to analogy to overcome the difficulties encountered. There exists a classical method developed by Schwarz and Christofell[1]) whereby the axis of reals in the plane of a given complex variable, say $\zeta = \xi + i\eta$, may be transformed into a closed polygon in another plane of a second complex variable, $z = x + iy$. A function which will effect this transformation may be written in the form of an integral,

$$z = A \int [(\xi_1 - \zeta)^{-\frac{\gamma_1}{\pi}} (\xi_2 - \zeta)^{-\frac{\gamma_2}{\pi}} (\xi_3 - \zeta)^{-\frac{\gamma_3}{\pi}} \ldots] \, d\zeta + B, \quad \ldots \quad (1)$$

where $\xi_1, \xi_2, \xi_3 \ldots$ are real quantities in ascending order of magnitude, and $\gamma_1, \gamma_2, \gamma_3 \ldots$ are the exterior angles of the desired polygon. A and B are complex constants which determine only the scale and position of the polygon in the z-plane. By means of this transformation the upper half of the ζ-plane maps into the interior of the polygon. The fundamental idea back of this method is to suppose that around each of the points $\xi_1, \xi_2, \xi_3 \ldots$ on the ξ-axis, a small semi-circle is drawn in the upper half of the ζ-plane. Then if the line consisting of the portions of the ξ-axis and these semi-circles is passed over from $\xi = -\infty$ to $\xi = +\infty$, it is seen that as the portions of the ξ-axis are traversed, only the modulus of the above integrand will change, but in passing over the semi-circular portions in a counter-clockwise direction[2]), the amplitude changes by the angles $\gamma_1, \gamma_2, \gamma_3 \ldots$ as the points $\xi_1, \xi_2, \xi_3 \ldots$ are successively passed so that these points correspond to the vertices of the desired polygon. If the integral (1) could be evaluated in the case of the bi-linear profile and a function found which would transform a circle into the real axis of the ζ-plane, a combination of these two functions would effect the desired transformation of the circle into the bi-linear profile, although it might be necessary to introduce certain modifications so that the region exterior to the circle would correspond to that outside the transformed profile. Now although the bi-linear profile may be considered as a quadrilateral of zero area, no method was found for evaluating the integral obtained from (1) after substituting the proper values for the different angles, and consequently it was necessary to proceed in a slightly different manner in order to obtain the desired function.

It is known that the function[3])

$$z = \frac{Z^2 + a^2}{Z} \quad \ldots \quad (2),$$

where $Z = X + iY$ is a new complex variable, will transform a circle of radius a with center at the origin in the Z-plane into a segment of the x-axis in the z-plane of length $4a$, symmetrically located with respect to the y-axis. If r and ϑ are the polar coordinates of any point in the Z-plane, ϑ being measured from the positive X-axis in a clockwise direction when positive, and $Z = re^{i\vartheta}$ is substituted in the above function (2), the result obtained on separating real and imaginary parts is

$$x = \frac{r^2 + a^2}{r} \cos\vartheta, \qquad y = \frac{r^2 - a^2}{r} \sin\vartheta$$

---

[1]) *H. Lamb*: "Hydrodynamics", (Cambridge University Press, 5th ed., 1924), pg. 87.

[2]) The positive ξ-axis is here taken as pointing to the left.

[3]) This is simply a special case of the well-known Joukovsky transformation.

and when $r = a$, this becomes

$$x = 2a \cos\vartheta, \qquad y = 0.$$

This, of course, is a special case of the bi-linear profile when the flap angle or flap-chord ratio is zero. Furthermore a function which will transform this same circle into the real axis in the ζ-plane is of the form[1])

$$\zeta = \frac{ik\,(Z - a)}{(Z + a)} \quad . \; . \; . \; . \; . \; . \; . \; . \; . \; . \; . \; . \; . \; . \quad (3)$$

where k is a real, positive constant, for when $Z = re^{i\vartheta}$, this gives

$$\xi = \frac{-2k\frac{r}{a}\sin\vartheta}{1 + \frac{2r}{a}\cos\vartheta + \frac{r^2}{a^2}}, \qquad \eta = \frac{-k\left(1 - \frac{r^2}{a^2}\right)}{1 + 2\frac{r}{a}\cos\vartheta + \frac{r^2}{a^2}}$$

which, when $r = a$, reduces to

$$\xi = -k \tan\frac{\vartheta}{2}, \qquad \eta = 0.$$

Now by reversing (3), that is, solving for Z in terms of ζ, it is possible to transform the axis of reals in the ζ-plane into the circle $Z = ae^{i\vartheta}$ in the Z-plane, and by substituting in (2) the value of Z thus obtained, a function is found whereby the axis of reals in the ζ-plane is transformed into the rectilinear profile, i. e., the above mentioned segment of the x-axis in the z-plane. This function is of the form

$$z = -2a\,\frac{(\zeta - k)\,(\zeta + k)}{\zeta^2 + k^2} \quad . \; . \; . \; . \; . \; . \; . \; . \; . \; . \; . \quad (4)$$

If ρ and δ are the polar coordinates of a point in the ζ-plane, the substitution of $\zeta = \rho e^{i\delta}$ gives

$$x = \frac{2a\left(1 - \frac{\rho^4}{k^4}\right)}{1 + 2\frac{\rho^2}{k^2}\cos 2\delta + \frac{\rho^4}{k^4}}, \qquad y = \frac{-4a\frac{\rho^2}{k^2}\sin 2\delta}{1 + 2\frac{\rho^2}{k^2}\cos 2\delta + \frac{\rho^4}{k^4}}.$$

When $\delta = n\pi$ and $\rho = \xi$, these expressions reduce to

$$x = -2a\,\frac{(\xi^2 - k^2)}{(\xi^2 + k^2)}, \qquad y = 0.$$

Thus by means of the functions (3) and (4), it is possible to transform the circle $Z = ae^{i\vartheta}$ in the Z-plane into the axis of reals in the ζ-plane and then this axis into a segment of

---

[1]) *H. Villat:* "Leçons sur l'Hydrodynamique", (Gauthier-Villars et Cie., Paris, 1929), pg. 40. The function given here is a generalized form of that given by Villat for transforming a unit circle, and the correspondence of areas has also been reversed,

the x-axis in the z-plane. The correspondence of the various points and areas in the three planes is shown in Figure 1 and in the accompanying table.

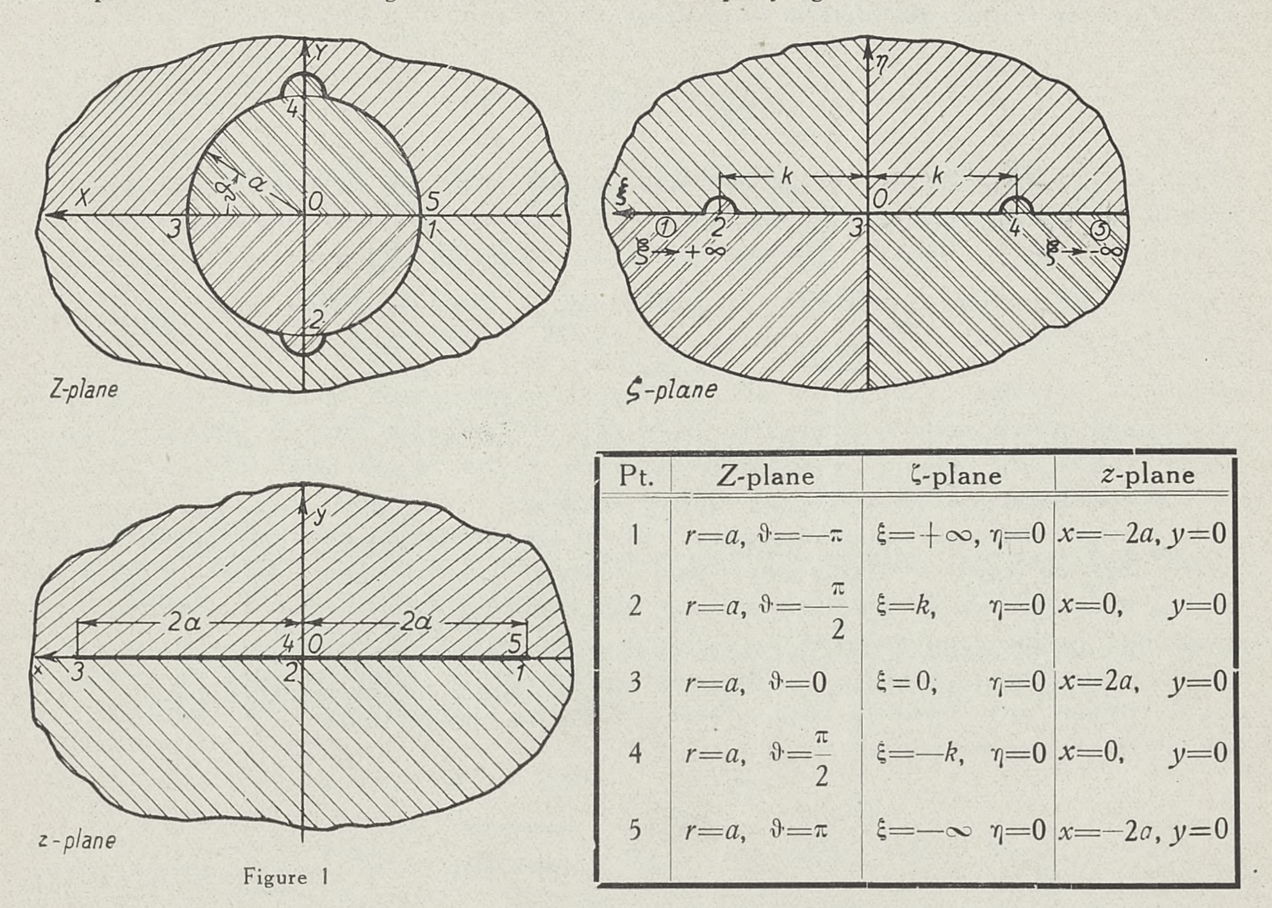


Figure 1

Pt.	Z-plane	ζ-plane	z-plane
1	$r=a,\ \vartheta=-\pi$	$\xi=+\infty,\ \eta=0$	$x=-2a,\ y=0$
2	$r=a,\ \vartheta=-\frac{\pi}{2}$	$\xi=k,\ \eta=0$	$x=0,\ y=0$
3	$r=a,\ \vartheta=0$	$\xi=0,\ \eta=0$	$x=2a,\ y=0$
4	$r=a,\ \vartheta=\frac{\pi}{2}$	$\xi=-k,\ \eta=0$	$x=0,\ y=0$
5	$r=a,\ \vartheta=\pi$	$\xi=-\infty\ \eta=0$	$x=-2a,\ y=0$

What has been done here is to show how the circle in the Z-plane is transformed into the rectilinear profile in the z-plane, introducing the intermediate ζ-plane which would be required if the method of Schwarz and Christofell could be applied directly. As a point passes around the circle $Z=ae^{i\vartheta}$ from $\vartheta=-\pi$ to $\vartheta=+\pi$, the corresponding point in the ζ-plane passes along the ξ-axis from $+\infty$ to $-\infty$, while in the z-plane the segment of the x-axis is traversed as shown in the figure. As the point in the z-plane passes the origin its amplitude experiences an increase of π at point 2 and again at point 4, so that it is necessary to suppose that in the upper half of the ζ-plane small semi-circles are drawn around the corresponding points on the real axis as in the method of Schwarz and Christofell. The curves in the Z-plane corresponding to these semi-circles lie outside the circle $Z=ae^{i\vartheta}$, but the nature of their equations is of no importance here. It should be noted that the area outside the circle in the Z-plane corresponds to the region around the rectilinear profile in the z-plane, while the interior of the circle, maps into the lower half of the ζ-plane and then covers the z-plane a second time. In physical applications, however, it is only the exterior of the circle that is to be considered, so that in the form given above the function is satisfactory, it only being necessary to stipulate that in the Z-plane, $Z \geqslant a$.

Now if it were desired to have the portion to the right of the origin of the segment in the z-plane, set at an angle β with the portion on the left, it is evident that such a result could be obtained by writing the function (4) in the form

$$z = -2a \frac{(\zeta - k)^{1-\frac{\beta}{\pi}} (\zeta + k)^{1+\frac{\beta}{\pi}}}{\zeta^2 + k^2}$$

Thus at point 2 ($\zeta = k$) the change in direction of z is $\pi - \beta$ while at point 4 ($\zeta = -k$) it is $\pi + \beta$. This function, however, gives a bi-linear profile with segments of equal length but it may be further generalized by writing

$$z = -2aK \frac{(\zeta - b)^{1 - \frac{\beta}{\pi}} (\zeta + c)^{1 + \frac{\beta}{\pi}}}{\zeta^2 + d^2}$$

where K, b, c, and d are all positive, real constants. By substituting the expression (3) for ζ in the above, a function of the form

$$z = \frac{-2aK\,(ik - b)^{1 - \frac{\beta}{\pi}} (ik + c)^{1 + \frac{\beta}{\pi}} \left[Z + a\frac{(b + ik)^2}{(b^2 + k^2)}\right]^{1 - \frac{\beta}{\pi}} \left[Z + a\frac{(c - ik)^2}{(c^2 + k^2)}\right]^{1 + \frac{\beta}{\pi}}}{Z^2\,(d^2 - k^2) + 2aZ\,(d^2 + k^2) + a^2\,(d^2 - k^2)}$$

is obtained which will transform the circle $Z = ae^{i\vartheta}$ directly into the required bi-linear profile, and it now remains to modify this function so that it will satisfy all the additional physical conditions of the problem.

It has been mentioned previously that the transformation function must be of such a form that the region at infinity will remain unchanged. This means that if Z approaches infinity, z as defined by this function must also approach infinity, and it is evident from the form of the above functionthat this will be true only when the denominator is of a degree less than that of the numerator, in other words when $d = k$. This restriction may be introduced without any difficulty since these constants are arbitrary. The transformation function then may be written as

$$z = \frac{-\frac{K}{2k^2}(ik - b)^{1 - \frac{\beta}{\pi}} (ik + c)^{1 + \frac{\beta}{\pi}} \left[Z + a\frac{(b + ik)^2}{(b^2 + k^2)}\right]^{1 - \frac{\beta}{\pi}} \left[Z + a\frac{(c - ik)^2}{(c^2 + k^2)}\right]^{1 + \frac{\beta}{\pi}}}{Z}$$

Let $\quad \frac{(b + ik)^2}{b^2 + k^2} = e^{2i\Theta_1}, \qquad \frac{(c - ik)^2}{c^2 + k^2} = e^{-2i\Theta_2}, \qquad$ where $0 \leqq \Theta_1 \leqq \frac{\pi}{2}$

and $0 \leqq \Theta_2 \leqq \frac{\pi}{2}$.

Then $$z = \frac{Ke^{i\left\{\pm\beta - \left(1 - \frac{\beta}{\pi}\right)\Theta_1 + \left(1 + \frac{\beta}{\pi}\right)\Theta_2\right\}}}{2\sin^{1 - \frac{\beta}{\pi}}\Theta_1 \sin^{1 + \frac{\beta}{\pi}}\Theta_2} \frac{\left[Z + ae^{2i\Theta_1}\right]^{1 - \frac{\beta}{\pi}} \left[Z + ae^{-2i\Theta_2}\right]^{1 + \frac{\beta}{\pi}}}{Z^2}$$

Now not only must z approach infinity with Z, but if the coordinate axes in the two planes are parallel, the derivative $\frac{dz}{dZ}$ must approach unity as Z approaches infinity [1]) in order that the direction and magnitude of the velocity will be unchanged in passing from one plane to the other. In this case, this derivative has the value

$$\frac{dz}{dZ} = \frac{Ke^{i\left\{\pm\beta - \left(1 - \frac{\beta}{\pi}\right)\Theta_1 + \left(1 + \frac{\beta}{\pi}\right)\Theta_2\right\}}}{2\sin^{1 - \frac{\beta}{\pi}}\Theta_1 \sin^{1 + \frac{\beta}{\pi}}\Theta_2} \left[\frac{Z + ae^{-2i\Theta_2}}{Z + ae^{2i\Theta_1}}\right]^{\frac{\beta}{\pi}} \frac{\left[Z^2 + \frac{\beta}{\pi}aZ\left(e^{2i\Theta_1} - e^{-2i\Theta_2}\right) - a^2 e^{2i(\Theta_1 - \Theta_2)}\right]}{Z^2}$$

[1]) C. *Witoszyński*: "La Mécanique des Profils d'Aviation", (E. Chiron, Paris, 1924), pg. 12.

and the limiting value as Z approaches infinity is

$$\lim_{Z\infty}\left(\frac{dz}{dZ}\right)=\frac{Ke^{i\left\{\pm\beta-\left(1-\frac{\beta}{\pi}\right)\Theta_1+\left(1+\frac{\beta}{\pi}\right)\Theta_2\right\}}}{2\sin^{1-\frac{\beta}{\pi}}\Theta_1\sin^{1+\frac{\beta}{\pi}}\Theta_2}$$

The fact that this limit is not in general unity indicates that the region at infinity in the z-plane has been stretched and rotated with respect to the same region of the Z-plane, due to the fact that in developing this function it was necessary to pass through the infinite point in the intermediate ζ- plane. The modulus of this limiting value, $\dfrac{K}{2\sin^{1-\frac{\beta}{\pi}}\Theta_1\sin^{1+\frac{\beta}{\pi}}\Theta_2}$ gives the ratio between corresponding lengths in the two planes, and the amplitude, $\pm\beta-\left(1-\frac{\beta}{\pi}\right)\Theta_1+\left(1+\frac{\beta}{\pi}\right)\Theta_2=\mu$, indicates that the whole z-plane is rotated through this angle with respect to the Z-plane. In order that this stretching shall be zero it is necessary to put $\dfrac{K}{2\sin^{1-\frac{\beta}{\pi}}\Theta_1\sin^{1+\frac{\beta}{\pi}}\Theta_2}=1$, and while μ may have any value whatsoever, it is most convenient to take it equal to zero, so that the axes in the two planes will be parallel. Under these restrictions the transformation function becomes

$$z=\frac{\left[Z+ae^{2i\Theta_1}\right]^{1-\frac{\beta}{\pi}}\left[Z+ae^{-2i\Theta_2}\right]^{1+\frac{\beta}{\pi}}}{Z}\quad\ldots\ldots\ldots\quad(5)$$

and its derivative is

$$\frac{dz}{dZ}=\left[\frac{Z+ae^{-2i\Theta_2}}{Z+ae^{2i\Theta_1}}\right]^{\frac{\beta}{\pi}}\frac{\left[Z^2+\frac{\beta}{\pi}aZ\left(e^{2i\Theta_1}-e^{-2i\Theta_2}\right)-a^2e^{2i(\Theta_1-\Theta_2)}\right]}{Z^2}$$

In the calculation of the forces and moment acting on an airfoil it is convenien to write the transformation function in such a way that the profile will be in the "zero position" [1]), so-called because the lift is zero when the airfoil is in this position and the relative velocity far away from it is in the direction of the negative x-axis. In order that the profile shall be in this position, it is necessary that the zero point at the trailing edge shall correspond to the point $Z=-a$ on the primitive circle. Now the derivative of the transformation function has three zero points corresponding to the three points where $\dfrac{dz}{dZ}=0$. The point $Z=ae^{-2i\Theta_2}$ evidently corresponds to the hinge point on the upper surface of the profile, while the two remaining points, the roots of the expression

$$Z^2+\frac{\beta}{\pi}aZ\left(e^{2i\Theta_1}-e^{-2i\Theta_2}\right)-a^2e^{2i(\Theta_1-\Theta_2)}=0,$$

correspond to the leading and trailing edges. These roots are found to be

$$Z=ae^{i(\Theta_1-\Theta_2)}\left[-\frac{\beta}{\pi}i\sin(\Theta_1+\Theta_2)\pm\sqrt{1-\frac{\beta^2}{\pi^2}\sin^2(\Theta_1+\Theta_2)}\right]=\pm ae^{i(\Theta_1-\Theta_2\pm\Theta_3)}$$

---

[1]) C *Witoszyński:* loc. cit. (reference 1, pg. 6) pg. 36.

where

$$-\frac{\beta}{\pi}\sin(\Theta_1+\Theta_2)=\sin\Theta_3\,,\ -\sqrt{1-\frac{\beta^2}{\pi^2}\sin^2(\Theta_1+\Theta_2)}=\cos\Theta_3\,,\qquad \frac{\pi}{2}\leqslant\Theta_3\leqslant\frac{3}{2}\pi.$$

Let it be assumed that the point $Z = ae^{i(\Theta_1 - \Theta_2 + \Theta_3)}$ corresponds to the trailing edge of the bi-linear profile. Then to put the profile in the zero position it must be turned in a clockwise direction through the angle $\pi - \Theta_1 + \Theta_2 - \Theta_3$. This may be accomplished by replacing[1]) a in (5) by $ae^{i(\pi - \Theta_1 + \Theta_2 - \Theta_3)}$ in which case the transformation function becomes

$$z=\frac{\left[Z-ae^{i(\Theta_1+\Theta_2-\Theta_3)}\right]^{1-\frac{\beta}{\pi}}\left[Z-ae^{-i(\Theta_1+\Theta_2+\Theta_2)}\right]^{1+\frac{\beta}{\pi}}}{Z}.$$

Let $\Theta_1 + \Theta_2 = \Theta$, $\Theta_3 = \varphi$, and this function becomes

$$z=\frac{\left[Z-ae^{i(\Theta-\varphi)}\right]^{1-\frac{\beta}{\pi}}\left[Z-ae^{-i(\Theta+\varphi)}\right]^{1+\frac{\beta}{\pi}}}{Z}\quad\ldots\ldots\quad(6)$$

From the relations existing between Θ_1, Θ_2, and Θ_3, it is easily shown that

$$\sin\varphi=-\frac{\beta}{\pi}\sin\Theta,\qquad \cos\varphi=-\sqrt{1-\frac{\beta^2}{\pi^2}\sin^2\Theta},\quad \frac{1}{2}\pi\leqslant\varphi\leqslant\frac{3}{2}\pi,$$

provided that $-\pi \leqslant \beta \leqslant \pi$ and $0 \leqslant \Theta \leqslant \pi$. The expression (6) then represents the function which transforms the primitive circle into the required bi-linear profile, the latter being in the so-called zero position, and the region at infinity remaining unchanged. It now remains to study some of the geometrical properties of this function.

In order to obtain expressions for the coordinates of the points of the transformed profile so as to demonstrate rigorously that it is the bi-linear profile, it is convenient to begin with a determination of the critical points of the transformation which will correspond to the leading and trailing edges and hinge point of the profile. These points are found by determining the poles and zeros of the derivative of the function (6), which may be written in the form

$$\frac{dz}{dZ}=\left[\frac{Z-ae^{-i(\Theta+\varphi)}}{Z-ae^{i(\Theta-\varphi)}}\right]^{\frac{\beta}{\pi}}\frac{[Z+a]\,[Z-ae^{-2i\varphi}]}{Z^2}\quad\ldots\ldots\quad(7)$$

This derivative has zeros at the points $Z_1 = ae^{\pm i\pi}$, $Z_3 = ae^{-2i(\varphi-\pi)}$, $Z_4 = ae^{i(2\pi - \Theta - \varphi)}$ and a pole at the point $Z_2 = ae^{i(\Theta-\varphi)}$. These four points all lie on the circle $Z = ae^{i\vartheta}$ and divide its circumference into the following four ranges:

I. $-\pi \leqslant \vartheta \leqslant \Theta - \varphi$

II. $\Theta - \varphi \leqslant \vartheta \leqslant -2(\varphi - \pi)$

III. $-2(\varphi - \pi) \leqslant \vartheta \leqslant 2\pi - \Theta - \varphi$

IV. $2\pi - \Theta - \varphi \leqslant \vartheta \leqslant \pi$

---

[1]) C. *Witoszyński*: loc. cit. (reference 1, pg. 6) pg. 13.

Now the expression for the coordinates of the points on the transformed profile, obtained by setting $Z = ae^{i\vartheta}$ in (6), is

$$z = x + iy = -4ae^{-i(\varphi + \frac{\beta}{\pi}\Theta)}\left[\sin\frac{(\vartheta - \Theta + \varphi)}{2}\right]^{1-\frac{\beta}{\pi}}\left[\sin\frac{(\vartheta + \Theta + \varphi)}{2}\right]^{1+\frac{\beta}{\pi}}$$

In range I, the second sine term in this expression is negative while the first is positive, in range II both sine terms are negative, in range III both terms are positive, in range IV the second term is again negative, hence there really exist two expressions for the coordinates of these points, which are as follows:

Ranges I and IV.

$$z = +4ae^{i(\beta - \varphi - \frac{\beta}{\pi}\Theta)}\left[\sin\frac{(\vartheta - \Theta + \varphi)}{2}\right]^{1-\frac{\beta}{\pi}}\left[\left|\sin\frac{(\vartheta + \Theta + \varphi)}{2}\right|\right]^{1+\frac{\beta}{\pi}}$$

$$x = 4a\cos(\beta - \varphi - \frac{\beta}{\pi}\Theta)\left[\sin\frac{(\vartheta - \Theta + \varphi)}{2}\right]^{1-\frac{\beta}{\pi}}\left[\left|\sin\frac{(\vartheta + \Theta + \varphi)}{2}\right|\right]^{1+\frac{\beta}{\pi}}$$

$$y = 4a\sin(\beta - \varphi - \frac{\beta}{\pi}\Theta)\left[\sin\frac{(\vartheta - \Theta + \varphi)}{2}\right]^{1-\frac{\beta}{\pi}}\left[\left|\sin\frac{(\vartheta + \Theta + \varphi)}{2}\right|\right]^{1+\frac{\beta}{\pi}}$$

Ranges II and III.

$$z = -4ae^{i(\varphi + \frac{\beta}{\pi}\Theta)}\left[\left|\sin\frac{(\vartheta - \Theta + \varphi)}{2}\right|\right]^{1-\frac{\beta}{\pi}}\left[\left|\sin\frac{(\vartheta + \Theta + \varphi)}{2}\right|\right]^{1+\frac{\beta}{\pi}}$$

$$x = -4a\cos(\varphi + \frac{\beta}{\pi}\Theta)\left[\left|\sin\frac{(\vartheta - \Theta + \varphi)}{2}\right|\right]^{1-\frac{\beta}{\pi}}\left[\left|\sin\frac{(\vartheta + \Theta + \varphi)}{2}\right|\right]^{1+\frac{\beta}{\pi}}$$

$$y = +4a\sin(\varphi + \frac{\beta}{\pi}\Theta)\left[\left|\sin\frac{(\vartheta - \Theta + \varphi)}{2}\right|\right]^{1-\frac{\beta}{\pi}}\left[\left|\sin\frac{(\vartheta + \Theta + \varphi)}{2}\right|\right]^{1+\frac{\beta}{\pi}}$$

The first of these expressions represents the equation of a straight line extending from the origin and making an angle $\beta - \varphi - \frac{\beta}{\pi}\Theta$ with the positive x-axis. Under the restrictions placed on the values of Θ and φ, this line will in general extend out into the second or third quadrant if β in assumed to lie in the range $-\frac{\pi}{2} \leqslant \beta \leqslant \frac{\pi}{2}$. The second expression represents another straight line making an angle $\pi - \varphi - \frac{\beta}{\pi}\Theta$ with the positive x-axis and in general extending out into the first or fourth quadrant. The critical points Z_3 and Z_1 correspond to the leading and trailing edges respectively, if the profile is assumed to be moving from right to left, while points Z_2 and Z_4 transform into the hinge point

which coincides with the origin in the transformed plane. In Figure 2 is shown a typical case with the corresponding points on the primitive circle indicated. From the figure

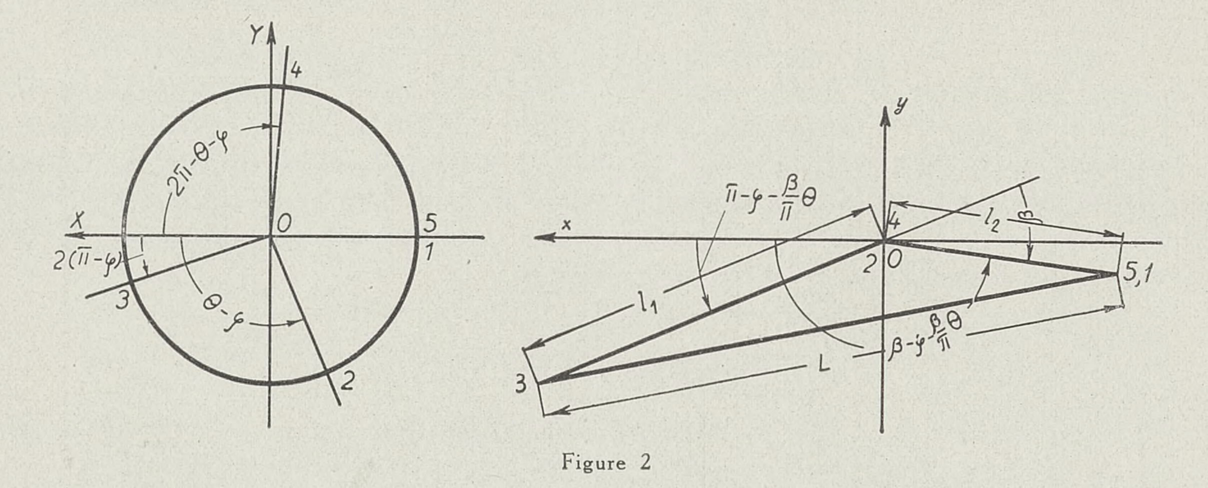


Figure 2

it is seen that the angle between these two lines is $\left(2\pi - \varphi + \beta - \frac{\beta}{\pi}\Theta\right) + \left(\varphi + \frac{\beta}{\pi}\Theta - \pi\right) =$ $= \pi + \beta$. The segment on the left thus forms the fixed part of the bi-linear profile and that on the right the flap.

In order to calculate the lengths of the two segments, the original function (6) may be written in the form

$$z = \left[\frac{Z - ae^{-i(\Theta+\varphi)}}{Z - ae^{i(\Theta-\varphi)}}\right]^{\frac{\beta}{\pi}} \frac{\left[Z^2 - aZe^{-i(\varphi - \frac{\beta}{\pi}\Theta)} + a^2 e^{-2i\varphi}\right]}{Z},$$

then substituting the values $Z_3 = ae^{-2i(\varphi-\pi)}$ and $Z_1 = -a$ corresponding to the leading and trailing edges respectively, the lengths of the segments in ratio to the diameter of the primitive circle are obtained as follows:

$$\frac{l_1}{2a} = [\cos\Theta - \cos\varphi]\left[\frac{\cos\varphi + \frac{\beta}{\pi}\cos\Theta}{\frac{\beta}{\pi} - 1}\right]^{-\frac{\beta}{\pi}} \quad \ldots\ldots\ldots \quad (8)$$

$$\frac{l_2}{2a} = -[\cos\Theta + \cos\varphi]\left[\frac{\cos\varphi - \frac{\beta}{\pi}\cos\Theta}{\frac{\beta}{\pi} - 1}\right]^{-\frac{\beta}{\pi}} \quad \ldots\ldots\ldots \quad (9)$$

It should be noted that when $\beta = \Theta$ or $\Theta = 0$ or π, that the profile becomes a single straight line segment of length $4a$, that is, the rectilinear profile, and also that for $\Theta = \frac{\pi}{2}$, the two segments are equal in length for all values of β. The length L of the chord, the line joining the leading and trailing edges, may be calculated by means of the formula

$$L = \sqrt{l_1^2 + l_2^2 + 2 l_1 l_2 \cos\beta} \quad \ldots\ldots\ldots \quad (10$$

Because of the exponential form of these expressions, it is impossible to calculate directly the values of Θ and φ which will give a desired flap-chord ratio, $\frac{l_2}{L}$, with a given flap angle β. The following table of values was obtained by calculating $\frac{l_1}{2a}$, $\frac{l_2}{2a}$, $\frac{L}{2a}$, and $\frac{l_2}{L}$ for a series of values of β and Θ and by reading from the curves of $\frac{l_2}{L}$ plotted against Θ, the values of Θ corresponding to the desired values of β and $\frac{l_2}{L}$. This data is also shown graphically in Figure 3.

Table I.

$\frac{l_2}{L}$	$\beta = 0^0$			$\beta = 5^0$			$\beta = 10^0$			$\beta = 15^0$		
	Θ	$\frac{L}{2a}$	$\frac{l_1}{2a}$	Θ	$\frac{L}{2a}$	$\frac{l_1}{2a}$	Θ	$\frac{L}{2a}$	$\frac{l_1}{2a}$	Θ	$\frac{L}{2a}$	$\frac{l_1}{2a}$
0	0	2,0000	2,0000	0	2,0000	2,0000	0	2,0000	2,0000	0	2,0000	2,0000
5	25,85	2,0000	1,9000	25,85	1,9997	1,9000	25,80	1,9992	1,9005	25,75	1,9981	1,9015
10	36,80	2,0000	1,8000	36,80	1,9996	1,8005	36,68	1,9984	1,8015	36,65	1,9964	1,8030
15	45,55	2,0000	1,7000	45,55	1,9994	1,7000	45 50	1,9977	1,7010	45,35	1,9949	1,7045
20	53,10	2,0000	1,6000	53,10	1,9992	1,6005	53,05	1,9970	1,6015	52,90	1,9935	1,6040
25	59,95	2,0000	1,5000	59,95	1,9991	1,5005	59,90	1,9966	1,5020	59,70	1,9925	1,5070
30	66,40	2,0000	1,3995	66,40	1,9990	1,4000	66,30	1,9962	1,4030	66,10	1,9916	1,4080
35	72,60	2,0000	1,2985	72,55	1,9990	1,2995	72,40	1,9959	1,3035	72,20	1,9908	1,3095
40	78,50	2,0000	1,1985	78,45	1,9990	1,2000	78,30	1,9957	1,2040	78,00	1,9902	1,2115
45	84,20	2,0000	1,1000	84,15	1,9989	1,1010	84,05	1,9955	1,1055	83,80	1,9899	1,1105
50	90,00	2,0000	1,0000	89,95	1,9989	1,0010	89,85	1,9955	1,0055	89,55	1,9897	1,0120

$\frac{l_2}{L}$	$\beta = 20^0$			$\beta = 25^0$			$\beta = 30^0$					
	Θ	$\frac{L}{2a}$	$\frac{l_1}{2a}$	Θ	$\frac{L}{2a}$	$\frac{l_1}{2a}$	Θ	$\frac{L}{2a}$	$\frac{l_1}{2a}$			
0	0	2,0000	2,0000	0	2,0000	2,0000	0	2,0000	2,0000			
5	25,70	1,9965	1.9025	25,60	1,9947	1,9040	25,50	1,9924	1,9060			
10	36,55	1,9935	1,8055	36,40	1,9900	1,8080	36,20	1,9858	1,8105			
15	45,20	1,9909	1,7080	45,00	1,9859	1,7120	44,80	1,9796	1,7160			
20	52,70	1,9885	1,6100	52,40	1,9822	1,6160	52,10	1,9745	1,6230			
25	59,50	1,9865	1,5125	59,20	1,9791	1,5200	58,80	1,9701	1,5285			
30	65,85	1,9850	1,4145	65,50	1,9765	1,4225	65,10	1,9664	1,4330			
35	71,90	1,9836	1,3160	71,50	1,9744	1,3260	71,00	1,9634	1,3385			
40	77.70	1,9826	1,2190	77,30	1,9730	1,2280	76,80	1,9612	1,2410			
45	83,50	1,9820	1,1190	83,00	1,9720	1,1310	82,40	1,9597	1,1460			
50	89,15	1,9818	1,0210	88,70	1,9716	1,0320	88,05	1,9591	1,0485			

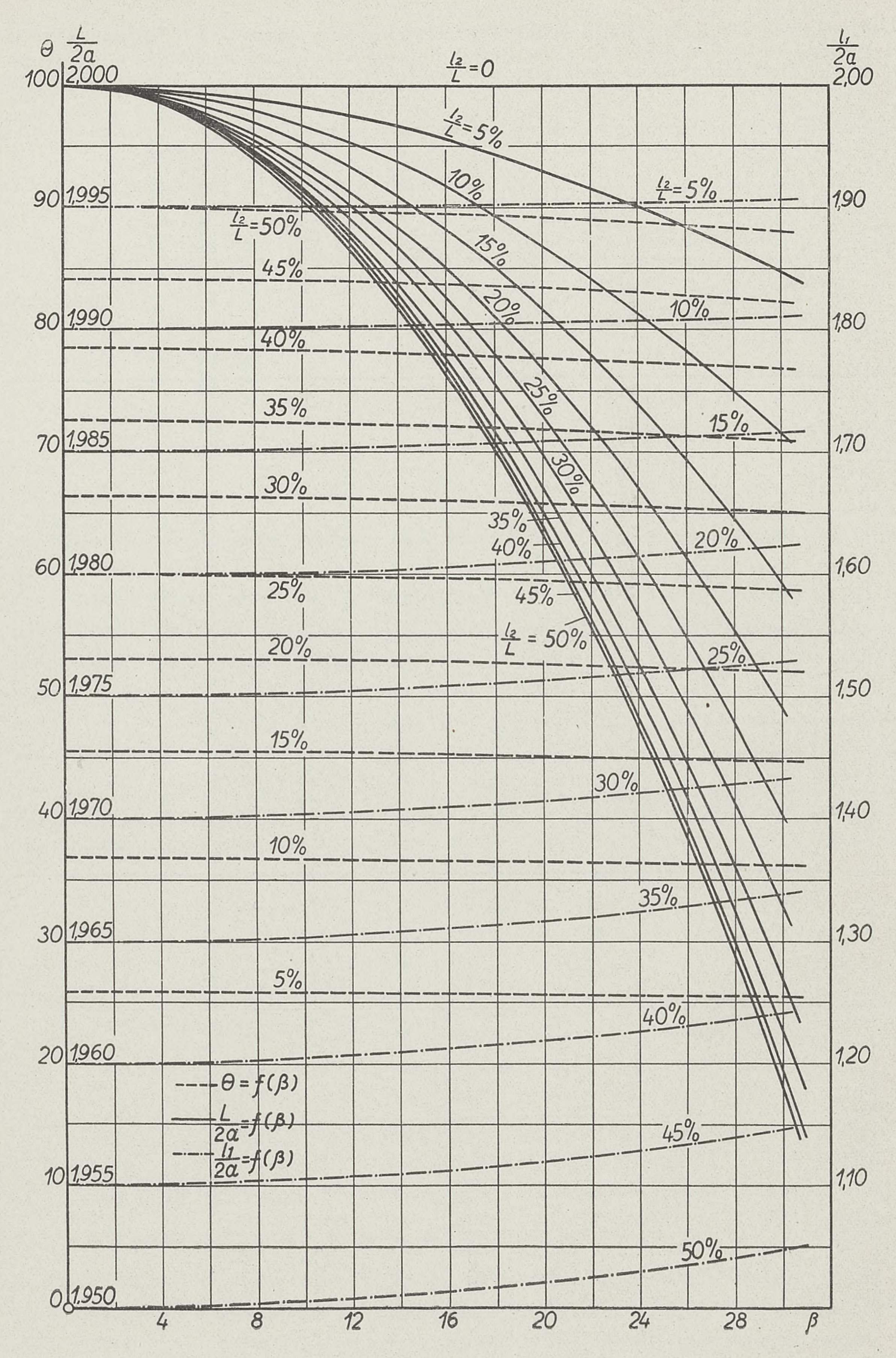

Θ
L/2a
l₁/2a
l₂/L = 0
100 2,000
2,00
l₂/L = 5%
10%
15%
20%
25%
30%
35%
40%
45%
l₂/L = 50%
90 1,995
1,90
80 1,990
1,80
70 1,985
1,70
60 1,980
1,60
50 1,975
1,50
40 1,970
1,40
30 1,965
1,30
20 1,960
1,20
10 1,955
1,10
0 1,950
4
8
12
16
20
24
28
β
Θ = f(β)
L/2a = f(β)
l₁/2a = f(β)

Figure 3

In experimental work in connection with profiles provided with flaps, it it usually more convenient to maintain the lengths of the two segments as constant rather than the flap chord ratio. In this case the ratio of the length of the flap to the total length, $\frac{l_2}{l_1 + l_2}$, remains constant but the difference between a given flap-chord ratio and the corresponding value of $\frac{l_2}{l_1 + l_2}$, is so small that it was deemed unnecessary to calculate the true values of this new ratio for the profiles here considered. It is also unnecessary to calculate all these values for negative values of β for as will be shown later on, the characteristics of such profiles may be obtained from those of profiles lying in the ranges given above in Table I. This completes the study of the geometrical properties of the bi-linear profile and the next step in this work will be to calculate the forces and moment acting on it.

II. Calculation of Forces and Moments.

As stated in the preceding paragraphs, the wing whose cross-section is the bi-linear profile is assumed to be of infinite span and the motion two-dimensional so that when calculating the forces and moment acting on this wing, it is therefore necessary to consider only a finite section of it, the length of which for convenience is taken as unity. It is also advantageous to consider the fluid as in motion and the wing as stationary instead of assuming that the wing is moving through the fluid which is at rest. The relative motion of the wing and fluid is of course the same in both cases. In order to determine the forces acting on a unit length of the wing, the first formula of Blasius, well-known in the literature of aerodynamics, will be employed. This formula may be written in the form

$$P_{y_1} - iP_{x_1} = -\frac{\sigma e^{-i\alpha}}{2} \oint \left(\frac{df}{dZ}\right)^2 \frac{dZ}{dz} dZ \quad \ldots \ldots \ldots \quad (11)$$

wherein P_{x_1} and P_{y_1} are the components of the air reaction parallel to and perpendicular to the direction of the velocity at an infinite distance from the profile, in other words the drag and lift, respectively, and α is the angle this velocity vector makes with the positive X-axis and is positive when measured in a counter-clockwise direction. The quantity σ is the mass density of the air, $\frac{df}{dZ}$ is the derivative of the complex potential $f(Z) = \Phi + i\Psi$ which represents the flow around the primitive circular profile, Φ and Ψ being the velocity potential and stream function respectively, and $\frac{dZ}{dz}$ is the reciprocal of the derivative of the transformation function. The path of integration is the primitive circle in the Z-plane.

For the calculation of the moment, the second formula of Blasius is usually used but a slightly modified form [1]), which is somewhat simpler, will be employed here. In its original form this formula is

$$M_0 + iN_0 = -\frac{\sigma}{2} \oint \left(\frac{df}{dZ}\right)^2 \frac{dZ}{dz} z\, dZ \quad \ldots \ldots \ldots \quad (12)$$

[1]) *C. Witoszyński:* "Aerodynamika", (według wykładów Prof. C. Witoszyńskiego, wydane staraniem Instytutu Aerodynamicznego w Warszawie z zapomogi Instytutu Badań Technicznych Lotnictwa, Warszawa, 1928) pg. 16 .

z being the transformation function, M_0 the moment about the origin in the z-plane, which is positive when it acts in the same direction as ϑ increasing, i. e. clockwise, while N_0 has no physical meaning. The modified form is based on the fact that for a circular profile this formula has only an imaginary value N_c, M_c being zero, and since $\frac{dZ}{dz} z = Z$ for the circle, formula (12) may be written in the form

$$M_0 + i(N_0 - N_c) = -\frac{\sigma}{2} \oint \left(\frac{df}{dZ}\right)^2 \left(\frac{dZ}{dz} z - Z\right) dZ \quad \ldots \ldots \quad (12')$$

The advantage in using this modified form is that the expression $\frac{dZ}{dz} z - Z$ is of a degree one less than $\frac{dZ}{dz} z$. In this case, as before, the path of integration is the circle $Z = ae^{i\vartheta}$, the entire circumference being passed over when the total moment is desired, and only those portions which correspond to the flap when the moment of the forces acting on the flap about the hinge point is wanted.

The derivative $\frac{df}{dZ}$ which enters in both the integrals (11) and (12′) depends on the function used as the complex potential of the flow, but the remaining parts which depend only on the transformation function may be calculated at once. Since $\frac{dZ}{dz}$ is the reciprocal of $\frac{dz}{dZ}$, the former may be obtained by inverting expression (7), giving

$$\frac{dZ}{dz} = \left[\frac{Z - ae^{i(\Theta - \varphi)}}{Z - ae^{-i(\Theta + \varphi)}}\right]^{\frac{\beta}{\pi}} \frac{Z^2}{[Z + a]\,[Z - ae^{-2i\varphi}]} \quad \ldots \ldots \quad (13)$$

which it is sometimes convenient to write in the form of a power series in $\frac{1}{Z}$, that is

$$\frac{dZ}{dz} = \left[1 + \frac{a^2 e^{-2i\varphi}}{Z^2} (\cos 2\varphi + 2i \sin\varphi \cos\Theta) + \ldots\right] \cdot \quad \ldots \ldots \quad (13')$$

Using expression (6) for z, the expression required in the calculation of the moment becomes

$$\frac{dZ}{dz} z - Z = \frac{-2aZe^{-i\varphi}\,[Z(\cos\Theta + i \sin\varphi) - ae^{-i\varphi}]}{[Z + a]\,[Z - ae^{-2i\varphi}]} \quad \ldots \ldots \quad (14)$$

or as a series in $\frac{1}{Z}$,

$$\frac{dZ}{dz} z - Z = -2ae^{-i\varphi} \Big[\cos\Theta + i\sin\varphi + \frac{a}{Z}\left\{(e^{-2i\varphi} - 1)(\cos\Theta + i\sin\varphi) - e^{-i\varphi}\right\} +$$

$$+ \frac{a^2}{Z^2}\left\{(e^{-4i\varphi} - e^{-2i\varphi} + 1)(\cos\Theta + i\sin\varphi) - e^{-i\varphi}(e^{-2i\varphi} - 1)\right\} +$$

$$+ \frac{a^3}{Z^3}\left\{(e^{-6i\varphi} - e^{-4i\varphi} + e^{-2i\varphi} - 1)(\cos\Theta + i\sin\varphi) - e^{-i\varphi}(e^{-4i\varphi} - e^{-2i\varphi} + 1)\right\} + \ldots\Big] \quad (14')$$

A. The Joukovsky Potential.

In order to obtain the values of the force components and moment acting on this profile, it is now necessary to assume a form for the potential function $f(Z)$ whose derivative, the complex velocity, appears in both the formulas of Blasius. The desired characteristics will first be computed by means of the Joukovsky potential, which may be written in the complex form as

$$f(Z) = -u\left(Ze^{i\alpha} + \frac{a^2 e^{-i\alpha}}{Z}\right) - \frac{iC}{2\pi}\log_e \frac{Z}{a} \quad \ldots\ldots \quad (15)$$

where $-u$ is the velocity of the fluid relative to the profile at an infinite distance from the latter, and the symbol $\log_e$ denotes the logarithm of a quantity taken with respect to the natural base e. The derivative of this function, the complex velocity, is

$$\frac{df}{dZ} = v_X - i v_Y = -u\left(e^{i\alpha} - \frac{a^2 e^{-i\alpha}}{Z^2}\right) - \frac{iC}{2\pi Z} \quad \ldots\ldots \quad (16).$$

As is well known this function represents the flow around the primitive circle obtained by the superposition of a plane translatory flow and a point vortex of circulation C, located at the center of the circle. Now the complex velocity in the plane of the transformed profile is [1])

$$v_x - i v_y = \frac{df}{dZ}\frac{dZ}{dz}.$$

From this formula it is evident that the points in the Z-plane where the derivative $\frac{dz}{dZ}$ vanishes, will be points of infinite velocity in the transformed plane. One such point is the trailing edge of this profile and in order to avoid an infinite value of the velocity at this point, Joukovsky proposed that the circulation C in his potential function be chosen in such a way that the velocity at the point in the plane of the primitive circle corresponding to the trailing edge of the transformed profile, should be equal to zero, so that the limit of the expression $\frac{df}{dZ}\frac{dZ}{dz}$ would remain finite. In order that this condition shall be fulfilled, it is necessary to take $C = 4\pi u a \sin\alpha$. But in attempting to apply this potential to the study of the bi-linear profile, it is impossible to avoid the infinite values of the velocity at the other points corresponding to the poles of the expression $\frac{dZ}{dz}$, i.e., the leading edge and the hinge point (on the upper surface only). However in making this application it will be supposed that these troublesome poles which lie on the circle $Z = ae^{i\vartheta}$ that forms the path of integration of the integrals required in the formulas of Blasius, may be considered as being inside this boundary. At the singular points corresponding to the hinge, it was already necessary to draw small curves about these points in the plane of the primitive circle in order to account for the sudden change of amplitude of the corresponding points in the transformed plane, so that it is only necessary to suppose that in the neighborhood of the point corresponding to the leading edge, the path of integration is infinitesimally larger than the primitive circle. Geometrically this may be interpreted as meaning that since the path of integration should really be a curve lying just outside the circle $Z = ae^{i\vartheta}$, the results obtained for the bi-linear profile are to be considered as a close approximation to the characteristics of a very thin profile whose mean camber line is approximately the bi-linear profile.

---

[1]) C. *Witoszyński*: "La Mécanique des Profils d'Aviation" (E. Chiron, Paris, 1924), pg. 11.

1. Lift and Drag.

In order to obtain the values of the components of the air reaction acting on the profile, the values (16) for $\frac{df}{dZ}$ and (13') for $\frac{dZ}{dz}$ must be substituted in the first formula of Blasius, (11), giving

$$P_{y_1} - i P_{x_1} = -\frac{\sigma e^{-i\alpha}}{2} \oint \left[u \left(e^{i\alpha} - \frac{a^2 e^{-i\alpha}}{Z^2} \right) + \frac{iC}{2\pi Z} \right]^2 \times$$

$$\times \left[1 + \frac{a^2 e^{-2i\varphi}}{Z^2} (\cos 2\varphi + 2i \sin\varphi \cos\Theta) + \ldots \right] dZ.$$

This integral is easily evaluated by the method of residues, and the results obtained are

$$P_{y_1} = \sigma u C = 4\pi\sigma u^2 a \sin\alpha \quad \ldots\ldots\ldots\ldots (17)$$

$$P_{x_1} = 0 \quad \ldots\ldots\ldots\ldots\ldots (17')$$

which is the Kutta-Joukovsky theorem.

2. Moment.

a. Total Moment. The total moment of the air reaction about the origin is obtained in a similar way by substituting expression (16) for $\frac{df}{dZ}$ and (14') for $\frac{dZ}{dz} z - Z$ in the modified form of the second formula of Blasius (12') giving

$$M_0 + i(N_0 - N_c) = a e^{-i\varphi} \oint \left[u \left(e^{i\alpha} - \frac{a^2 e^{-i\alpha}}{Z^2} \right) + \frac{iC}{2\pi} \right]^2 \left[\cos\Theta + i \sin\varphi + \right.$$

$$\left. + \frac{a}{Z} \left\{ (e^{-2i\varphi} - 1)(\cos\Theta + i\sin\varphi) - e^{-i\varphi} \right\} + \ldots \right] dZ.$$

After evaluating this integral by the method of residues, the real part of the resulting expression is found to be

$$M_0 = -2\pi\sigma a^2 u^2 \left[\left\{ 1 + 2\cos 2\varphi \cos\varphi (\cos\Theta - \cos\varphi) \right\} \sin 2\alpha + \right.$$

$$\left. + 4 \sin 2\varphi \cos\varphi (\cos\Theta - \cos\varphi) \sin^2\alpha - 2\cos 2\varphi \sin\varphi (\cos\Theta - \cos\varphi) \right]$$

or

$$\left.\begin{aligned} M_0 &= \sigma u^2 a^2 [K_4 \sin 2\alpha + K_5 \sin^2\alpha + K_6] \\ K_4 &= -2\pi(1 + 2h\cos 2\varphi \cos\varphi) \\ K_5 &= -8\pi h \sin 2\varphi \cos\varphi \\ K_6 &= 4\pi h \cos 2\varphi \sin\varphi \\ h &= \cos\Theta - \cos\varphi \end{aligned}\right\} \quad \ldots\ldots\ldots (18).$$

where

b. Hinge Moment. In case the hinge moment is desired, the path of integration of the above integral consists of those portions of the circumference of the primitive circle which correspond to the flap, that is from $Z_1 = a\,e^{-i\pi}$ to $Z_2 = a\,e^{i(\Theta-\varphi)}$ and from $Z_4 = a\,e^{i(2\pi-\Theta-\varphi)}$ to $Z_5 = a\,e^{i\pi}$. The evaluation of these two integrals is a rather long and tedious process and since the details are of no interest here, only the final result is given. It should be noted that in this case the path of integration is not a closed curve so that the method of residues cannot be employed and the expression for $\frac{dZ}{dz}\,z - Z$ must be written in the form (14). The final expression obtained for the hinge moment is

$$M_f = \sigma u^2 a^2 \left[K_{4_f} \sin 2\alpha + K_{5_f} \sin^2\alpha + K_{6_f}\right]$$

where

$$K_{4_f} = -2\Big[\cos 2\varphi \sin\Theta\,(h - \cos\varphi) + \Theta\,(1 + 2h\cos 2\varphi\cos\varphi) - $$
$$- h \sin 2\varphi \cos\varphi \log_e \left\{\frac{1-\cos(\Theta+\varphi)}{1-\cos(\Theta-\varphi)}\right\}\Big]$$

$$K_{5_f} = -4\cos\varphi\Big[2\sin\varphi\,\{\sin\Theta\,(h-\cos\varphi) + 2h\,\Theta\cos\varphi\} + $$
$$+ h\cos 2\varphi \log_e \left\{\frac{1-\cos(\Theta+\varphi)}{1-\cos(\Theta-\varphi)}\right\}\Big] \qquad \ldots (19)$$

$$K_{6_f} = 2\sin\varphi\Big[2\sin\Theta\,\{1 + \cos\varphi\,(h - \cos\varphi)\} + 2h\,\Theta\cos 2\varphi - $$
$$- h\sin 2\varphi \log_e \left\{\frac{1-\cos(\Theta+\varphi)}{1-\cos(\Theta-\varphi)}\right\}\Big]$$

The integrals required above were first evaluated in terms of the parameters ϑ_2 and ϑ_4, the amplitudes of the points on the primitive circle corresponding to the hinge. A partial check on the calculations was thus obtained for when $\vartheta_2 = \vartheta_4 = 0$, the flap becomes the whole profile and the hinge moment must be equal to the total moment about the leading edge. The formulas for both the total moment and hinge moment were also checked for the limiting cases where β and Θ are so chosen that the rectilinear profile is obtained, and the results were found to be satisfactory in every case.

From formulas (17), (18), and (19), the usual lift and moment coefficients as well as the position of the center of pressure, may be determined, but this work will be taken up later on.

B. The Discontinuous Potential.

Another complex potential function which may be used for the calculation of the force components and moments has been developed by Witoszyński[1]) and will now be applied to the study of the bi-linear profile. Assuming, as has been done here, that the profile is always fixed in the zero position, and that the direction of the velocity must be

---

[1]) *C. Witoszyński:* "La Mécanique des Profils d'Aviation", (E. Chiron, Paris, 1924). "Aerodynamika", (reference 1, pg. 13), Chap. 8.

changed in order to obtain different angles of attack, this function may be written in the form [1]).

$$f(Z) = -u\left(Ze^{i\alpha} + \frac{a^2e^{-i\alpha}}{Z}\right) + \frac{8\,i\,u\,a^{1/2}\sin\alpha}{Z^{1/2} + a^{1/2}} \quad \ldots\ldots \quad (20)$$

while its derivative, the complex velocity, is

$$\frac{df}{dZ} = -u\left(e^{i\alpha} - \frac{a^2e^{-i\alpha}}{Z^2}\right) - \frac{4\,i\,u\,a^{3/2}\sin\alpha}{Z^{1/2}\left(Z^{1/2} + a^{1/2}\right)^2} \quad \ldots\ldots \quad (21)$$

On comparing this function with the Joukovsky potential (15), it is seen that only the second term of the latter has been changed. The vortex has been replaced by a sort of cyclic movement about the circle, the circulation of which is [2])

$$C = 8\,u\,a\sin\alpha \quad \ldots\ldots\ldots\ldots \quad (22),$$

about 64% of the strength of the vortex in the Joukovsky potential. Now if $Z = re^{i\vartheta}$ is substituted in expression (20) and the velocity potential and stream function of the flow determined, it will be found [3]) that the stream-line $\Psi = 4ua\sin\alpha$ consists of three parts, a line in the region in front of the circle which ends at a point of zero velocity on its contour, the primitive circle itself, and two lines issuing from the second stagnation point $Z = -a$ and extending out to infinity in the wake. The system of stream-lines around the circle is shown schematically in Figure 4. If a point P, situated on the uppermost

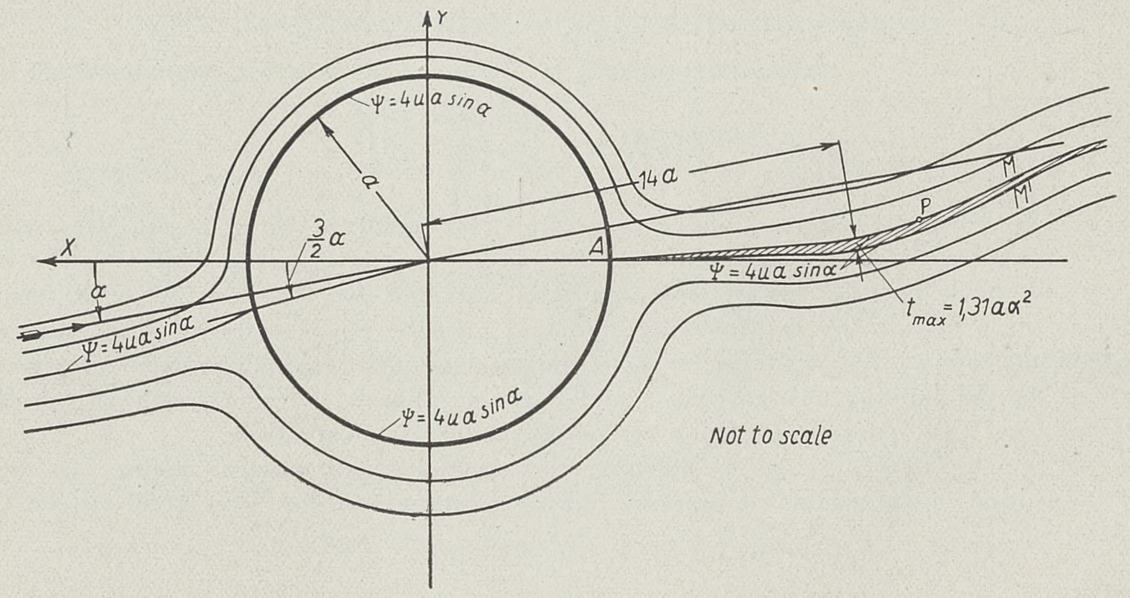


Figure 4.

of these last two stream-lines, AM, be considered, and its coordinates be taken as r_p and ϑ_p $(0 \leqslant \vartheta_p < \pi)$, the velocity at this point calculated by means of expression (21) will be found to be tangential to this stream-line, but if the amplitude of P be taken

[1]) *S. Neumark:* "Sur les Formes diverses du Potentiel servant à calculer les Forces qui agissent sur les Profils d'Aviation", (Travaux de l'Institut Aérodynamique de Varsovie, Fascicule I, Warszawa, 1927), pg. 43.

[2]) *S. Neumark:* loc. cit., pg. 45.

[3]) *C. Witoszyński:* "Modification du Principe de Circulation", (Proceedings of the International Congress for Applied Mechanics, Delft, 1924), pgs. 5, 6.

as — $(2\pi - \vartheta_p)$, a different value will be obtained which in general will be such that the line AM can no longer be regarded as a stream-line through P. A similar situation may be shown to exist for a point on the lower stream-line AM', this line being a stream-line only when the points on it are approached in a counter-clockwise direction. This mathematical phenomenon is due to the fact that the function (20) is multiple-valued, and in order that it may be used in physical applications, it is necessary to consider the lines AM and AM' as constituting a branch-cut [1]) so that the region between them is excluded from the Z-plane and the potential of the flow is not defined therein. The extension of the branch-cut from the point A to the origin, which is a branch point of the function, is here replaced by the circle $Z = a e^{i\vartheta}$, since it is not possible to consider the points within this circle, as was shown in the development of the transformation function. Analytically these restrictions may be expressed by stipulating that $|Z| \geqslant a$ and that $-\pi - \xi \leqslant \vartheta \leqslant \pi - \eta$, the angles ξ and η being functions of the modulus of Z and equal to zero for $|Z| = a$. The region included between the lines AM and AM' which may be shown to have only the one point A in common, is known as the "layer of discontinuity" and is to be considered as replacing the vortex-filled space which actually does exist in the wake of a profile moving through the air, giving rise to a discontinuity of the velocity and constituting the cause of a large part of the resistance of the profile.

The discontinuous potential was originally developed by Witoszyński on the basis that the energy of the fluid contained between two planes parallel to the direction of motion and extending out to infinity in all directions, should be finite. In the case of the Joukovsky potential this energy is infinite. Several other writers [2]) in discussing this point have shown that in the case of a body moving through a fluid against a certain resistance, the laws of rational mechanics demonstrate that the energy of the fluid must increase indefinitely as time goes on, while if the resistance were equal to zero, the energy possessed by the fluid would remain constant. Since the discontinuous potential gives a drag for a wing moving through a fluid which is infinite in extent, according to this law, known as the principle of kinetic energy and work, the energy of the fluid should be infinite instead of finite as stipulated by Witoszyński. The infinite energy of the fluid in the case of the Joukovsky potential is explained by considering the regime during which the movement is unstable and vortices are periodically discharged from the trailing edge of the wing. Assuming that an infinitely long period of time is necessary to establish the permanent movement represented by the Joukovsky potential, it may be said that this infinite amount of energy is acquired by the fluid during this time. If all the vortices in the rear of the wing be concentrated into a single vortex, and the flow during this period of establishment be considered as due to a pair of conjugate vortices, the external one moving out to infinity in the negative direction while the internal one approaches the center of the primitive circle, then the Joukovsky potential may be considered as the limiting case of such a flow. However, the transmission of energy to the fluid during the beginning of this period takes place at a rate which is much higher than seems physically possible, so that this explanation is not entirely satisfactory.

---

[1]) *J. Bonder et P. Szymański:* "Sur le Multiplan en Tandem", (Travaux de l'Institut Aérodynamique de Varsovie, Fascicule II, Warszawa, 1928), pg. 2.

[2]) *E. Carafoli:* "Confrontations des Théories Aérodynamiques Modèrnes avec les Lois de la Mécanique Rationelle", (L'Aérophile, 1927), pgs. 71 — 77.

"Sur une Remarque au Sujet du Théorème des Forces Vives Appliqué à l'Hydrodynamique Rationelle", (L'Aérophile, 1927), pgs. 217 — 18.

M. Roy: "À propos des Théories Aérodynamiques et l'Hydrodynamique Rationelle", (L'Aérophile, 1927), pgs. 185 — 87 and 215 — 17. See also

P. Dupont: "Sur la Confrontation des Théories Aérodynamiques Modèrnes avec les Lois de la Mécanique Rationelle", (L'Aèrophile, 1927), pgs. 218 — 20.

In explaining the disagreement of the discontinuous potential with the principle of kinetic energy and work, it is necessary to go back to the fundamental ideas underlying the development of this theory. It should be remembered in the first place that this theory is not a rational development based on certain assumptions concerning the nature of the fluid and its movement, but is rather an attempt to obtain a mathematical expression that represents approximately the motion around the wing under consideration, that is, the discontinuous potential is not the real potential of the flow but merely a formula which gives a velocity distribution around the profile agreeing closely with that which exists in the actual motion. From this standpoint, the only condition which this "potential" must satisfy is that its velocity field in the neighborhood of the profile should resemble as closely as possible the actual one, and all considerations concerning the energy of a real fluid having a motion governed by this function are unnecessary, since it is not assumed that such a motion exists.

If a strict rational theory were developed for this motion of the air around a wing not assuming a "potential" of the flow "a priori", but developing a solution to the problem from the basic equations of motion and considerations concerning the nature of the fluid, the solution thus obtained, or potential assuming that the movement possessed one, would represent a real flow and would naturally have to conform to all the laws of rational mechanics, including the principle of kinetic energy and work.

From this point of view both the Joukovsky and the discontinuous potentials are nothing more than methods of representing approximately the flow around a wing and are not to be considerered as real potentials of this motion but rather as mathematical tools by means of which the characteristics of the profile may be determined. The justification of their use therefore depends only on how well the results thus obtained agree with experimental data. One of the purposes of this paper is to consider to a certain extent the relative merits of the two functions, using the bi-linear profile as a basis of comparison.

1. Exact Method of Computing Lift and Drag.

With the completion of this introduction concerning the general theory of the discontinuous potential, the calculations for the lift and drag of the bi-linear profile will now be made using this function as a basis. As in the case of the Joukovsky potential, the first formula of Blasius will be employed, so that it is necessary to substitute the expression (21) for the complex velocity and (13) for the reciprocal of the derivative of the transformation function in formula (11), which then becomes

$$P_{y_1} - iP_{x_1} = -\frac{\sigma e^{-i\alpha}}{2} \oint \left[u\left(e^{i\alpha} - \frac{a^2 e^{-i\alpha}}{Z^2}\right) + \frac{4\, i u a^{3/2} \sin\alpha}{Z^{1/2}(Z^{1/2} + a^{1/2})^2} \right]^2 \left[\frac{Z - a e^{(i\Theta - \varphi)}}{Z - a e^{-i(\Theta+\varphi)}} \right]^{\frac{\beta}{\pi}} \times$$

$$\times \frac{Z^2\, dZ}{[Z+a]\,[Z - a e^{-2i\varphi}]} \quad \ldots\ldots\ldots\ldots \quad (22).$$

This expression may now be split into two others and the integral in the first of these evlauated by the method of residues. Writing $\frac{dZ}{dz}$ in the form (13′), the first part is

$$I_1 = -\frac{\sigma e^{-i\alpha}}{2} \oint \left[u^2 \left(e^{2i\alpha} - \frac{2a^2}{Z^2} + \frac{a^4 e^{-2i\alpha}}{Z^4} \right) \right] \times$$

$$\times \left[1 + \frac{a^2 e^{-2i\varphi}}{Z^2} (\cos 2\varphi + 2i \sin\varphi \cos\Theta) + \ldots \right] dZ = 0.$$

The remaining part which cannot be determined by this method is

$$I_2 = P_{y_1} - P_{x_1} = -4\sigma u^2 e^{-i\alpha} \sin\alpha \oint \left[\frac{i\,a^{3/2}}{Z^{1/2}(Z^{1/2}+a^{1/2})^2} \left(e^{i\alpha} - \frac{a^2 e^{-i\alpha}}{Z^2} \right) - \frac{2a^3 \sin\alpha}{Z(Z^{1/2}+a^{1/2})^4} \right] \times$$

$$\times \left[\frac{Z - ae^{i(\Theta-\varphi)}}{Z - ae^{-i(\Theta+\varphi)}} \right]^{\frac{\beta}{\pi}} \frac{Z^2\,dZ}{[Z+a]\,[Z-ae^{-2i\varphi}]} \quad \ldots\ldots \quad (23).$$

The evaluation of this integral is not a tremendously difficult task but the presentation of the results in a form suitable for rapid numerical computations is considerably harder, and several methods were tried before a satisfactory one was developed. The evaluation of expression (23) will first be made by an exact method, and then after calculating the total moment and hinge moment, several approximate methods for the determination of the lift and drag which were applied to the problem will be discussed, and finally one will be given whereby these results may be obtained with considerably greater facility than by means of the formulas obtained with the exact method.

Now the above integral, which is complex and therefore a line integral, may be transformed into an ordinary real integral in the following manner. The path of integration, as stated previously, is the circle $Z = ae^{i\vartheta}$, the limits being taken as $-\pi$ and $+\pi$ in order to conform to the restrictions made on the discontinuous potential when drawing the branch-cut which bounds the layer of discontinuity. If $Z = a\zeta^2$, where $\zeta = \tau + i\rho$ is a new complex variable, be substituted in expression (23), the result is a function of ζ which is to be integrated along the half of the unit circle $|\zeta| = 1$ from $\zeta = -i$ to $\zeta = +i$, that is, along the path ABC in Figure 5. Now it may be shown that if the poles of this function which lie on this semi-circle are considered as being inside it, then the function is regular outside the region bounded by the semi-circle and the segment of the imaginary axis which is its diameter, and consequently the path of integration may be replaced by any ordinary curve joining the end-points A and C and lying entirely in the region of regularity. Suppose that the path ABC is replaced by the path AD-DEF-FC, where DEF is a semi-circle of arbitrary radius R, with center at the origin and situated in the left-hand half of the ζ-plane, and AD and FC are segments of the axis of imaginaries. Since R is arbitrary it may be allowed to approach infinity, in which case the integral along the semi-circle DEF vanishes and there remains only the integrals along the imaginary axis from A to $-\infty$ and from $+\infty$ to C. These may be determined by substituting $\zeta = -i\rho$ in the integral along AD and $\zeta = +i\rho$ in that along FC, where ρ is a real variable and the limits in both cases are 1 and ∞. By combining these two integrals, the expression for the lift and drag is obtained in the form

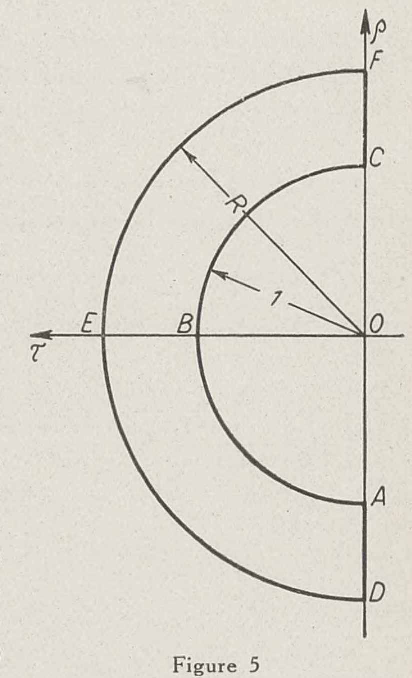


Figure 5

$$P_{y_1} - iP_{x_1} = 16\sigma u^2 a e^{-i\alpha} \sin\alpha \int_1^{\infty} \left[\frac{e^{i\alpha}}{(1+\rho^2)^2} - \frac{e^{-i\alpha}}{\rho^4(1+\rho^2)^2} - \frac{8i\,\sin\alpha}{(1+\rho^2)^4} \right] \times$$

$$\times \left[\frac{\rho^2 + e^{i(\Theta-\varphi)}}{\rho^2 + e^{-i(\Theta+\varphi)}} \right]^{\frac{\beta}{\pi}} \frac{\rho^4\,d\rho}{[\rho_2 + e^{-2i\varphi}]}$$

This expression, which is an improper integral, may be transformed into an ordinary definite integral by substituting $\rho = \frac{1}{t}$. After rationalizing the denominator and simplifying, the result is

$$P_{y_1} - iP_{x_1} = 16\,\sigma u^2 a \sin\alpha \int_0^1 \left[\frac{1}{1+2t^2\cos 2\varphi + t^4}\right] \times$$

$$\times \left[\frac{\sqrt{(1-t^4)^2 + 4t^2(1-t^4)(\cos\varphi + t^2\cos\Theta)\cos\Theta + 4t^4(\cos\varphi + t^2\cos\Theta)^2}}{1+2t^2\cos(\Theta+\varphi)+t^4}\right]^{\frac{\beta}{\pi}} \times$$

$$\times \left[\frac{1-t^2}{1+t^2} + \frac{2t^4(t^4+2t^2-3)\sin^2\alpha}{(1+t^2)^4} + \frac{2it^4(t^4+2t^2-3)\sin\alpha\cos\alpha}{(1+t^2)^4}\right] \times$$

$$\times \left[(1+t^2\cos 2\varphi)\cos\left(\frac{\beta}{\pi}\arctan\left\{\frac{2t^2(\cos\varphi+t^2\cos\Theta)\sin\Theta}{1-t^4+2t^2(\cos\varphi+t^2\cos\Theta)\cos\Theta}\right\}\right) - \right.$$

$$- t^2\sin 2\varphi \sin\left(\frac{\beta}{\pi}\arctan\left\{\frac{2t^2(\cos\varphi+t^2\cos\Theta)\sin\Theta}{1-t^4+2t^2(\cos\varphi+t^2\cos\Theta)\cos\Theta}\right\}\right) +$$

$$+ it^2\sin 2\varphi \cos\left(\frac{\beta}{\pi}\arctan\left\{\frac{2t^2(\cos\varphi+t^2\cos\Theta)\sin\Theta}{1-t^4+2t^2(\cos\varphi+t^2\cos\Theta)\cos\Theta}\right\}\right) +$$

$$\left. + i(1+t^2\cos 2\varphi)\sin\left(\frac{\beta}{\pi}\arctan\left\{\frac{2t^2(\cos\varphi+t^2\cos\Theta)\sin\Theta}{1-t^4+2t^2(\cos\varphi+t^2\cos\Theta)\cos\Theta}\right\}\right)\right] dt$$

In order to simplify this expression, let

$$S_1 = \left[\frac{1}{\sqrt{1+2t^2\cos 2\varphi + t^4}}\right] \times$$

$$\times \left[\frac{\sqrt{(1-t^4)^2 + 4t^2(1-t^4)(\cos\varphi + t^2\cos\Theta)\cos\Theta + 4t^4(\cos\varphi + t^2\cos\Theta)^2}}{1+2t^2\cos(\Theta+\varphi)+t^4}\right]^{\frac{\beta}{\pi}}$$

$$S_2 = \frac{1-t^2}{1+t^2}, \qquad S_3 = \frac{2t^4(t^4+2t^2-3)}{(1+t^2)^4},$$

$$\gamma = \arctan\frac{t^2\sin 2\varphi}{1+t^2\cos 2\varphi}, \qquad \left\{\begin{array}{lll} 0 \leqslant \gamma \leqslant \frac{\pi}{2} & \text{for} & 0 \leqslant \beta \leqslant \pi \\ -\frac{\pi}{2} \leqslant \gamma \leqslant 0 & \text{for} & -\pi \leqslant \beta \leqslant 0 \end{array}\right\}$$

so that

$$t^2\sin 2\varphi = \sin\gamma\sqrt{1+2t^2\cos 2\varphi + t^4}$$

$$1+t^2\cos 2\varphi = \cos\gamma\sqrt{1+2t^2\cos 2\varphi + t^4},$$

$$\lambda = \frac{\beta}{\pi}\arctan\left\{\frac{2t^2(\cos\varphi+t^2\cos\Theta)\sin\Theta}{1-t^4+2t^2(\cos\varphi+t^2\cos\Theta)\cos\Theta}\right\}, \qquad \left\{\begin{array}{l} -\pi \leqslant \lambda \leqslant 0 \text{ for } 0 \leqslant \beta \leqslant \pi. \\ 0 \leqslant \lambda \leqslant \pi \text{ for } -\pi \leqslant \beta \leqslant 0 \end{array}\right\}$$

The preceding expression then becomes

$$P_{y_1} - iP_{x_1} = 16\,\sigma u^2 a \sin\alpha \int_0^1 \left[S_1 \left(S_2 + S_3 \sin^2\alpha + i\,S_3 \sin\alpha \cos\alpha\right)\right] \times$$

$$\times \left[\cos(\gamma+\lambda) + i\sin(\gamma+\lambda)\right] dt$$

and on separating real and imaginary parts, formulas for the lift and drag are obtained as follows:

$$P_{y_1} = 16\,\sigma u^2 a \left\{ \sin\alpha \int_0^1 \left[S_1 S_2 \cos(\gamma+\lambda)\right] dt - \sin^2\alpha \cos\alpha \int_0^1 \left[S_1 S_3 \sin(\gamma+\lambda)\right] dt + \right.$$

$$\left. + \sin^3\alpha \int_0^1 \left[S_1 S_3 \cos(\gamma+\lambda)\right] dt \right\}$$

$$P_{x_1} = -\,16\,\sigma u^2 a \left\{ \sin\alpha \int_0^1 \left[S_1 S_2 \sin(\gamma+\lambda)\right] dt + \sin^2\alpha \cos\alpha \int_0^1 \left[S_1 S_3 \cos(\gamma+\lambda)\right] dt + \right.$$

$$\left. + \sin^3\alpha \int_0^1 \left[S_1 S_3 \sin(\gamma+\lambda)\right] dt \right\}$$

It was found after making calculations for several different profiles that the magnitudes of these integrals were such that for small values of α, corresponding to the range for which the lift curve is approximately a straight line, these formulas may be written as

$$P_{y_1} \simeq 16\,\sigma u^2 a \sin\alpha \int_0^1 \left[S_1 S_2 \cos(\gamma+\lambda)\right] \mathrm{dt},$$

$$P_{x_1} \simeq -16\,\sigma u^2 a \left\{ \sin\alpha \int_0^1 \left[S_1 S_2 \sin(\gamma+\lambda)\right] dt + \sin^2\alpha \cos\alpha \int_0^1 \left[S_1 S_3 \cos(\gamma+\lambda)\right] \mathrm{dt} \right\}$$

or

$$P_{y_1} = \sigma u^2 a\, K_1 \sin\alpha \qquad (24)$$

$$P_x = \sigma u^2 a \left[K_2 \sin\alpha + K_3 \sin^2\alpha \cos\alpha\right] \qquad (25)$$

where

$$K_1 = 16 \int_0^1 \left[S_1 S_2 \cos(\gamma+\lambda)\right] dt$$

$$K_2 = -\,16 \int_0^1 \left[S_1 S_2 \sin(\gamma+\lambda)\right] dt$$

$$K_3 = -\,16 \int_0^1 \left[S_1 S_3 \cos(\gamma+\lambda)\right] dt$$

The best method for evaluating these integrals is a graphical one or one using Simpson's rule, but in either case the computations are very long and tedious. Later on a method will be given whereby results closely approximating those given by formulas (24) and (25) may be obtained with considerable less effort.

As a check on these formulas the rectilinear profile was considered, that is $\beta = 0^0$, $\Theta = 90^0$, $\varphi = 180^0$, in which case the integrals may be evaluated by analytical methods. The results obtained are

$$P_{y_1} = 8\,\sigma u^2 a \left[\sin\alpha - \left(1 - \frac{9\pi}{32}\right)\sin^3\alpha\right] \simeq 8\,\sigma u^2 a \sin\alpha$$

$$P_{x_1} = 8\,\sigma u^2 a \left[1 - \frac{9\pi}{32}\right]\sin^2\alpha\cos\alpha$$

which agree with the results obtained by Witoszyński [1]) if the semi-residue corresponding to the leading edge is not subtracted from his result. It should be noted that in this case the term in the drag which depends on sin α is zero. In case the flap angle is different from zero, this term will have a finite value, as for example in the case where $\beta = 30^0$, $\Theta = 90^0$, $\frac{l_2}{L} = 51{,}77\%$, the results being

$$P_{y_1} = 7{,}9811\ \sigma u^2 a\ \sin\alpha$$

$$P_{x_1} = \sigma u^2 a\ [0{,}0685\ \sin\alpha + 0{,}9238\ \sin^2\alpha\ \cos\alpha]$$

It can easily be shown that the value of K_2 is equal to zero only in the case of symmetric profiles, while for asymmetric profiles it has a value different from zero. But if the formula (25) is employed for the calculation of the resistance, it will be found that in these cases ($K_2 \neq 0$), this formula gives a negative resistance for small negative values of α which of course is physically imposible. The expression for the resistance may be written in the form

$$P_{x_1} = \sigma u^2 a \left[K_2 + \frac{K_3}{2}\sin 2\alpha\right]\sin\alpha$$

and since sin α is negative for negative values of α, it is necessary that the quantity inside the brackets should also be negative. Although the term $\frac{K_3}{2}\sin 2\alpha$ is negative in this range, it is always possible to find a sufficiently small value of α such that $\left|\frac{K_3}{2}\sin 2\alpha\right| < |K_2|$, thus making the quantity $K_2 + \frac{K_3}{2}\sin 2\alpha$ positive when K_2 and K_3 are positive, and leading to a negative value for P_{x_1}.

This fact, which has never been noted by any of the previous writers on this subject, would at first seem to indicate that the discontinuous potential is not a satisfactory means for the calculation of the characteristics of a wing profile, but the following considerations will show that with a slight correction, the theory and the results given above may still be used. Instead of the form (21) for the complex velocity, let it be supposed that the second term of this expression is an infinite series and that the derivative $\frac{df}{dZ}$ is of the form

$$\frac{df}{dZ} = -u\left(e^{i\alpha} - \frac{a^2 e^{-i\alpha}}{Z^2}\right) - 4\,iua\sin\alpha\sum_{n=}^{\infty}\frac{2^{n-1} B_n\, a^{\frac{n}{2}}}{Z^{1-\frac{n}{2}}\,(Z^{1/2} + a^{1/2})^{2n}} \quad . \; . \; . \; (26),$$

subject to the condition that $\sum\limits_{n=1}^{\infty} B_n = 1$ in order that the velocity on the primitive circle at the point corresponding to the trailing edge shall be equal to zero. On substituting this

[1]) *C. Witoszyński:* "La Mécanique des Profils d'Aviation", (E. Chiron, Paris, 1924), pg. 51.

value in the first formula of Blasius, it will be found that that portion of the complex expression for the lift and drag which depends on sin α is of the form

$$P'_{y_1} - iP'_{x_1} = -4 i\sigma u^2 a \sin\alpha \oint \left[\left(1 - \frac{a^2}{Z^2}\right) \left\{ \frac{B_1 a^{1/2}}{Z^{1/2}\,(Z^{1/2} + a^{1/2})^2} + \right.\right.$$

$$\left.\left. + \frac{2\,B_2 a}{(Z^{1/2} + a^{1/2})^4} + \frac{4\,B_3 Z^{1/2} a^{3/2}}{(Z^{1/2} + a^{1/2})^6} + \ldots \right\} \right] \frac{dZ}{dz}\, dZ$$

Now another condition which the constants B_1, B_2, ... B_n... must fulfill is that their values must be so chosen that the imaginary part of this expression, P'_{x_1}, should be equal to zero, in order to avoid negative values of the drag. After making the same substitutions as in the calculations on pages 21 and 22, the above expression for $P'_{y_1} - iP'_{x_1}$ becomes

$$P'_{y_1} - iP'_{x_1} = 8\,\sigma u^2 \sin\alpha \int_0^1 \left[(t^4 - 1)\,(t^2 - 1) \left\{ \frac{B_1}{(t^2+1)^2} + \frac{8\,B_2 t^2}{(t^2+1)^4} - \right.\right.$$

$$\left.\left. - \frac{4\,B_3 t^2\,(t^4 - 14\,t^2 + 1)}{(t^2+1)^6} + \ldots \right\} \frac{dZ}{dz} \right] dZ$$

where the same substitutions are of course to be made in the expression for $\frac{dZ}{dz}$. The transformation function for an airfoil section may always be written in the form [1])

$$z = Z + \frac{A_1}{Z} + \frac{A_2}{Z^2} + \frac{A_3}{Z^3} + \frac{A_4}{Z^4} \ldots\ldots\ldots\ldots$$

and it can be shown that the coefficients in this series and hence in the series for $\frac{dZ}{dz}$, are all real in the case of a symmetric profile and some of them, at least, are complex in all other cases. Since the part of the integrand in the expression for $P'_{y_1} - iP'_{x_1}$ which is obtained from the complex velocity is real, it is easily seen why the coefficient K_2 in the formula for the drag is zero only in the case of a symmetric profile. For asymmetric profiles the values of these coefficients in the expression for the complex velocity will depend on the transformation function and will therefore be functions of the shape of the profile.

As a third condition on the coefficients in the series representing the new discontinuous potential function, it will be supposed that the circulation around the primitive circle shall be the same as that given by the original function (20), in other words, $8\,u\,a \sin\alpha$. The basis for this assumption is that experience has shown that the lift of an airfoil depends very closely on the circulation around it, and since it is here desired that the lift remain unchanged, it is necessary that the circulation maintain its original value. The simplest way of calculating this circulation is to determine the expression for the velocity on the primitive circle as a function of the polar angle ϑ and then substitute this value in the integral

$$C = \int_{-\pi}^{\pi} V_c\, a\, d\vartheta$$

---

[1]) *A. Toussaint et E. Carafoli:* loc. cit. (reference 5, pg. 2), pg. 11.

where C represents the circulation in question. Since the circulation due to the plane translatory flow represented by the first term of the function (26) is zero, it is necessary to consider only that portion of the velocity on the primitive circle which is due to the second term. The velocity due to this complementary term is found by using the formula[1])

$$V_c = i \frac{df}{dZ} e^{i\vartheta} \quad \ldots\ldots\ldots\ldots \quad (27)$$

wherein $Z = ae^{i\vartheta}$ must be substituted. In this case the result is

$$V'_c = 2\,u \sin\alpha \left[\frac{B_1}{1+\cos\frac{\vartheta}{2}} + \frac{B_2}{(1+\cos\frac{\vartheta}{2})^2} + \frac{B_3}{(1+\cos\frac{\vartheta}{2})^2} + \ldots\ldots\right] \quad \ldots\ldots \quad (28)$$

so that the circulation is

$$C = 8\,ua \sin\alpha \left[B_1 + \frac{2}{3} B_2 + \frac{7}{15} B_3 + \ldots\ldots\right]$$

Since this value is to be the same as that obtained with the original potential, the following relation between the coefficients is obtained:

$$B_1 + \frac{2}{3} B_2 + \frac{7}{15} B_3 + \ldots\ldots = 1.$$

Inasmuch as these considerations have led to three conditions which the coefficients in expression (26) must satisfy, it seems natural to consider the series in the second term as consisting of only the first three terms so that only three arbitrary constants will be involved and the function will be in the simplest possible form. The new expression for the complex velocity may then be written as

$$\frac{df_1\,(Z)}{dZ} = -u\left(e^{i\alpha} - \frac{a^2 e^{-i\alpha}}{Z^2}\right) - 4\,iua \sin\alpha \left\{\frac{B_1\,a^{1/2}}{Z^{1/2}\,(Z^{1/2}+a^{1/2})^2} + \frac{2\,B_2\,a}{(Z^{1/2}+a^{1/2})^4} + \frac{4\,B_3\,Z^{1/2} a^{3/2}}{(Z^{1/2}+a^{1/2})^6}\right\}$$

where the conditions determining the B's are

$$B_1 + B_2 + B_3 = 1 \quad \ldots\ldots\ldots\ldots \quad (29),$$

$$P'_{x_1} = \Re\left(8\,\sigma u^2 a \sin\alpha \int_0^1 \left[(t^4-1)(t^2-1)\left\{\frac{B_1}{(t^2+1)^2} + \frac{8\,B_2\,t^2}{(t^2+1)^4} - \frac{4\,B_3 t^2\,(t^4-14\,t^2+1)}{(t^2+1)^6}\right\}\frac{dZ}{dz}\right] dt\right) = 0 \quad \ldots\ldots\ldots \quad (30),$$

(where $\Re$ denotes the real part of a complex quantity) and

$$B_1 + \frac{2}{3} B_2 + \frac{7}{15} B_3 = 1 \quad \ldots\ldots\ldots\ldots \quad (31).$$

In order to solve these three equations, it is necessary to consider a definite profile so that the value of $\frac{dZ}{dz}$ may be determined. For the purpose of obtaining an idea as to the relation

[1]) C. *Witoszyński:* "La Mécanique des Profils d'Aviation", (E. Chiron, Paris, 1924), pg. 10.

between the values of B_1, B_2, and B_3 and the shape of the profile, calculations were made for the simplest possible asymmetric profile that may be considered, a circular arc. Such a profile may be obtained by using the Joukovsky transformation function

$$z = \frac{(Z + a)^2}{Z + kae^{i\mu}},$$

setting $\mu = 90^0$. The reciprocal of the derivative of this function is then found to be

$$\frac{dZ}{dz} = \frac{(Z + kai)^2}{[Z + a]\,[Z + a\,(2ki - 1)]}$$

which, after the proper substitutions for Z, becomes

$$\frac{dZ}{dz} = \frac{(1 - k^2t^4)\,(1 - t^2) + 4k^2t^4 - 2ikt^4\,(k^2t^2 + 1)}{(1 - t^2)\,[(1 + t^2)^2 + 4k^2t^4]},$$

and equation (30) then reduces to

$$\int_0^1 \left[\frac{B_1}{(t^2 + 1)^2} + \frac{8B_2t^2}{(t^2 + 1)^4} - \frac{4B_3t^2\,(t^4 - 14t^2 + 1)}{(t^2 + 1)^6}\right]\left[\frac{t^4\,(1 - t^4)\,(1 + k^2t^2)}{(t^2 + 1)^2 + 4k^2t^4}\right] dt = 0$$

The special case where $k = 0{,}2$, corresponding to a circular arc having a ratio of camber to chord of approximately 0,1, was first considered, and after evaluating the above integral, equation (30) was found to be

$$B_1 + 1{,}5972\,B_2 - 1{,}8913\,B_3 = 0$$

and the simultaneous solution of this equation with the other remaining two gave the following values for the three arbitrary constants:

$$B_1 = 1{,}1560$$
$$B_2 = -0{,}4159$$
$$B_3 = 0{,}2600$$

The case of $k = 0{,}4$ was also considered, for which equation (30) takes the form

$$B_1 + 1{,}5987\,B_2 - 1{,}8952\,B_3 = 0,$$

and the values of the coefficients were found to be

$$B_1 = 1{,}1557$$
$$B_2 = -0{,}4152$$
$$B_3 = 0{,}2595$$

These calculations showed that the camber of the profile apparently has little influence on the values of these coefficients and that for all practical purposes, B_1, B_2, and B_3 could be considered as constants. In order to investigate the effect of a change in the thickness

of a profile on these quantities, a Joukovsky airfoil section with $\mu \neq 90^0$ was considered. This necessitated a new calculation for the value of $\frac{dZ}{dz}$, after which equation (30) could be written in the form

$$\int_0^1 \left[\frac{B_1}{(t^2+1)^2} + \frac{8B_2t^2}{(t^2+1)^4} - \frac{4B_3t^2(t^4-14t^2+1)}{(t^2+1)^6}\right]\left[\frac{t^4(1-t^4)\{1+k^2t^2-(1+t^2)k\cos\mu\}}{(1+t^2)^2+4t^2k^2-4t^2(1+t^2)k\cos\mu}\right]dt = 0.$$

For the special case [1]) where $k = 0,2$ and $\mu = 30^0$, this equation reduces to

$$B_1 + 1,6117\,B_2 - 1,9239\,B_3 = 0$$

and the values of the constants were computed as

$$B_1 = 1,1538$$
$$B_2 = -0,4100$$
$$B_3 = 0,2562$$

so that the assumption that these numbers are practically the same for all profiles was again verified.

It is now of interest to determine just what is the difference, as it affects the lift and drag, between this new function and the original potential whose complementary function consisted of only one term. With this end in mind, the velocity distribution on the primitive circle, corresponding to the complementary function only, was calculated by means of formula (28), the values of B_1, B_2, and B_3 being those obtained for the above example of the circular arc with $k = 0,2$. A comparison of these results with similar ones for the original discontinuous potential [2]) showed that the velocity distributions on the primitive circle were practically identical, and that if the new function was assumed to be correct, the maximum error, ε, in the velocity on the circle was less than 1,3%. The results of these calculations are given in Table II and are shown graphically in Figure 6.

Table II.

$\pm\vartheta$	$\frac{V'c_2}{2u\sin\alpha}$	$\frac{Vc'}{2u\sin\alpha}$	ε—%	$\pm\vartheta$	$\frac{V'c_2}{2u\sin\alpha}$	$\frac{V'c}{2u\sin\alpha}$	ε—%
0	0,5000	0,5065	1,283	100	0,6086	0,6081	— 0,082
10	0,5010	0,5074	1,260	110	0,6353	0,6332	— 0,332
20	0,5038	0,5100	1,215	120	0,6667	0,6628	— 0,588
30	0,5086	0,5145	1,147	130	0,7027	0,6971	— 0,802
40	0,5155	0,5210	1,055	140	0,7452	0,7381	— 0,962
50	0,5247	0,5296	0,925	150	0,7943	0,7861	— 1,041
60	0,5359	0,5401	0,776	160	0,8518	0,8436	— 0,972
70	0,5498	0,5531	0,596	170	0,9200	0,9140	— 0,656
80	0,5663	0,5684	0,387	180	1,0000	1,0000	0,000
90	0,5858	0,5868	0,171				

$V'c_2$ = velocity due to original function.
$V'c$ = velocity due to new function of three terms.
ε = error in $V'c_2$.

[1]) C. Witoszyński: "La Mécanique des Profils d'Aviation", (E. Chiron, Paris, 1924) profil no. 19, pg. 69

[2]) S. Neumark: loc. cit. (reference 1, pg. 18) pgs. 44, 71.

Now experience with other functions [1]) giving a circulation and a velocity distribution agreeing closely with those of the original discontinuous potential (20) has shown that under such conditions the values of the coefficients K_1 and K_3 in the formulas for the lift and drag will remain practically unchanged. The above calculations show there-

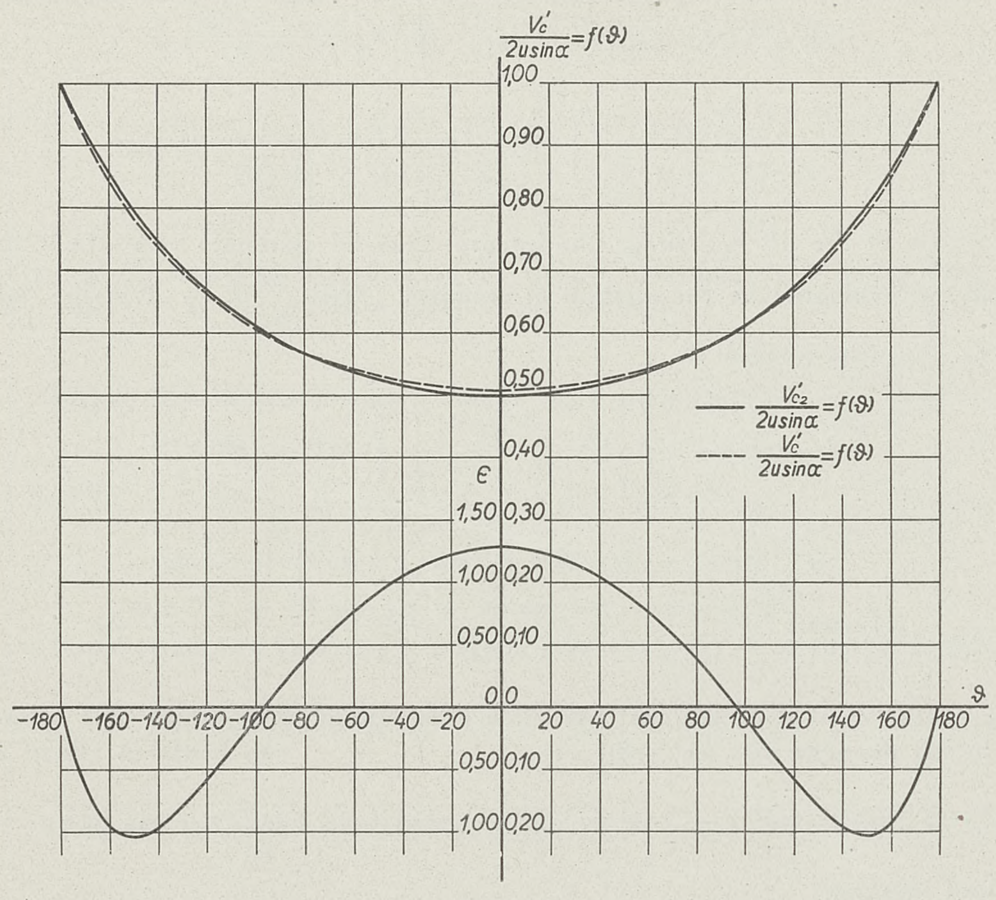


Figure 6

fore that the values of these factors obtained with the new potential, whose derivative is the expression (26) may be taken as the same as those given by formulas (24) and (25). Thus the discontinuous potential (20) may be considered as an approximation to a similar potential of three complementary terms and formulas (24) and (25) may be used for calculating the lift and drag, it only being necessary to introduce the correction that in the case of asymmetric profiles, $K_2 = 0$.

2. Exact Method for Determining the Moment.

a. Total Moment. The calculation of the moment by means of the discontinuous potential is considerably simpler than that required for obtaining the lift and drag because of the fact that the terms in the second formula of Blasius which are due to the transformation function no longer contain any expressions having the fractional exponent $\frac{\beta}{\pi}$. [Compare (13) and (14)]. The integral in formula (12′) for the moment about the origin or hinge point can therefore be evaluated by analytical methods so that it was deemed unnecessary to attempt to develop an approximate method as in the case of the lift and drag.

---

[1]) *S. Neumark:* loc. cit. (reference 1, pg. 18).
See also § II B — 3 c of the present paper concerning the "potential" of three vortices.

To obtain the moment M_0 about the origin of coordinates in the plane of the transformed profile, it is necessary to substitute in formula (12′) the expression (21) for $\frac{df}{dZ}$ and (14) for $\frac{dZ}{dz} z - Z$. This gives

$$M_0 + i(N_0 - N_c) = -\sigma a e^{-i\varphi} \oint \left[u \left(e^{i\alpha} - \frac{a^2 e^{-i\alpha}}{Z^2} \right) + \right.$$

$$\left. + \frac{4 i u a^{3/2} \sin\alpha}{Z^{1/2}(Z^{1/2} + a^{1/2})^2} \right]^2 \left[\frac{Z\{a e^{-i\varphi} - Z(\cos\Theta + i \sin\varphi)\}}{(Z + a)(Z - a e^{-2i\varphi})} \right] dZ \quad . \quad . \quad . \quad . \quad (32)$$

As in the case of the lift and drag, this integral may be split into two others, the first of which may be evaluated by the method of residues. With $\frac{dZ}{dz} z - Z$ in the form of the series (14′), this first integral is

$$J_1 = \sigma u^2 a e^{-i\varphi} \oint \left[e^{i\alpha} - \frac{a^2 e^{-i\alpha}}{Z^2} \right]^2 \left[\cos\Theta + i \sin\varphi + \right.$$

$$\left. + \frac{a}{Z} \left\{ (e^{-2i\varphi} - 1)(\cos\Theta + i \sin\varphi) - e^{-i\varphi} \right\} + \ldots \right] dZ$$

$$= 2\pi\sigma u^2 a^2 i e^{2i\alpha} \left[(\cos 3\varphi - \cos\varphi)(\cos\Theta - \cos\varphi) - 1 - i(\sin 3\varphi - \sin\varphi)(\cos\Theta - \cos\varphi) \right].$$

Denoting by the symbol $\Re$, the real part of a complex quantity, the value which J_1 contributes to the moment may be written as

$$\Re(J_1) = 2\pi\sigma u^2 a^2 \left[\sin 2\alpha + 2 \sin\varphi (\cos\Theta - \cos\varphi)(\cos 2\varphi \cos 2\alpha + \sin 2\varphi \sin 2\alpha) \right] \quad . \quad (33)$$

The second integral,

$$J_2 = -8\sigma u^2 a e^{-i\varphi} \sin\alpha \oint \left[\frac{i a^{3/2}}{Z^{1/2}(Z^{1/2} + a^{1/2})^2} \left(e^{i\alpha} - \frac{a^2 e^{-i\alpha}}{Z^2} \right) - \frac{2 a^3 \sin\alpha}{Z(Z^{1/2} + a^{1/2})^4} \right] \times$$

$$\times \left[\frac{Z\{a e^{-i\varphi} - Z(\cos\Theta + i \sin\varphi)\}}{(Z + a)(Z - a e^{-2i\varphi})} \right] dZ,$$

is treated in the same way as the corresponding integral in the determination of the lift and drag; first $Z = a\zeta^2$ is substituted, then the integral is reduced to two others along the imaginary axis, in which ζ is put equal to $\pm i\rho$, finally giving

$$J_2 = -32\sigma u^2 a^2 e^{-i\varphi} \sin\alpha \int_1^\infty \left[\frac{e^{i\alpha}}{(1 + \rho^2)^2} - \frac{e^{-i\alpha}}{\rho^4 (1 + \rho^2)^2} - \right.$$

$$\left. - \frac{8 i \sin\alpha}{(1 + \rho^2)^4} \right] \left[\rho^2 e^{i\varphi} + \frac{\rho^4 (\cos\Theta - \cos\varphi)}{\rho^2 + e^{-2i\varphi}} \right] d\rho$$

It is convenient to again divide this integral into two parts,

$$T_1 = -32\sigma u^2 a^2 \sin\alpha \int_1^\infty \left[\frac{e^{i\alpha}}{(1 + \rho^2)^2} - \frac{e^{-i\alpha}}{\rho^4 (1 + \rho^2)^2} - \frac{8 i \sin\alpha}{(1 + \rho^2)^4} \right] \rho^2 d\rho$$

and

$$T_2 = -32\,\sigma u^2 a^2 e^{-i\varphi}\,(\cos\Theta - \cos\varphi)\,\sin\alpha \int_1^\infty \left[\frac{e^{i\alpha}}{(1+\rho^2)^2} - \right.$$

$$\left. - \frac{e^{-i\alpha}}{\rho^4(1+\rho^2)^2} - \frac{8\,i\sin\alpha}{(1+\rho^2)^4}\right]\left[\frac{\rho^4}{\rho^2 + e^{-2i\varphi}}\right] d\rho$$

the first of which is a function of α alone and contributes to M_0 the quantity

$$\Re(T_1) = -\,8\,\sigma u^2 a^2\,(\pi - 2)\sin 2\,\alpha \quad \ldots\ldots\ldots\ldots \quad (34).$$

The evaluation of T_2 based on the method of partial fractions, is a rather long process and only the real part of the result is given here. This is

$$\Re(T_2) = 32\,\sigma u^2 a^2(\cos\Theta - \cos\varphi)\sin\alpha\left[\frac{1}{4}\cot\varphi\,\cos\alpha\,\log_e\left(\frac{1-\sin\varphi}{1+\sin\varphi}\right) + \right.$$

$$+ \left\{\frac{(\cos 8\varphi - 6\cos 6\varphi + 8\cos 4\varphi + 6\cos 2\varphi - 9)}{32\,(1-\cos 2\varphi)^4}\log_e\left(\frac{1-\sin\varphi}{1+\sin\varphi}\right) + \right.$$

$$\left.\left. + \frac{(\sin 7\varphi - 10\sin 5\varphi + 36\sin 3\varphi - 65\sin\varphi)}{12\,(1-\cos 2\varphi)^4}\right\}\sin\alpha\right] \quad \ldots\ldots \quad (35).$$

On combining the terms (33), (34), and (35), and simplifying, the expression for the moment is finally obtained as

$$M_0 = 2\,\sigma u^2 a^2\left[\left\{-(3\pi - 8) + 2\pi\sin\varphi\sin 2\varphi\,(\cos\Theta - \cos\varphi) - \right.\right.$$

$$\left. - 2\cot\varphi\,(\cos\Theta - \cos\varphi)\log_e\left(\frac{1+\sin\varphi}{1-\sin\varphi}\right)\right\}\sin 2\,\alpha$$

$$-4\,(\cos\Theta - \cos\varphi)\left\{\pi\sin\varphi\cos 2\varphi + \frac{4\sin^2\varphi + 3}{3\sin^3\varphi} + \frac{(2\sin^4\varphi - \sin^2\varphi - 1)}{2\sin^4\varphi}\log_e\left(\frac{1+\sin\varphi}{1-\sin\varphi}\right)\right\}\sin^2\alpha$$

$$\left. + 2\pi\sin\varphi\cos 2\varphi\,(\cos\Theta - \cos\varphi)\right] =$$

$$= \sigma u^2 a^2\,[K_4 \sin 2\alpha + K_5 \sin^2\alpha + K_6] \quad \ldots\ldots\ldots, \quad (36)$$

where

$$K_4 = 2\left\{-(3\pi - 8) + 2\pi h\sin\varphi\sin 2\varphi - 2\,h\cot\varphi\,\log_e\left(\frac{1+\sin\varphi}{1-\sin\varphi}\right)\right\},$$

$$K_5 = -\,8\,h\left\{\pi\sin\varphi\cos 2\varphi + \frac{4\sin^2\varphi + 3}{3\sin^3\varphi} + \frac{(2\sin^4\varphi - \sin^2\varphi - 1)}{2\sin^4\varphi}\log_e\left(\frac{1+\sin\varphi}{1-\sin\varphi}\right)\right\},$$

$$K_6 = 4\pi h\sin\varphi\cos 2\varphi$$

$$h = \cos\Theta - \cos\varphi.$$

A trial computation for a special case will show that the term K_5 in general contains two very large quantities with opposite signs whose difference is relatively small, making it necessary to use a large number of significant figures in the value of $\sin\varphi$ in order to obtain accurate results. Consequently it is more convenient to write the term $\log_e\left(\frac{1+\sin\varphi}{1-\sin\varphi}\right)$ in the form of a series in $\sin\varphi$ and then neglect higher powers of this quantity, since for flap angles up to 30^0, φ will lie between 180^0 and 190^0. The expression for K_4 may also be simplified somewhat in this way, and the results, after subtituting the value

$$\log_e\left(\frac{1+\sin\varphi}{1-\sin\varphi}\right) = 2\left[\sin\varphi + \frac{1}{3}\sin^3\varphi + \frac{1}{5}\sin^5\varphi + \frac{1}{7}\sin^7\varphi + \ldots\ldots\right]$$

in the expressions for K_4 and K_5 are

$$\left.\begin{aligned} K_4 &= 2\left[-(3\pi-8) - 4h\cos\varphi\left\{1 - \left(\pi - \frac{1}{3}\right)\sin^2\varphi + \frac{1}{5}\sin^4\varphi + \ldots\ldots\right\}\right] \\ &\simeq -2\left[(3\pi-8) + 4h\cos\varphi\left\{1 - \left(\pi - \frac{1}{3}\right)\sin^2\varphi\right\}\right] \\ K_5 &= -8h\left[\pi + \frac{22}{15} - \left(2\pi - \frac{34}{105}\right)\sin^2\varphi + \frac{46}{315}\sin^4\varphi + \ldots\ldots\ldots\right]\sin\varphi \\ &\simeq -8h\left[\pi + \frac{22}{15} - \left(2\pi - \frac{34}{105}\right)\sin^2\varphi\right]\sin\varphi \\ K_6 &= 4\pi h\sin\varphi\cos 2\varphi \end{aligned}\right\} \quad (36')$$

These formulas were checked by considering the limiting case of the bi-linear profile, the rectilinear profile, which is obtained when the flap angle β approaches zero. In this case the value of Θ merely determines the position of the profile on the x-axis with respect to the origin in the z-plane. In the original expressions for K_4 and K_5, certain terms become indeterminate as β approaches zero ($\varphi \rightarrow \pi$) but their limits may be evaluated by applying the rule of l'Hospital. However it is simpler to consider the second form of these coefficients where K_4 and K_5 are written as infinite series in $\sin\varphi$. In this case it is immediately evident that the limiting values as β approaches zero are

$$K_4 = -2(3\pi - 12 - 4\cos\Theta)$$

$$K_5 = 0$$

$$K_6 = 0$$

When $\Theta = 0^0$, the trailing edge of the rectilinear profile is at the origin of coordinates and the moment about this point is thus the moment about the trailing edge, i. e.,

$$M_t = 2\sigma u^2 a^2 (16 - 3\pi)\sin 2\alpha$$

which agrees with the result obtained by applying the discontinuous potential directly to the rectilinear profile [1]).

---

[1]) C. *Witoszyński*: "Aerodynamika" (reference 1, pg. 13), pg. 168.

b. Hinge Moment. In order to calculate the hinge moment for the bi-linear profile by means of the discontinuous potential, it is necessary to evaluate the integral (*32*) along those portions of the circle $Z = ae^{i\vartheta}$ which correspond to the flap, that is, from $-\pi$ to ϑ_2 and from ϑ_4 to π, where $\vartheta_2 = \Theta - \varphi$ and $\vartheta_4 = 2\pi - \Theta - \varphi$. Two integrals are thus obtained which are

$$M_f + i\,(N_f - N_c) = -\frac{\sigma}{2}\oint_{Z=ae^{-i\pi}}^{Z=ae^{i\vartheta_2}}\left(\frac{df}{dZ}\right)^2\left(\frac{dZ}{dz}z - Z\right)dZ - \frac{\sigma}{2}\oint_{Z=ae^{i\vartheta_4}}^{Z=ae^{i\pi}}\left(\frac{df}{dZ}\right)^2\left(\frac{dZ}{dz}z - Z\right)dZ.$$

In case $\vartheta_2 = \vartheta_4 = 0$, the path of integration becomes the complete circle and the hinge moment then becomes the total moment, consequently these integrals were first evaluated in terms of ϑ_2 and ϑ_4, and the calculations checked by putting these values equal to zero, as was done in the case of the Joukovsky potential. When the values of ϑ_2 and ϑ_4 corresponding to the hinge point on the upper and lower surfaces of the bi-linear profile were substituted, the results obtained for the real parts of the above integrals were as follows:

$$M_f = \sigma u^2 a^2\left[K_{4_f}\sin 2\alpha + K_{5_f}\sin^2\alpha + K_{6_f}\right] \quad \ldots\ldots \quad (37)$$

where

$$K_{4_f} = 2\Bigg[-(3\Theta - 8) + 2h\left\{\Theta\sin 2\varphi\sin\varphi - \cot\varphi\log_e\left(\frac{1+\sin\varphi}{1-\sin\varphi}\right)\right\} - 8\sin\frac{\varphi}{2}\cos\frac{\Theta}{2} -$$

$$-\sin\Theta\left\{2\cos\varphi + \cos 2\varphi\,(h - \cos\varphi)\right\} + 2h\left\{\cot\varphi\,(\cos\varphi + 1) + \cos\varphi\sin 2\varphi\right\}\log_e\left\{\left|\frac{\cos\frac{(\Theta+\varphi)}{4}}{\sin\frac{(\Theta-\varphi)}{4}}\right|\right\} -$$

$$-2h\left\{\cot\varphi\,(\cos\varphi - 1) + \cos\varphi\sin 2\varphi + \frac{2}{\sin\varphi}\right\}\log_e\left\{\left|\frac{\cos\frac{(\Theta-\varphi)}{4}}{\sin\frac{(\Theta+\varphi)}{4}}\right|\right\}\Bigg],$$

$$K_{5_f} = -8h\left\{\Theta\sin\varphi\cos 2\varphi + \frac{3 + 4\sin^2\varphi}{3\sin^3\varphi} + \frac{(2\sin^4\varphi - \sin^2\varphi - 1)}{2\sin^4\varphi}\log_e\left(\frac{1+\sin\varphi}{1-\sin\varphi}\right)\right\} +$$

$$+ 32\cos\frac{\varphi}{2}\cos\frac{\Theta}{2} - 8\sin\varphi\sin\Theta\left\{1 + \cos\varphi\,(h - \cos\varphi)\right\} -$$

$$-\frac{h(4 + 5\sin^2\varphi)}{\sin^3\varphi}\left\{\tan\frac{(\Theta-\varphi)}{4} - \cot\frac{(\Theta+\varphi)}{4}\right\} - \frac{(h\cos\varphi - 2\sin^2\varphi)}{\sin^2\varphi}\left\{\tan^2\frac{(\Theta-\varphi)}{4} - \cot^2\frac{(\Theta+\varphi)}{4}\right\} -$$

$$-\frac{h}{3\sin\varphi}\left\{\tan^3\frac{(\Theta-\varphi)}{4} - \cot^3\frac{(\Theta+\varphi)}{4}\right\} +$$

$$+2\left[h\left\{\frac{2(2\sin^4\varphi-\sin^2\varphi-1)-(4\sin^4\varphi-9\sin^2\varphi-6)\cos\varphi}{\sin^4\varphi}+4\cos\varphi\cos 2\varphi\right\}-12\right]\log_e\left\{\left|\frac{\cos\frac{(\Theta-\varphi)}{4}}{\sin\frac{(\Theta+\varphi)}{4}}\right|\right\}+$$

$$+2h\left[\frac{2(2\sin^4\varphi-\sin^2\varphi-1)+(4\sin^4\varphi-3\sin^2\varphi-2)\cos\varphi}{\sin^4\varphi}-4\cos\varphi\cos 2\varphi\right]\log_e\left\{\left|\frac{\cos\frac{(\Theta+\varphi)}{4}}{\sin\frac{(\Theta-\varphi)}{4}}\right|\right\},$$

$$K_{6_f}=2\sin\varphi\left[2\sin\Theta\left\{1+\cos\varphi\,(h-\cos\varphi)\right\}+2h\Theta\cos 2\varphi-h\sin 2\varphi\log_e\left\{\frac{1-\cos(\Theta+\varphi)}{1-\cos(\Theta-\varphi)}\right\}\right].$$

A partial check on these results is obtained by noting that the expresion for K_{6_f} is identical with that obtained by the Joukovsky potential. This is to be expected for when $\alpha=0$, the circulations of both the vortex of Joukovsky and the complementary function in the discontinuous potential are zero, the motion then being due to the plane translatory flow alone. Since the flow is the same in both cases, the hinge moment, which is $\sigma u^2 a^2 K_{6_f}$, should also be the same for both potentials. These remarks also apply to the total moment.

The above expressions for the coefficients K_{4_f} and K_{5_f} in the hinge moment are not well suited to numerical calculations and also involve terms which are indeterminate when β approaches zero, making it difficult to investigate the limiting case of the rectilinear profile. In order to overcome these difficulties, the indeterminate expressions were treated as in the total moment and expanded into series in $\sin\varphi$. After this expansion the following results were obtained:

$$K_{4_f}=2\left[-(3\Theta-8)-4h\cos\varphi\left\{1-\left(\Theta-\frac{1}{3}\right)\sin^2\varphi\right\}-8\sin\frac{\varphi}{2}\cos\frac{\Theta}{2}-\right.$$

$$-\sin\Theta\left\{2\cos\varphi+\cos 2\varphi\,(h-\cos\varphi)\right\}+$$

$$\left.+A_0+A_2\sin^2\varphi+A_4\sin^4\varphi+A_6\sin^6\varphi+\ldots\ldots\right]$$

where

$$A_0=-8\left(1-\sin\frac{\Theta}{2}\right)\cos\frac{\Theta}{2},$$

$$A_2=\frac{\left(7+19\sin\frac{\Theta}{2}+16\sin^2\frac{\Theta}{2}\right)\cos\frac{\Theta}{2}}{3\left(1+\sin\frac{\Theta}{2}\right)},$$

$$A_4=\frac{\left(131-1789\sin\frac{\Theta}{2}-1979\sin^2\frac{\Theta}{2}+1541\sin^3\frac{\Theta}{2}+1616\sin^4\frac{\Theta}{2}\right)}{240\left(1+\sin\frac{\Theta}{2}\right)\cos\frac{\Theta}{2}},$$

$$A_6=\left(1827+5087\sin\frac{\Theta}{2}+2686\sin^2\frac{\Theta}{2}-6274\sin^3\frac{\Theta}{2}+2371\sin^4\frac{\Theta}{2}+\right.$$

$$\left.+7187\sin^5\frac{\Theta}{2}-14128\sin^6\frac{\Theta}{2}\right)\frac{1}{13440\left(1+\sin\frac{\Theta}{2}\right)\cos^3\frac{\Theta}{2}},$$

$$K_{5f} = -8h \sin\varphi \left\{\Theta + \frac{22}{15} - \left(2\Theta - \frac{34}{105}\right)\sin^2\varphi\right\} + 32 \cos\frac{\varphi}{2} \cos\frac{\Theta}{2} -$$

$$- 8 \sin\varphi \sin\Theta \{1 + \cos\varphi\,(h - \cos\varphi)\} + A_1 \sin\varphi + A_3 \sin^3\varphi + A_5 \sin^5\varphi + \ldots$$

where

$$A_1 = \frac{8\left(14 + 28 \sin\frac{\Theta}{2} - 8 \sin^2\frac{\Theta}{2} - 19 \sin^3\frac{\Theta}{2}\right)\cos\frac{\Theta}{2}}{15\left(1 + \sin\frac{\Theta}{2}\right)^2},$$

$$A_3 = -\left(9864 + 125778 \sin\frac{\Theta}{2} + 236645 \sin^2\frac{\Theta}{2} + 6262 \sin^3\frac{\Theta}{2} - 233501 \sin^4\frac{\Theta}{2} - \right.$$

$$\left. - 124888 \sin^5\frac{\Theta}{2}\right)\frac{1}{3360\left(1 + \sin\frac{\Theta}{2}\right)^2 \cos\frac{\Theta}{2}},$$

$$A_5 = -\left(643988 - 4187984 \sin\frac{\Theta}{2} - 10195548 \sin^2\frac{\Theta}{2} + 3431713 \sin^3\frac{\Theta}{2} + \right.$$

$$+ 17327893 \sin^4\frac{\Theta}{2} + 2983707 \sin^5\frac{\Theta}{2} - 6219609 \sin^6\frac{\Theta}{2} -$$

$$\left. - 2074592 \sin^7\frac{\Theta}{2}\right)\frac{1}{322560\left(1 + \sin\frac{\Theta}{2}\right)^2 \cos^3\frac{\Theta}{2}}.$$

Computations for a typical case showed that the error committed in neglecting the terms above $A_4 \sin^4\varphi$ in K_{4f} and above $A_3 \sin^3\varphi$ in K_{5f} was so small that for practical purposes, these formulas could be written in the form

$$\left.\begin{aligned}
K_{4f} &= 2\left[-(3\Theta - 8) - 4h\cos\varphi\left\{1 - \left(\Theta - \frac{1}{3}\right)\right\}\sin^2\varphi - 8\sin\frac{\varphi}{2}\cos\frac{\Theta}{2} - \right.\\
&\quad \left. - \sin\Theta\left\{2\cos\varphi + \cos 2\varphi\,(h - \cos\varphi) + A_0 + A_2\sin^2\varphi + A_4\sin^4\varphi\right]\right.,\\
K_{5f} &= -8h\sin\varphi\left\{\Theta + \frac{22}{15} - \left(2\Theta - \frac{34}{105}\right)\sin^2\varphi\right\} + 32\cos\frac{\varphi}{2}\cos\frac{\Theta}{2} -\\
&\quad - 8\sin\varphi\sin\Theta\left\{1 + \cos\varphi\,(h - \cos\varphi)\right\} + A_1\sin\varphi + A_3\sin^3\varphi,\\
K_6 &= 2\sin\varphi\left[2\sin\Theta\left\{1 + \cos\varphi\,(h - \cos\varphi)\right\} + 2h\Theta\cos 2\varphi - \right.\\
&\quad \left. - h\sin 2\varphi\,\log_e\left\{\frac{1 - \cos(\Theta + \varphi)}{1 - \cos(\Theta - \varphi)}\right\}\right].
\end{aligned}\right\} \quad . \quad . \quad (37')$$

These formulas were checked for the limiting cases where the flap becomes the whole rectilinear profile or vanishes entirely and the results were found to be satisfactory in every case.

3. Approximate Methods for Calculating Lift and Drag.

Although none of the formulas obtained for the characteristics of the bi-linear profile using the discontinuous potential are particularly simple, from the standpoint of numerical calculations, the formulas for the lift and drag are the most unsatisfactory since they involve integrals which cannot in general be evaluated exactly by analytical methods. For this reason several different approximate methods were applied to this phase of the problem in an attempt to obtain these results in a simpler form.

a. **Bonder's Method.** The first of these approximate methods consisted in the employment of an unpublished theory developed by Juljan Bonder of the Aerodynamic Institute of Warsaw, which was used in this problem with his kind permission. A brief résumé of this method will now be given. The velocity distribution on the primitive circle as given by the discontinuous potential is determined by the expression

$$V_c = 2u \left[\sin(\vartheta + \alpha) + \frac{\sin \alpha}{1 + \cos \frac{\vartheta}{2}} \right] \quad . \; . \; . \; . \; . \; . \; . \; . \; . \quad (38)$$

as may be shown by substituting the value (21) for $\frac{df}{dZ}$ in the formula (27). Now the lift and drag of a profile are dependent on the square of this velocity, which may be written in the form of a Fourier's series, as

$$V_c^2 = 4u^2 \left[\frac{1}{2} a_0 + a_1 \cos\vartheta + a_2 \cos 2\vartheta + \ldots\ldots + a_n \cos n\vartheta + \ldots \right.$$

$$\left. + b_1 \sin\vartheta + b_2 \sin 2\vartheta + \ldots\ldots + b_n \sin n\vartheta + \ldots \right], \qquad -\pi \leqslant \vartheta \leqslant \pi,$$

where the coefficients are calculated by the usual formulas

$$a_n = \frac{1}{\pi} \int_{-\pi}^{\pi} f(\vartheta) \cos n\vartheta \, d\vartheta, \qquad n = 0, 1, 2, \ldots\ldots$$

$$b_n = \frac{1}{\pi} \int_{-\pi}^{\pi} f(\vartheta) \cos n\vartheta \, d\vartheta, \qquad n = 1, 2, \ldots\ldots$$

Now consider the complex function

$$-4u^2 \frac{a^2}{Z^2} \left[\frac{a_0}{2} + \frac{a_1}{2}\left(\frac{Z}{a} + \frac{a}{Z}\right) + \frac{a_2}{2}\left(\frac{Z^2}{a^2} + \frac{a^2}{Z^2}\right) + \ldots + \frac{a_n}{2}\left(\frac{Z^n}{a^n} + \frac{a^n}{Z^n}\right) + \ldots \right.$$

$$\left. + \frac{b_1}{2i}\left(\frac{Z}{a} - \frac{a}{Z}\right) + \frac{b_2}{2i}\left(\frac{Z^2}{a^2} - \frac{a^2}{Z^2}\right) + \ldots\ldots + \frac{b_n}{2i}\left(\frac{Z^n}{a^n} - \frac{a^n}{Z^n}\right) + \ldots \right] \quad . \; . \quad (39).$$

If this function be considered as representing the square of the complex velocity obtained with a certain potential, it will be found that the velocity distribution on the primitive circle is identical with that obtained by expression (38) for the discontinuous potential, the coefficients

a_n and b_n being the same as in the Fourier development for the square of the velocity due to the latter. Hence for the calculation of the lift and drag, the square of the derivative (21) of the discontinuous potential may be replaced by the expression (39). Of course it is not supposed that the velocity defined by this new function will be identical with that given by the discontinuous potential at points outside the profile contour. Since the function (39) is single-valued the integral obtained after substitution in the first formula of Blasius may be evaluated by the method of residues, it being necessary, however, to write the expression for $\frac{dZ}{dz}$ in the form of a series, as follows:

$$\frac{dZ}{dz} = 1 + \frac{a^2 (c_2 + id_2)}{Z^2} + \frac{a^3 (c_3 + id_3)}{Z^3} + \ldots\ldots$$

The results for the lift and drag are thus obtained in the form of infinite series and the practicability of this method depends on the rapidity with which these series converge. Computations were made for a special case of the bi-linear profile using the first six terms in these series, but the results did not agree very well with those of the exact method, probably due to the fact that the series for $\frac{dZ}{dz}$ did not converge with sufficient rapidity. It was concluded that even if satisfactory results could be obtained by taking a few more terms into consideration, the numerical calculations would be so long that this method would have no appreciable advantage over the exact method, and the attempt to apply it to the bi-linear profile was therefore abandoned. It is possible that this method may be of value in cases where the reciprocal of the derivative of the transformation function converges more rapidly.

b. A Graphical Method. After the failure of the above process, a graphical method for obtaining the lift and drag was developed and will now be discussed briefly. Instead of the usual lift and drag, let it be supposed that the resultant air force has been divided into two other components P_x and P_y, parallel to the x and y coordinate axes, P_y acting vertically upward and P_x horizontally in the direction of the negative x-axis. By means of the elementary principles of hydrodynamics, it may be shown that

$$P_y = -\frac{\sigma}{2}\oint V_c^2 \left(\frac{dS}{ds}\right)^2 dx$$

$$P_x = -\frac{\sigma}{2}\oint V_c^2 \left(\frac{dS}{ds}\right)^2 dy,$$

these formulas forming the basis on which the first formula of Blasius is developed, In these integrals V_c is the velocity at a point on the primitive circle, $\frac{dS}{ds}$ is the ratio of the length of an element of arc of this circle to the length of the corresponding element of arc of the transformed profile, and dx and dy are the projections of this second element, ds, on the x- and y-axes. Now all these quantities may be expressed as functions of ϑ and the expressions for P_y and P_x thus transformed into integrals along the "ϑ" axis, instead of along the x- and y-axes in the plane of the transformed profile. As in the exact method these integrals contained the fractional exponent $\frac{\beta}{\pi}$ and an attempt was therefore made to evaluate them by means of Simpson's rule but because of the fact that the integrands become infinite at the points $\vartheta_3 = 2(\pi - \varphi)$ and $\vartheta_4 = 2\pi - \Theta - \varphi$ corresponding

to the leading edge and hinge point (on the upper surface) of the bi-linear profile, considerable difficulty was experienced in evaluating the integrals in the neighborhood of these critical points, and since accurate results could not be obtained even when analytical methods were applied in these ranges, this method was finally rejected as being impractical.

c. The Potential of Three Vortices. After the failure of the two approximate methods discussed above to give satisfactory results for the forces acting on the bi-linear profile, a third method based on an "artificial" potential was developed with which sufficiently accurate results were obtained for profiles such as are employed in practice, that is, for flap angles from 0^0 to 30^0 and for flap-chord ratios up to 50%. The function employed in this case was based on the same general considerations discussed in the application of the Bonder method and is called an artificial potential because it does not represent a motion which is physically possible but merely gives a velocity distribution on the primitive circle closely approximating that obtained with the discontinuous potential. In Bonder's method a single-valued complex function in the form of an infinite series was employed which gave a velocity distribution on the primitive circle identical with that given by the discontinuous potential, but as shown above, the results were unsatisfactory in the case of the bi-linear profile. The supposition on which this new potential is based is that it might be possible to find another function consisting of a finite number of terms whose derivative at least is single-valued so that the integrals required could be evaluated by the method of residues. It of course is necessary that the velocity distribution on the primitive circle given by this new function shall closely approximate that given by the discontinuous potential. For this purpose the original discontinuous potential (20) was split into two terms

$$f_1(Z) = -u\left(Ze^{i\alpha} + \frac{a^2 e^{-i\alpha}}{Z}\right),$$

$$f_2(Z) = \frac{8ia^{3/2} u \sin\alpha}{Z^{1/2} + a^{1/2}}.$$

As mentioned previously the potential $f_1(Z)$ represents the movement around the circle due to a plane translatory flow and is identical with the first term of the Joukovsky potential, so that in developing this new artificial potential, it was decided to leave this term intact and try to find only a new function $f_3(Z)$ which could be used to replace the original complementary function $f_2(Z)$. Since $f_2(Z)$ represents a type of circulatory flow around the profile, it was to be expected that the new function should also give a circulation of the same magnitude for it is known that in general the lift force acting on a profile is directly proportional to the circulation around it. The function proposed as the new complementary term represents the flow around the profile due to a system of three stationary vortices, one placed at the center of the primitive circle, the second outside it on the negative X-axis, and the third inside the circle at the image point of this external one. The circulation of the first vortex was C_1 while the remaining pair had equal and opposite circulations, C_2. The function representing this configuration is

$$f_3(Z) = -\frac{iC_1}{2\pi}\log_e\frac{Z}{a} + \frac{iC_2}{2\pi}\log_e\left(\frac{Z+R}{Z+\frac{a^2}{R}}\right) \quad \ldots\ldots\ldots \quad (40)$$

and in Figure 7 the arrangement of the vortices is shown. The complete complex potential is

$$f_4(Z) = -u\left(Ze^{i\alpha} + \frac{a^2 e^{-i\alpha}}{Z}\right) - \frac{iC_1}{2\pi}\log_e\frac{Z}{a} + \frac{iC_2}{2\pi}\log_e\left(\frac{Z+R}{Z+\frac{a^2}{R}}\right) \quad \ldots \quad (41),$$

It is easily demonstrated that this function gives the circle $Z = ae^{i\vartheta}$ as a stream-line, for the flow may be considered as due to the superposition of three different movements; the plane translatory flow, the vortex at the origin, and the conjugate pair of vortices. Since the primitive circle is a stream-line for each of these, it follows that it is a stream-line for the combined flow.

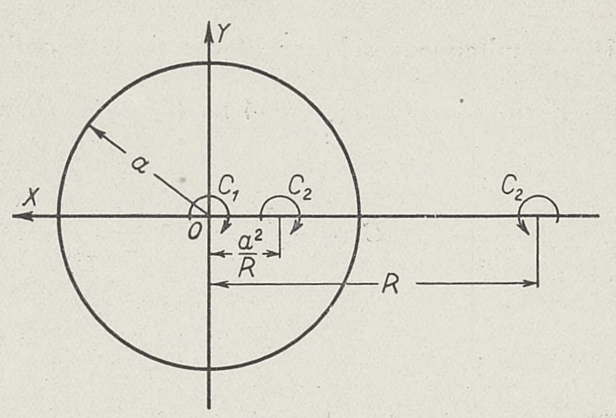


Figure 7

The complex velocity now is

$$\frac{df_4(Z)}{dz} = -u\left(e^{i\alpha} - \frac{a^2 e^{-i\alpha}}{Z^2}\right) - \frac{iC_1}{2\pi Z} + \frac{iC_2}{2\pi}\left(\frac{1}{Z+R} - \frac{1}{Z+\dfrac{a^2}{R}}\right) \quad . \quad . \quad . \quad (42).$$

The artificialness of this function is immediately evident for this system of vortices is unstable, the external one moving out to infinity while the two internal ones coincide at the origin after the lapse of an infinite length of time. However, a stable system is needed here and so the vortices will be considered as fixed, that is, R is a constant, and the velocity distribution that would be obtained with such an arrangement will be investigated although its physical existence is impossible.

The velocity distiibution on the circle $Z = ae^{i\vartheta}$ due to this complementary function is

$$V'_{c_3} = \frac{C_1}{2\pi a} + \frac{C_2}{2\pi a}\left(\frac{R^2 - a^2}{R^2 + a^2 + 2aR\cos\vartheta}\right) \quad . \quad . \quad . \quad . \quad . \quad . \quad (43)$$

while that due to the second term in the discontinuous potential is

$$V'_{c_2} = \frac{2u\sin\alpha}{1 + \cos\dfrac{\vartheta}{2}} \quad . \quad . \quad . \quad . \quad . \quad . \quad . \quad . \quad . \quad . \quad . \quad . \quad (44)$$

and it now remains to determine the constants C_1, C_2, and R in (41) so that V'_{c_3} and V'_{c_2} will agree as closely as posible for all values of ϑ from $-\pi$ to π. It has already been mentioned that the circulations given by the two functions should be equal. Now by Stokes' theorem, the circulation around the profile due to $f_3(Z)$ is $C_1 + C_2$, while that due to the discontinuous potential is $8\,ua\sin\alpha$, (see pg. 18), so that the first restricting condition on these constants becomes

$$C_1 + C_2 = 8\,ua\sin\alpha \quad . \quad . \quad . \quad . \quad . \quad . \quad . \quad . \quad . \quad . \quad . \quad (45).$$

As in the previous cases the velocity at the point $Z = -a$ on the primitive circle, corresponding to the trailing edge of the transformed profile must be zero, therefore the second condition is

$$\frac{C_1}{2\pi a} + \frac{C_2}{2\pi}\left(\frac{R+a}{R-a}\right) = 2u\sin\alpha \quad . \quad . \quad . \quad . \quad . \quad . \quad . \quad . \quad . \quad (46).$$

Since there are three constants to be determined, a third equation is required and to obtain this it was arbitrarily stipulated that the velocities at the point $Z = a$, given by $f_2(Z)$ and $f_3(Z)$, should be identical. The equation based on this condition is

$$\frac{C_1}{2\pi a} + \frac{C_2}{2\pi}\left(\frac{R-a}{R+a}\right) = u\sin\alpha \quad . \quad . \quad . \quad . \quad . \quad . \quad . \quad . \quad . \quad (47).$$

The simultaneous solution of the three equations, (45), (46), and (47) gives

$$\left.\begin{aligned} C_1 &= \frac{4\,ua\,(\pi^2 - 8)\sin\alpha}{3\,\pi - 8} = 5{,}2488\;ua\sin\alpha \\ C_2 &= -\frac{4\,ua\,(\pi^2 - 6\,\pi + 8)\sin\alpha}{3\,\pi - 8} = 2{,}7512\,ua\sin\alpha \\ R &= \frac{\pi\,a}{3\pi - 8} = 2{,}2050\;a \end{aligned}\right\} \quad \ldots\ldots \quad (48).$$

The curves showing the velocity distribution on the circular profile due to these complementary functions are plotted in Figure 8 as functions of ϑ, the velocity for $f_3(Z)$ being given in Table III while that for $f_2(Z)$ is obtained from Table II, page 28. It is seen that the two curves are very nearly identical but the real test of this new function will be on how the values it gives for the forces acting on the profile agree with those obtained by the discontinuous potential.

Table III.

$\pm\vartheta$	$\frac{V'_{c_3}}{2\,u\sin\alpha}$	$\pm\vartheta$	$\frac{V'_{c_3}}{2\,u\sin\alpha}$
0	0,5000	100	0,5837
10	0,5006	110	0,6119
20	0,5022	120	0,6489
30	0,5051	130	0,6970
40	0,5092	140	0,7577
50	0,5150	150	0,8312
60	0,5225	160	0,9102
70	0,5324	170	0,9742
80	0,5452	180	1,0000
90	0,5618		

Before attempting to apply this function to the calculation of the lift and drag of the bi-linear profile, a simplified method for evaluating the line integral which occurs in the first formula of Blasius will be discussed briefly. It is at once evident from the form of (42) that in determining the value of this integral by the method of residues, the integrand has in addition to the poles of $\frac{dZ}{dz}$, poles at the points $Z = 0$, $Z = -R$, and

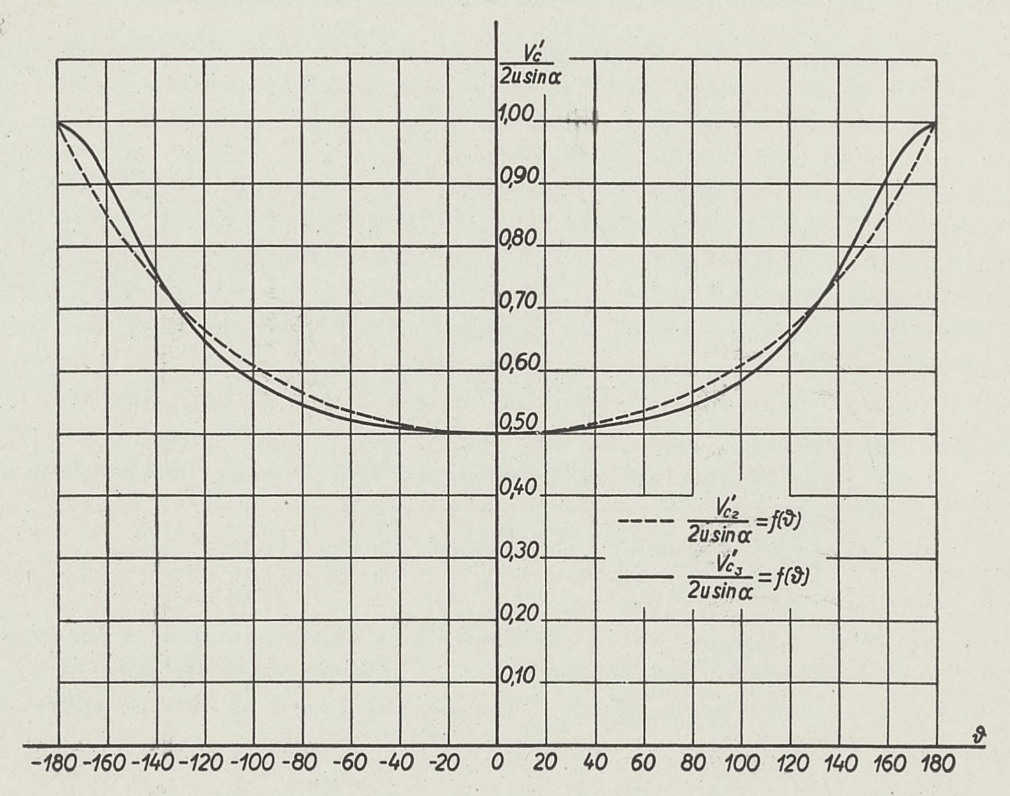


Figure 8

$Z = -\frac{a^2}{R}$. Now consider any closed curve S which encloses all the singular points of the integrand and divide the area within this curve into two parts, such that in one the only pole is the point $Z = -R$, while the second area contains all the others. If S_1 is the boundary of the first area and S_2 that of the second, then

$$\oint_S \left(\frac{df_4}{dZ}\right)^2 \frac{dZ}{dz}\, dZ = \oint_{S_1} \left(\frac{df_4}{dZ}\right)^2 \frac{dZ}{dz}\, dZ + \oint_{S_2} \left(\frac{df_4}{dZ}\right)^2 \frac{dZ}{dz}\, dZ.$$

But the circle $Z = ae^{i\vartheta}$ may be replaced by S_2 if the singular points on its boundary be taken as inside it, so that it is possible to write

$$P_{y_1} - iP_{x_1} = -\frac{\sigma e^{-i\alpha}}{2} \oint_S \left(\frac{df_4}{dZ}\right)^2 \frac{dZ}{dz}\, dZ + \frac{\sigma e^{-i\alpha}}{2} \oint_{S_1} \left(\frac{df_4}{dZ}\right)^2 \frac{dZ}{dz}\, dZ.$$

If $\frac{dZ}{dz}$ be written in the form $\quad 1 + \frac{a^2 A_2}{Z^2} + \frac{a^3 A_3}{Z^3} + \ldots\ldots,$

then the integral around S is found to be $\sigma u C_1$ and the above expression becomes

$$P_{y_1} - iP_{x_1} = \sigma u C_1 + \frac{\sigma e^{-i\alpha}}{2} \oint_{S_1} \left(\frac{df_4}{dZ}\right)^2 \frac{dZ}{dz}\, dZ \quad \ldots\ldots (49).$$

In this way the calculation of P_{y_1} and P_{x_1} is reduced to the evaluation of an integral around a curve containing only the singular point $Z = -R$ instead of around the circle $Z = ae^{i\vartheta}$ which in the case of the bi-linear profile contains five singular points.

As a preliminary check on the potential of three vortices, calculations were made for the two limiting cases, the rectilinear profile and the circular profile, in order to get some idea as to what sort of an approximation could be expected to the results obtained with the discontinuous potential. In the case of the rectilinear profile, the transformation function was taken in the form $z = Z + \frac{a^2}{Z}$ and the results obtained are as follows:

$$P_{y_1} = \sigma \left[u\,(C_1 + C_2) - \frac{C_2^2\, R\,(R^2 + a^2)\sin\alpha}{2\pi\,(R^2 - a^2)^2} - \frac{C_1 C_2\, R \sin\alpha}{2\pi\,(R^2 - a^2)} + \frac{2\, C_2 u a^2 \sin^2\alpha}{R^2 - a^2} \right],$$

$$P_{x_1} = \sigma \left[\frac{C_2^2\, R\,(R^2 + a^2)\cos\alpha}{2\pi\,(R^2 - a^2)} + \frac{C_1 C_2\, R\cos\alpha}{2\pi\,(R^2 - a^2)} - \frac{2\, u C_2 a^2 \sin\alpha\, \cos\alpha}{R^2 - a^2} \right].$$

When the values (48) for C_1, C_2, and R are substituted, these expressions become

$$P_{y_1} = 8\,\sigma u^2 a \left[\sin\alpha - \left(1 - \frac{9\pi}{32}\right) \sin^3\alpha \right] \cong 8\,\sigma u^2 a \sin\alpha,$$

$$P_{x_1} = 8\,\sigma u^2 a \left[1 - \frac{9\pi}{32} \right] \sin^2\alpha\, \cos\alpha.$$

The lift and drag by means of the discontinuous potential have already been computed on page 24 and what is indeed remarkable, the two sets of results are found to be identical.

In the case of the circular profile the transformation function is $z = Z$ and the desired results are easily obtained. By means of the potential of three vortices, they are

$$P_{y_1} = \sigma \left[u\,(C_1 + C_2) - \frac{uC_2a^2}{R^2} + \frac{2\,uC_2a^2\,\sin^2\alpha}{R^2} - \frac{C_1\,C_2\,\sin\alpha}{2\,\pi R} - \frac{C_2{}^2 R\,\sin\alpha}{2\,\pi\,(R^2 - a^2)} \right]$$

$$\simeq 7{,}4341\ \sigma u^2 a\,\sin^2\alpha\ ,$$

$$P_{x_1} = \sigma \left[\frac{C_1\,C_2\,\cos\alpha}{2\,\pi R} + \frac{C_2{}^2 R\,\cos\alpha}{2\,\pi\,(R^2 - a^2)} - \frac{2\,uC_2a^2\,\sin\alpha\,\cos\alpha}{R^2} \right]$$

$$\simeq 0{,}5959\ \sigma u^2 a\,\sin^2\alpha\,\cos\alpha,$$

while by means of the discontinuous potential[1]), the expressions for the lift and drag are

$$P_{y_1} = \frac{16}{3}\,\sigma u^2 a \left[3\,\pi - 8 + (28 - 9\,\pi)\,\sin^2\alpha \right] \sin\alpha \simeq 7{,}60\ \sigma u^2 a\,\sin\alpha\,,$$

$$P_{x_1} = \frac{8}{3}\,\sigma u^2 a \left[9\,\pi - 28 \right] \sin^2\alpha\,\cos\alpha = 0{,}732\ \sigma u^2 a\,\sin^2\alpha\,\cos\alpha.$$

Here the expresions for the lift agree sufficiently well, but in the drag as calculated by the potential of three vortices, there is an error amounting to 18,6%. However, most of the profiles which it is desired to study here will resemble the rectilinear profile much more closely than the circle, so that in spite of this large error, it was concluded that the possibility of obtaining satisfactory results with the potential of three vortices was quite strong if the study was limited to profiles having flap-chord ratios and flap angles such as are used in practice.

With the completion of this preliminary work, the potential of three vortices is now ready to be applied to the study of the bi-linear profile. In order to determine the lift and drag the expression (42) for the complex velocity and (13) for $\frac{dZ}{dz}$ must be substituted in the formula (49) which then becomes

$$P_{y_1} - iP_{x_1} = \sigma u\,C_1 + \frac{\sigma\,e^{-i\alpha}}{2} \oint_{S_1} \left[-\,u \left(Ze^{i\alpha} + \frac{a^2\,e^{-i\alpha}}{Z} \right) - \frac{iC_1}{2\pi Z} + \frac{iC_2}{2\pi} \left(\frac{1}{Z+R} - \frac{1}{Z + \frac{a^2}{R}} \right) \right]^2 \times$$

$$\times \left[\frac{Z - ae^{i(\Theta-\varphi)}}{Z - ae^{-i(\Theta+\varphi)}} \right]^{\frac{\beta}{\pi}} \frac{Z^2\,dZ}{[Z+a]\,[Z - ae^{-2i\varphi}]}$$

where the curve S_1 encloses no other singular points but the pole at $Z = -R$. This integral is most conveniently evaluated by the method of residues but the details of this work are of little interest here so that only the final results will be given. After neglecting the relatively small terms in α and, as in the case of the discontinuous potential, supposing

[1]) *S. Neumark:* loc. cit., (reference 1, pg. 18) pg. 46.

that the coefficient of the term in sin α in the resistance is always zero, the expressions for the lift and drag, using an abridged notation, are

$$P_{y_1} = \sigma\left\{C_1 u + M_1 (M_2 \cos\mu - N_2 \sin\mu)\, C_2\left(1 - \frac{a_2}{R^2}\right)\right\}$$
$$= \sigma u^2 a K'_1 \sin\alpha \quad . \; . \; . \; . \; . \; . \; . \; . \; . \; . \; . \; . \; . \; . \; (50),$$

$$P_{x_1} = \sigma\left[\left\{M_1 (M_2 \cos\mu - N_2 \sin\mu)\right\}\left\{\frac{C_2^2}{4\pi}\left(M_3 + M_4 - \frac{2}{R}\right) - \frac{2\, C_2\, u a^2 \sin\alpha}{R^2} +\right.\right.$$
$$\left.\left. + \frac{C_1\, C_2}{2\pi R} + \frac{C_2^2\, R}{2\pi\,(R^2 - a^2)}\right\} - \left\{M_1 (M_2 \sin\mu + N_2 \cos\mu)\right\}\left\{\frac{C_2^{\,2}}{4\pi}(N_3 + N_4)\right\}\right] \cos\alpha$$
$$= \sigma u^2 a K'_3 \sin^2\alpha \cos\alpha \quad . \; . \; . \; . \; . \; . \; . \; . \; . \; . \; . \; . \; (51)$$

where

$$K_1' = 5{,}2488 + 2{,}1853\, M_1 (M_2 \cos\mu - N_2 \sin\mu)\,,$$

$$K_3' = \left\{M_1 (M_2 \cos\mu - N_2 \sin\mu)\right\}\left\{0{,}6023a\,(M_3 + M_4) + 0{,}05204\right\} -$$
$$- \left\{M_1 (M_2 \sin\mu + N_2 \cos\mu)\right\}\left\{0{,}6023a\,(N_3 + N_4)\right\}$$

and

$$M_1 = \left[\frac{\sqrt{(R^2 + a^2)^2 + 4a^2 R^2 (\cos^2\Theta - \sin^2\varphi) + 4aR\,(R^2 + a^2) \cos\Theta \cos\varphi}}{R^2 + 2aR \cos(\Theta + \varphi) + a^2}\right]^{\frac{\beta}{\pi}}$$

$$= \left[\frac{\sqrt{1 + 0{,}56596\,(\cos^2\Theta - \sin^2\varphi) + 1{,}5046 \cos\Theta \cos\varphi}}{1 + 0{,}75359 \cos(\Theta + \varphi)}\right]^{\frac{\beta}{\pi}},$$

$$\mu = \frac{\beta}{\pi} \arctan\left[\frac{2a\,(R \cos\varphi + a \cos\Theta) \sin\Theta}{R^2 + 2aR \cos\Theta \cos\varphi + a^2 \cos 2\Theta}\right] =$$

$$= \frac{\beta}{\pi} \arctan\left[\frac{4{,}4100 \cos\varphi \sin\Theta + \sin 2\Theta}{4{,}8620 + 4{,}4100 \cos\varphi \cos\Theta + \cos 2\Theta}\right],$$

$$-\frac{\pi}{2} \leqslant \mu \leqslant 0 \text{ for } 0 \leqslant \beta \leqslant \pi, \quad 0 \leqslant \mu \leqslant \frac{\pi}{2} \text{ for } -\pi \leqslant \beta \leqslant 0,$$

$$M_2 = \frac{R^2\,[R + a \cos 2\varphi]}{[R - a]\,[(R + a)^2 - 4aR \sin^2\varphi]} = \frac{0{,}86612 + 0{,}39280 \cos 2\varphi}{1 - 0{,}85864 \sin^2\varphi},$$

$$N_2 = \frac{R^2 a \sin 2\varphi}{[R - a]\,[(R + a)^2 - 4aR \sin^2\varphi]} = \frac{0{,}39280 \sin 2\varphi}{1 - 0{,}85864 \sin^2\varphi},$$

$$M_3 = \frac{-2a\,(R^2 - a^2) \sin^2\varphi}{[(R^2 + a^2)^2 + 4a^2 R^2 (\cos^2\Theta - \sin^2\varphi) + 4aR\,(R^2 + a^2) \cos\Theta \cos\varphi]} =$$

$$= \frac{-0{,}22478 \sin^2\varphi}{a\,[1 + 0{,}56596\,(\cos^2\Theta - \sin^2\varphi) + 1.5046 \cos\Theta \cos\varphi]},$$

$$N_3 = \frac{-2a\,[(R^2+a^2)\cos\varphi + 2aR\cos\Theta]\sin\varphi}{[(R^2+a^2)^2 + 4a^2R^2(\cos^2\Theta - \sin^2\varphi) + 4a\,R\,(R^2+a^2)\cos\Theta\cos\varphi]} =$$

$$= \frac{-0{,}17059\sin 2\varphi - 0{,}25667\cos\Theta\sin\varphi}{a\,[1 + 0{,}56596\,(\cos^2\Theta - \sin^2\varphi) + 1{,}5046\cos\Theta\cos\varphi]},$$

$$M_4 = \frac{2\,[R\,(R+a) - a\,(3R - a)\sin^2\varphi]}{[R-a]\,[(R+a)^2 - 4aR\sin^2\varphi]} = \frac{1{,}1419 - 0{,}90727\sin^2\varphi}{a\,[1 - 0{,}85864\sin^2\varphi]},$$

$$N_4 = \frac{a\,(R-a)\sin 2\varphi}{[R-a]\,[(R+a)^2 - 4aR\sin^2\varphi]} = \frac{0{,}09735\sin 2\varphi}{a\,[1 - 0{,}85864\sin^2\varphi]}.$$

Although these results can hardly be said to be in a simple form, the advantage of this method over the discontinuous potential from the standpoint of computations is at once evident from the fact that here there are no integrals to be calculated. Experience has shown that the results can be obtained for a given profile in from a fourth to an eighth of the time required by the method based on the discontinuous potential.

It still remains, however, to show that these formulas give results which are in sufficiently close agreement with those obtained by the discontinuous potential. For this purpose calculations were made for a series of eleven profiles which cover the range of flap angles and flap-chord ratios such as are used in practice, the results being shown in Table IV. From this data it was concluded that the formulas based on the "potential of three vortices" may be used for the determination of the lift and drag of the bi-linear profile.

Table IV.

No.	β	Θ	$\frac{l_2}{L}$—%	K_1	K_3	K'_1	K'_3
1	5°	35°	9,052	7,9986	0,9309	7,9987	0,9306
2	5°	60°	25,027	7,9990	0,9310	7,9985	0,9306
3	5°	72°	34,587	7,9991	0,9311	7,9988	0,9308
4	5°	90°	50,068	7,9992	0,9315	7,9992	0,9311
5	10°	60°	25,102	7,9962	0,9297	7,9948	0,9285
6	20°	35°	9,173	7,9856	0,9238	7,9799	0,9186
7	20°	90°	50,782	7,9915	0,9280	7,9882	0,9257
8	30°	35°	9,337	7,9677	0,9144	7,9555	0,9031
9	30°	47° 45′	16,959	7,9637	0,9103	7,9495	0,9014
10	30°	60°	25,922	7,9666	0,9151	7,9504	0,9043
11	30°	90°	51,769	7,9811	0,9238	7,9754	0,9193

III. Determination of Numerical Values of Profile Characteristics.

A. Theoretical Results.

In the previous pages theoretical formulas have been developed for calculating the lift, drag, total moment, and hinge moment acting on the bi-linear profile when moving through the air with a uniform velocity. These formulas, unfortunately, are of such a complex nature that it is practically impossible to directly obtain from them any concrete results concerning the influence of the flap angle and flap-chord ratio on the aerodynamic characteristics of the profile. For this purpose numerical calculations have been made for a large number of bi-linear profiles covering the range of flap-chord ratios from 0 to 50% and of flap angles from 0 to 30°. It will be explained later on how the characteristics of profiles having negative flap angles may be obtained from those of profiles in the above ranges.

In determining the characteristics of the bi-linear profile, it is most convenient to proceed as in experimental work and determine the values of the absolute lift, drag, and moment coefficients rather than the total values of these quantities. The first step in these calculations will therefore be to transform the theoretical formulas for the lift and drag forces and the moments so that the corresponding absolute coefficients may be obtained as quickly as possible. If P_{y_1} represents the lift force acting on a unit length of an infinitely long wing, the so-called lift coefficient may be written in the form

$$C_{y_1} = \frac{100\ P_{y_1}}{\frac{\sigma u^2}{2} L}$$

but in the theoretical work [formulas (17) and (50)], it has been demonstrated that

$$P_{y_1} = \sigma u^2 a\ K_1 \sin\alpha$$

so that

$$C_{y_1} = 100\ \frac{K_1}{L/2a} \sin\alpha \qquad \text{. . . . . (52).}$$

The drag coefficient is defined in a similar way as

$$C_{x_1} = \frac{100\, P_{x_1}}{\frac{\sigma u^2}{2} L}$$

where P_{x_1} represents the drag force acting on a unit length of the wing. This quantity, according to formula (51) obtained in the theoretical work, may be written in the form

$$P_{x_1} = \sigma\, u^2\, a\, K_3 \sin^2\alpha \cos\alpha$$

and consequently

$$C_{x_1} = 100\ \frac{K_3}{L/2a} \sin^2\alpha \cos\alpha \qquad \text{. . . . . (53).}$$

In computing the moment coefficient it is necessary to select a point of reference and this will be taken as the leading edge in accordance with the standard procedure followed in laboratory work. The theoretical formulas (18) and (36), however, give the moment about the hinge point, which may be written in the general form

$$M_0 = \sigma\, u^2\, a^2\, [K_4 \sin 2\alpha + K_5 \sin^2\alpha + K_6]$$

In this formula a clockwise moment or one tending to increase the angle of attack is positive. Now if c is the distance along the chord from the leading edge to the center

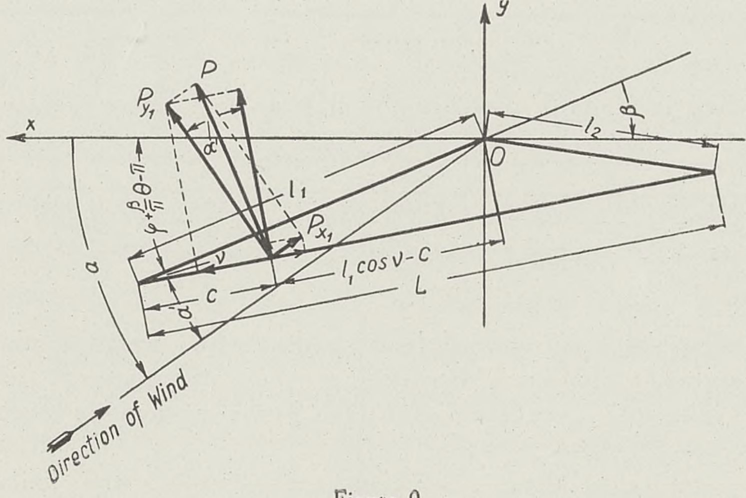


Figure 9

of pressure, and M_{LE} is the moment about the leading edge taken as positive when it tends to decrease the angle of attack, then it is easily seen from Figure 9 that

$$M_0 = \frac{(l_1 \cos\nu - c)\,(P_{y_1} \cos\alpha' + P_{x_1} \sin\alpha') + l_1 \sin\nu\,(P_{y_1} \sin\alpha' + P_{x_1} \cos\alpha')}{P_{y_1} \cos\alpha' + P_{x_1} \sin\alpha'}$$

so that

$$c = \frac{l_1 \cos\nu\,(P_{y_1} \cos\alpha' + P_{x_1} \sin\alpha') + l_1 \sin\nu\,(P_{y_1} \sin\alpha' + P_{x_1} \cos\alpha') - M_0}{P_{y_1} \cos\alpha' + P_{x_1} \sin\alpha'}.$$

The angle $\nu = \arcsin\left(\frac{l_2}{L}\sin\beta\right)$ is the angle between the fixed part and the chord of the profile, while α' is the true angle of attack, that is, the angle between the velocity vector and the chord. Now

$$M_{LE} = c\,(P_{y_1} \cos\alpha' + P_{x_1} \sin\alpha') = l_1 \left[P_{y_1} \cos(\alpha' - \nu) + P_{x_1} \sin(\alpha' - \nu)\right] - M_0$$

sothat if the moment coefficient is defined as

$$C_m = \frac{100\,M_{LE}}{\frac{\sigma u^2}{2} L^2}$$

the final expression for this quantity becomes

$$C_m = \frac{1}{L/2a}\left[\frac{l_1}{2a}\left\{C_{y_1} \cos\left(\alpha - \varphi - \frac{\beta}{\pi}\Theta + \pi\right) + C_{x_1} \sin\left(\alpha - \varphi - \frac{\beta}{\pi}\Theta + \pi\right)\right\} - \right.$$

$$\left. - \frac{50}{L/2a}\left\{K_4 \sin 2\alpha + K_5 \sin^2\alpha + K_6\right\}\right] \quad . \; . \; . \; . \; . \; . \; . \; . \quad (54).$$

As in the case of the total moment about the leading edge, a positive value of C_m indicates that the moment tends to decrease the angle of attack.

The calculation of the hinge moment coefficient is somewhat simpler than that for the total moment. According to the theoretical results [formulas (19) and (37)], the total moment about the hinge point of the forces acting on the flap is of the form

$$M_f = \sigma u^2 a^2\,[K_{4_f} \sin 2\alpha + K_{5_f} \sin^2\alpha + K_{6_f}]$$

and is positive when it tends to increase the flap angle. Consequently the hinge moment coefficient may be written as

$$C_{mf} = \frac{-100\,M_f}{\frac{\sigma u^2}{2} L^2} = -\frac{50}{(L/2a)^2}\left[K_{4_f} \sin 2\alpha + K_{5_f} \sin^2\alpha + K_{6_f}\right] \quad . \; . \; . \quad (55).$$

The negative sign has been introduced here so that when positive, this coefficient represents a moment acting in the same direction as the total moment when C_m is positive. Hence a positive value of C_{mf} indicates that the hinge moment is tending to decrease the flap angle.

When the values of these coefficients as given by the Joukovsky potential are desired, it is evident from formulas (17) and (17′) that $K_1 = 4\pi$ and $K_3 = 0$, while the values of the

K'_s in the moment coefficients are to be determined by the expressions (18) and (19). In the case of the discontinuous potential, K_1 and K_3 are equal to the values K'_1 and K'_3 respectively, defined on pages 43-44, while expressions (36′) and (37′) are to be used in the determination of the moment coefficients.

Before proceeding to the actual computations, it should be noted that the angle α which enters into the above formulas is not the usual angle of attack but differs therefrom by a constant for a given profile. Since α is measured from the zero lift axis of the profile, the angle of attack measured from the chord is seen from Figure 9 to be

$$\alpha' = \alpha - \varphi - \frac{\beta}{\pi}\Theta + \pi + \nu .$$

The angle of attack corresponding to zero lift is thus

$$\alpha'_0 = -\varphi - \frac{\beta}{\pi}\Theta + \pi + \nu \quad . \; . \; . \; . \; . \; . \; . \; . \; . \; . \quad (56).$$

The angle α may conveniently be called the theoretical angle of attack or angle of position. In experimental work with profiles having symmetrical sections, it is more convenient to measure the angle of attack from the line of symmetry of the stationary part of the profile and to maintain the lengths of the two parts of the profile as constant rather than the flap-chord ratio. In this case the angle of attack is

$$\alpha'_s = \alpha - \varphi - \frac{\beta}{\pi}\Theta + \pi$$

and the value for zero lift

$$\alpha'_{s_0} = -\varphi - \frac{\beta}{\pi}\Theta + \pi \quad . \; . \; . \; . \; . \; . \; . \; . \; . \; . \; . \; . \quad (57).$$

The difference between the values of $l_1 + l_2$ and L for the profiles studied here is so small (see Table I) that it is permissible to take these quantities as equal and to consider only the change in the angle of attack when passing from one system of measurement to the other. The values of α'_0 and α'_{s_0} for all the profiles considered have been calculated,

Table V

β	$\frac{l_2}{L} = 0$		$\frac{l_2}{L} = 10\%$		$\frac{l_2}{L} = 20\%$		$\frac{l_2}{L} = 30\%$		$\frac{l_2}{L} = 40\%$		$\frac{l_2}{L} = 50\%$	
	α'_0	α'_{s_0}	α'_0	α'_{s_0}	α'_0	α'_{s_0}	α'_0	α'_{s_0}	α'_0	α'_{s_0}	α'_0	α'_{s_0}
0	0,0000	0,0000	0,0000	0,0000	0,0000	0,0000	0,0000	0,0000	0,0000	0,0000	0,0000	0,0000
5	0,0000	0,0000	— 1,4806	— 1,9750	— 1,7489	— 2,7481	— 1,8039	— 3,3033	— 1,7403	— 3,7397	— 1,5944	— 4,0936
10	0,0000	0,0000	— 2,9528	— 3,9372	— 3,5031	— 5,4917	— 3,6167	— 6,6028	— 3,4889	— 7,4722	— 3,1956	— 8,1767
15	0,0000	0,0000	— 4,4211	— 5,9044	— 5,2525	— 8,2192	— 5,4217	— 9,8772	— 5,2331	—11,1753	— 4,8056	—12,2417
20	0,0000	0,0000	— 5,9011	— 7,8667	— 6,9992	—10,9225	— 7,2442	—13,1336	— 7,0000	—14,8667	— 6,4378	—16,2878
25	0,0000	0,0000	— 7,3544	— 9,7756	— 8,7456	—13,5950	— 9,0722	—16,3556	— 8,7869	—18,5203	— 8,1031	—20,3031
30	0,0000	0,0000	— 8,8167	—11,6833	—10,5044	—16,2439	—10,9167	—19,5439	—10,6011	—22,1389	— 9,7839	—24,2564

the results being tabulated in Table V and plotted graphically in Figure 10. It is interesting to note that for a given value of the flap-chord ratio, $\frac{l_2}{L}$, both α'_0 and α'_{s_0} are

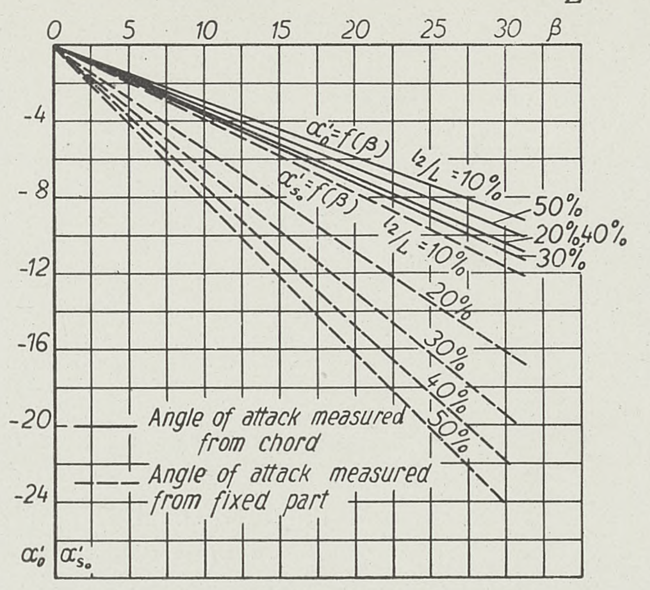


Figure 10

approximately linear functions of β. That this is very close to the actual fact may be demonstrated by inspecting the formulas (56) and (57). In the first case

$$\alpha'_0 = -\varphi - \frac{\beta}{\pi}\Theta + \pi + \nu \text{ [illegible]}$$

$$= -\arcsin\left(-\frac{\beta}{\pi}\sin\Theta\right) - \frac{\beta}{\pi}\Theta + \text{[illegible]} \arcsin\left(\frac{l_2}{L}\sin\beta\right)$$

$$= -\left\{\frac{\beta}{\pi}\sin\Theta + \frac{1}{6}\left(\frac{\beta}{\pi}\sin\Theta\right)^3 + \frac{3}{40}\left(\frac{\beta}{\pi}\sin \text{[illegible]}\right) + \ldots\right\} - \frac{\beta}{\pi}\Theta +$$

$$+ \frac{l_2}{L}\sin\beta + \frac{1}{6}\left(\frac{l_2}{L}\sin\beta\right)^3 + \frac{3}{40}\left(\frac{l_2}{L}\sin\beta\right)^5 + \ldots\ldots$$

Now the maximum values of β, Θ, and $\frac{l_2}{L}$ that are considered here are 30°, 90°, and 50%, respectively, so that the maximum value of $\frac{\beta}{\pi}\sin\Theta$ is $\frac{1}{6}$ and that of $\frac{l_2}{L}\sin\beta$ is $\frac{1}{4}$. Consequently it is permissible to write the expression for α'_0 in the approximate form

$$\alpha'_0 \cong -\frac{\beta}{\pi}\left(\sin\Theta + \Theta - \pi\frac{l_2}{L}\right)$$

In the second case when the angle of attack is measured from the fixed part of the profile, the formula for the angle of zero lift is

$$\alpha'_{s_0} = -\varphi - \frac{\beta}{\pi}\Theta + \pi$$

which in a similar way reduces to

$$\alpha'_{s_0} \cong -\frac{\beta}{\pi}\left(\sin\Theta + \Theta\right).$$

The error in the values of α'_0 and α'_{s_0} obtained by using these approximate formulas may be as high as 5% or 6% for the larger values of β and $\frac{l_2}{L}$, and since they are not much simpler than the exact formulas, there is little advantage in using them for the calculation of these quantities. However in these forms it is possible to see at once that α'_0 and α'_{s_0} are approximately linear functions of β for as can be seen from Table I, Θ changes but slightly with β for a given flap-chord ratio, so that the terms $\left(\sin\Theta + \Theta - \pi\frac{l_2}{L}\right)$ and $(\sin\Theta + \Theta)$ are practically constant.

With the completion of these necessary preliminary remarks, the determination of the profile characteristics will now be discussed. The first step in this work is the calculation of the various coefficients which enter into the formulas for the lift, drag, and moments. These quantities were determined for six families of profiles having constant flap-chord ratios of 0, 10, 20, 30, 40, and 50% and in each family, profiles with flap angles of 0, 5, 10, 15, 20, 25, and 30° were considered. The values of the coefficients K_4, K_5, and K_6 in the case of the Joukovsky potential are given in Table VI and in Figure 11, while those of $\frac{K'_1}{L/2a}$, $\frac{K'_3}{L/2a}$, K_4, K_5, K_{4f}, K_{5f}, and K_{6f} for the discontinuous potential are shown in Figures 12-a and 12-b with the numerical values in Table VII. The values of K_6 are the same for both functions. The calculations for the hinge moment based on the Joukovsky potential have not been made.

Table VI

β	$\frac{l_2}{L}=0$			$\frac{l_2}{L}=10\%$			$\frac{l_2}{L}=20\%$		
	K_4	K_5	K_6	K_4	K_5	K_6	K_4	K_5	K_6
0	18,850	0,00000	0,00000	16,336	0,00000	0,00000	13,823	0,00000	0,00000
5	18,850	0,00000	0,00000	16,328	0,37643	— 0,37629	13,801	0,44649	— 0,44641
10	18,850	0,00000	0,00000	16,293	0,75009	— 0,74955	13,726	0,89096	— 0,88937
15	18,850	0,00000	0,00000	16,210	1,12306	— 1,12010	13,614	1,33128	— 1,32523
20	18,850	0,00000	0,00000	16,103	1,49352	— 1,48455	13,458	1,76407	— 1,75152
25	18,850	0,00000	0,00000	15,973	1,85110	— 1,84050	13,268	2,19090	— 2,16451
30	18,850	0,00000	0,00000	15,816	2,20800	— 2,18601	13,026	2,60790	— 2,56182

β	$\frac{l_2}{L}=30\%$			$\frac{l_2}{L}=40\%$			$\frac{l_2}{L}=50\%$		
	K_4	K_5	K_6	K_4	K_5	K_6	K_4	K_5	K_6
0	11,310	0,00000	0,00000	8,7965	0,00000	0,00000	6,2832	0,00000	0,00000
5	11,281	0,44755	— 0,44740	8,7671	0,41017	— 0,40981	6,2650	0,34903	— 0,34876
10	11,204	0,89316	— 0,89079	8,7015	0,81895	— 0,81655	6,1999	0,69681	— 0,69467
15	11,083	1,33480	— 1,32687	8,6031	1,22560	— 1,21749	6,1195	1,04439	— 1,03709
20	10,908	1,76966	— 1,75212	8,4407	1,62760	— 1,60793	6,0017	1,39179	— 1,37332
25	10,692	2,19770	— 2,16261	8,2371	2,02330	— 1,98565	5,8368	1,73340	— 1,69930
30	10,426	2,61640	— 2,55545	7,9898	2,41250	— 2,34718	5,6548	2,07610	— 2,01673

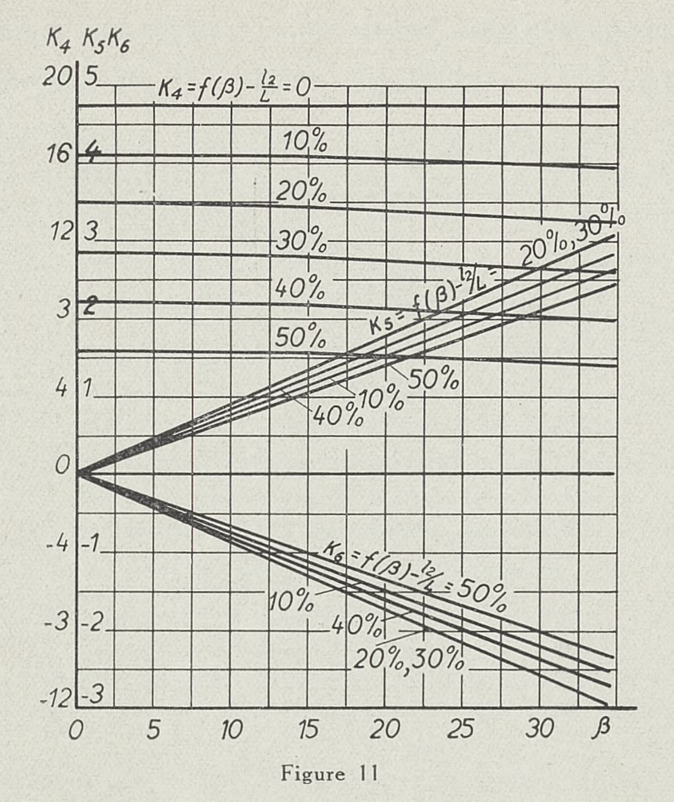


Figure 11

Table VII

$\frac{l_2}{L} = 0$

β	$\frac{K_1'}{L/2a}$	$\frac{K_3'}{L/2a}$	K_4	K_5	K_{4f}	K_{5f}	K_{6f}
0	4,0000	0,46572	13,150	0,00000	0,00000	0,00000	0,00000
5	„	„	„	„	„	„	„
10	„	„	„	„	„	„	„
15	„	„	„	„	„	„	„
20	„	„	„	„	„	„	„
25	„	„	„	„	„	„	„
30	„	„	„	„	„	„	„

$\frac{l_2}{L} = 10\%$

β	$\frac{K_1'}{L/2a}$	$\frac{K_3'}{L/2a}$	K_4	K_5	K_{4f}	K_{5f}	K_{6f}
0	4,0000	0,46572	11,551	0,0000	0,02092	0,00000	0,00000
5	4,0002	0,46544	11,542	1,1041	0,02072	0,00515	— 0,00518
10	4,0007	0,46448	11,510	2,2005	0,02064	0,00988	— 0,01015
15	4,0016	0,46292	11,441	3,2921	0,02038	0,01494	— 0,01503
20	4,0030	0,46534	11,351	4,3688	0,02026	0,01807	— 0,01955
25	4,0051	0,45829	11,240	5,4258	0,02006	0,02606	— 0,02358
30	4,0060	0,45309	11,107	6,4581	0,02192	0,02319	— 0,02674

Table VII (contd.)

$\frac{l_2}{L} = 20\%$							
β	$\frac{K'_1}{L/2a}$	$\frac{K'_3}{L/2a}$	K_4	K_5	K_{4f}	K_{5f}	K_{6f}
0	4,0000	0,46572	9,9505	0,0000	0,05504	0,00000	0,00000
5	4,0009	0,46549	9,9311	1,3099	0,05466	0,01649	—0,01804
10	4,0031	0,46478	9,8681	2,6125	0,05396	0,03572	—0,03577
15	4,0065	0,46352	9,7715	3,9001	0,05330	0,05237	—0,05265
20	4,0115	0,46586	9,6370	5,1671	0,05204	0,07044	—0,06843
25	4,0182	0,45970	9,4714	6,4055	0,05026	0,08550	—0,08252
30	4,0225	0,45551	9,2651	7,6108	0,04866	0,10068	—0.09509

$\frac{l_2}{L} = 30\%$							
β	$\frac{K'_1}{L/2a}$	$\frac{K'_3}{L/2a}$	K_4	K_5	K_{4f}	K_{5f}	K_{6f}
0	4,0000	0,46572	8,3505	0,0000	0,07018	0,00000	0,00000
5	4,0014	0,46560	8,3266	1,3130	0,06994	0,03767	—0,03453
10	4,0051	0,46525	8,2597	2,6179	0,06910	0,06657	—0,06845
15	4,0111	0,46460	8,1536	3,9087	0,06816	0,09880	—0,10094
20	4,0198	0,46737	8,0019	5,1781	0,06620	0,10651	—0,13176
25	4,0313	0,46259	7,8133	6,4185	0,06222	0,18678	—0,15972
30	4,0447	0,46122	7,5817	7,6237	0,06086	0,20036	—0,18487

$\frac{l_2}{L} = 40\%$							
β	$\frac{K'_1}{L/2a}$	$\frac{K'_3}{L/2a}$	K_4	K_5	K_{4f}	K_{5f}	K_{6f}
0	4,0000	0,46572	6,7505	0,0000	0,04268	0,00000	0,00000
5	4,0015	0,46569	6,7258	1,2029	0,04212	0,05150	—0,05082
10	4,0066	0,46568	6,6669	2,4005	0,04180	0,09531	—0.10082
15	4,0149	0,46566	6,5759	3,5886	0,04140	0,14196	—0,14891
20	4,0267	0,46844	6,4325	4,7575	0,03984	0,18779	—0,19493
25	4,0416	0,46583	6,2516	5,9036	0,03992	0,23342	—0,23678
30	4,0570	0,46512	6,0329	7,0214	0,03496	0,27634	—0,27686

$\frac{l_2}{L} = 50\%$							
β	$\frac{K'_1}{L/2a}$	$\frac{K'_3}{L/2a}$	K_4	K_5	K_{4f}	K_{5f}	K_{6f}
0	4,0000	0,46572	5,1505	0,0000	— 0,05224	0,00000	0,00000
5	4,0018	0,46579	5,1338	1,0237	— 0,05202	0,05893	— 0,06323
10	4,0076	0,46609	5,0774	2,0423	— 0,05228	0,11103	— 0 12617
15	4,0173	0,46647	5,0014	3,0578	— 0,05146	0,16623	— 0,18701
20	4,0315	0,46953	4,8916	4,0653	— 0,05028	0,21669	— 0,24438
25	4,0479	0,46768	4,7414	5,0561	— 0,05000	0,27522	— 0,30164
30	4,0692	0,46847	4,5699	6,0391	— 0,04890	0,32932	— 0.35334

Average value of $\frac{K_1'}{L/2a} = 4{,}0130$. Average value of $\frac{K_3'}{L/2a} = 0{,}46496$.

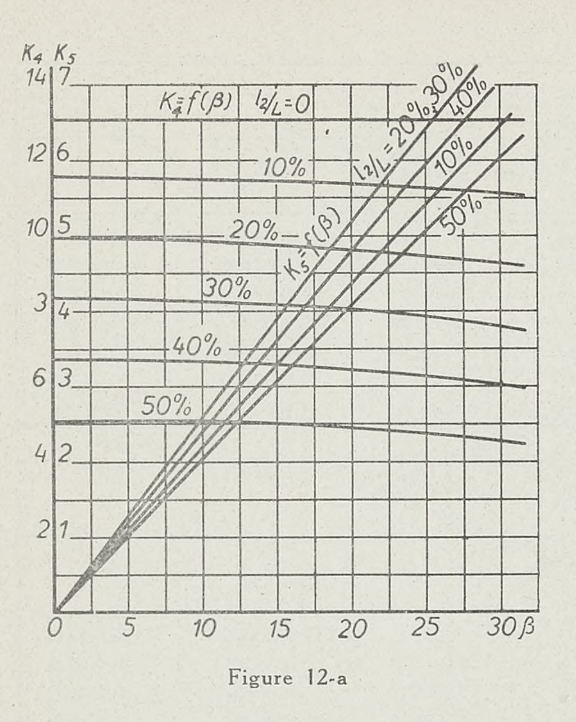


Figure 12-a

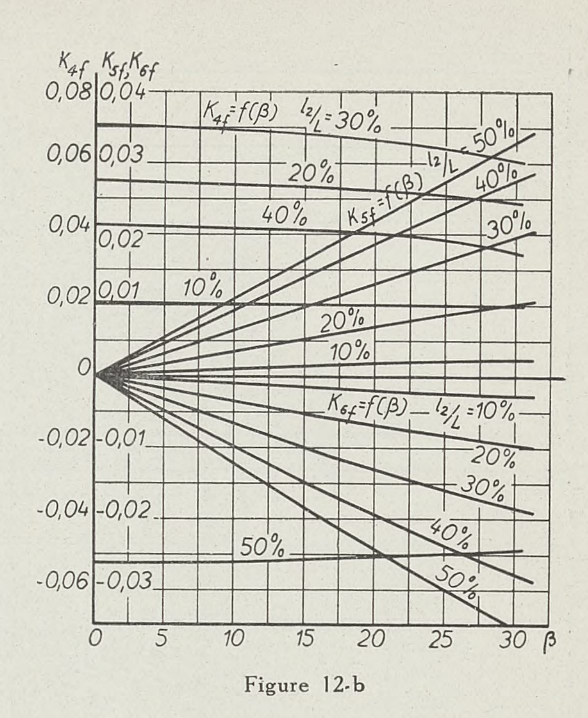


Figure 12-b

From this data it is seen that in the case of the lift and drag coefficients as obtained by the discontinuous potential, the values of the quantities $\frac{K'_1}{L/2a}$ and $\frac{K'_3}{L/2a}$ are practically constant, and in the remaining work the average values of these quantities have been used. Similarly in the case of the lift coefficient when calculated by the Joukovsky potential, K_1 is constant and $\frac{L}{2a}$ varies so slightly that for the profiles considered here, it is permissable to use its average value, 1,9908. It should also be noted that certain values of K_{4f} and K_{5f} seem to be in error since they do not all lie on smooth curves. The reason for this discrepancy is that these values are very sensitive to slight changes in the value of Θ and since the latter were determined graphically from Figure 3 and are not accurate to more than 0,1 of a degree, the values of K_{4f} and K_{5f} may be slightly irregular. However the error in any case is not very great and the results given in Table VII were deemed to be satisfactory for practical purposes.

Having determined these quantities for all the profiles under consideration, the actual values of the force and moment coefficients may now be calculated. These have been computed for values of α at intervals of $2{,}5^0$ between 0^0 and 20^0, the results for the Joukovsky potential being given in Tables VIII-a, b, c, d, and e, and those for the discontinuous potential in Tables IX-a, b, c, d, and e. In case it is desired to obtain these coefficients as functions of the angle of attack, it is simply necessary to add to α the proper value of α_0' or α'_{s_0} depending on whether the angle of attack is to be measured from the chord or the fixed part of the profile. In Figures 13-a, b, c, d, e and 14-a, b, c, d, e, these characteristics as obtained by the Joukovsky and discontinuous potentials respectively are given when the angle of attack is measured from the chord of the profile, the values of C_{y_1} and C_{x_1} being plotted directly as functions of α', while the moment coefficients C_m and C_{mf} are plotted against C_{y_1}. The polar curve, $C_{y_1} = f\,(C_{x_1})$ has also been drawn in the the case of the discontinuous potential.

The characteristics for profiles having negative flap angles may be obtained very easily from the above data, It is not difficult to show that for a profile having a given flap-chord ratio and set at a certain angle of attack α', the characteristics for a negative

Table VIII-a

$\frac{l_2}{L} = 10\%$								
α	C_{y_1}	C_m						
		$\beta = 0^0$	$\beta = 5^0$	$\beta = 10^0$	$\beta = 15^0$	$\beta = 20^0$	$\beta = 25^0$	$\beta = 30^0$
0	0	0	4,706	9,373	14,056	18,739	23,184	27,726
2,5	27,535	6,909	11,693	16,384	21,128	25,874	30,378	34,977
5	55,019	13,759	18,632	23,463	28,318	33,183	37,800	42,512
7,5	82,396	20,517	25,491	30,549	35,567	40,604	45,389	50,267
10	109,614	27,113	32,207	37,589	42,818	48,084	53,089	58,184
12,5	136,625	33,501	38,733	44,532	50,018	55,562	60,841	66,202
15	163,377	39,636	45,018	51,323	57,124	62,983	68,585	74,258
17,5	189,820	45,469	51,014	57,912	63,993	70,285	76,259	82,285
20	215,896	50,953	56,671	64,240	70,752	77,409	83,794	90,215

Note: C_{y_1} is the same for all profiles.

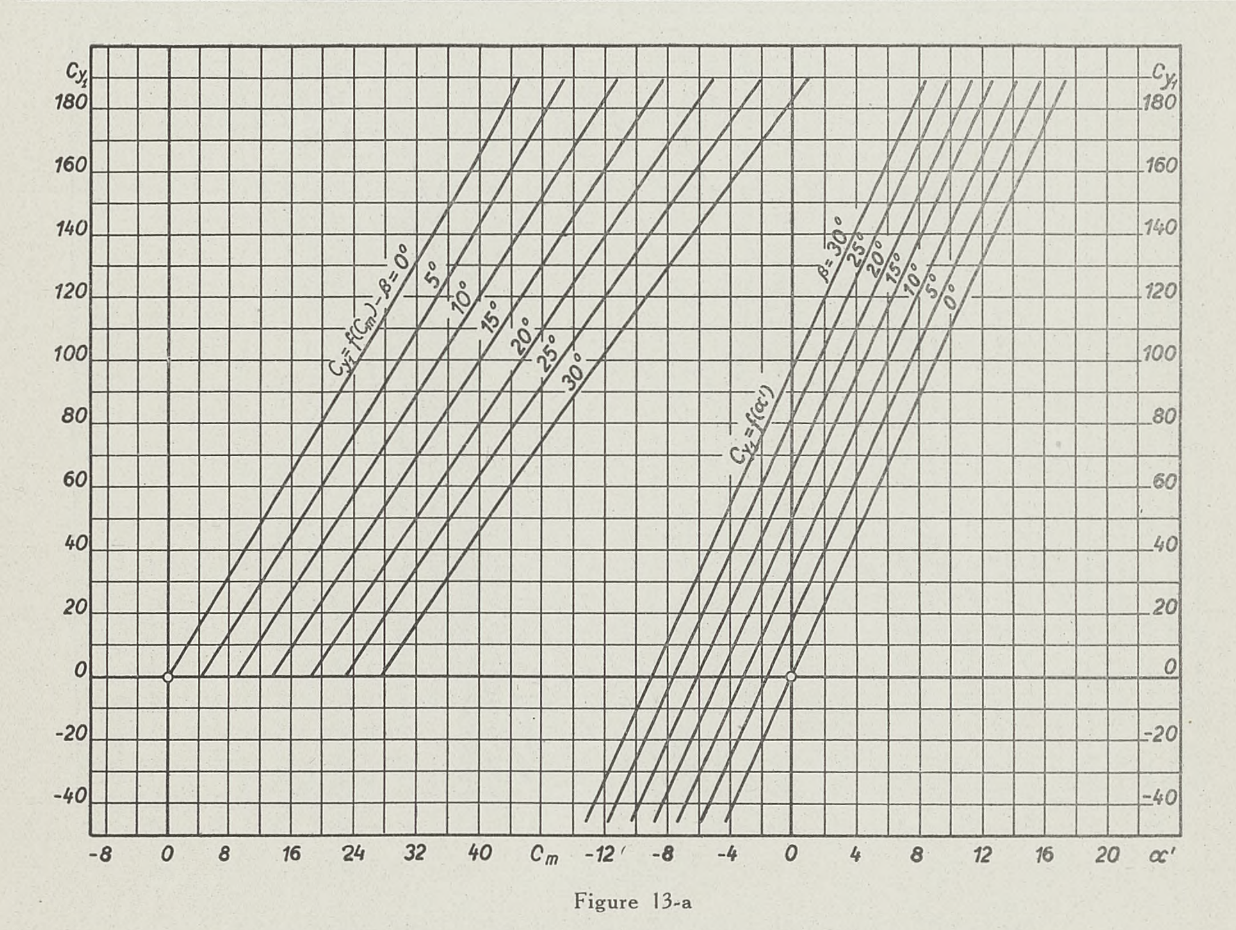


Figure 13-a

Characteristics of the Bi-Linear Profile, Joukovsky Potential.

$$\frac{l_2}{L} = 10\%$$

Table VIII-b

α	C_m ($\frac{l_2}{L} = 20\%$)						
	$\beta = 0^0$	$\beta = 5^0$	$\beta = 10^0$	$\beta = 15^0$	$\beta = 20^0$	$\beta = 25^0$	$\beta = 30^0$
0	0	5,581	11,147	16,677	22,115	27,534	32,858
2,5	6,909	12,564	18,178	23,761	29,293	34,793	40,219
5	13,759	19,571	25,300	31,005	36,703	42,353	47,951
7,5	20,517	26,537	32,434	38,350	44,281	50,151	55,988
10	27,113	33,415	39,584	45,743	51,972	58,127	64,266
12,5	33,501	40,151	46,639	53,119	59,716	66,220	72,734
15	39,636	46,694	53,564	60,429	67,453	74,366	81,310
17,5	45,469	52,993	60,303	67,614	75,119	82,501	89,931
20	50,953	58,995	66,801	74,612	82,651	90,553	98,520

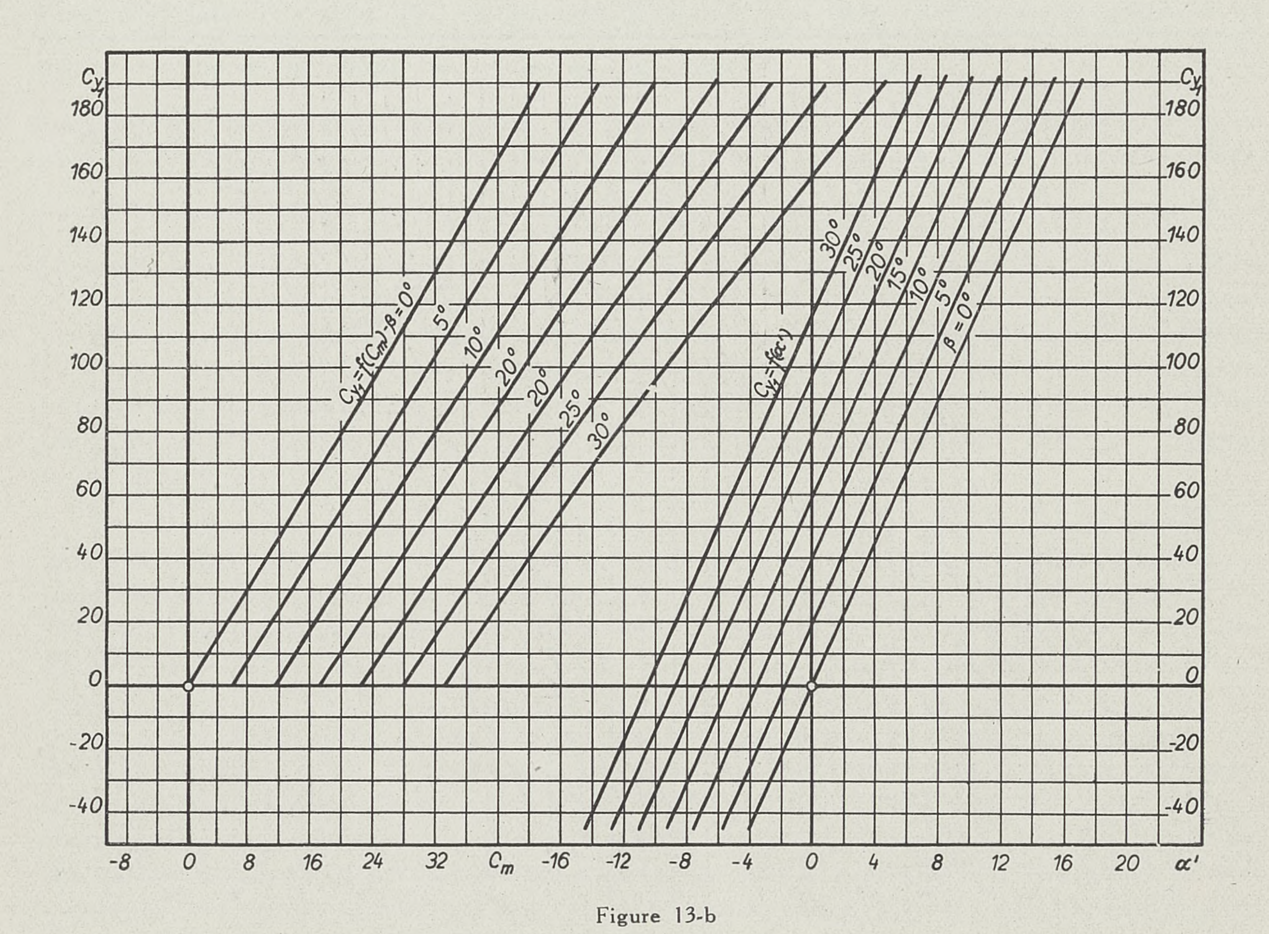


Figure 13-b

Characteristics of the Bi-Linear Profile, Joukovsky Potential.

$$\frac{l_2}{L} = 20\%$$

Table VIII-c

$\frac{l_2}{L} = 30\%$							
α	C_m						
	$\beta = 0^0$	$\beta = 5^0$	$\beta = 10^0$	$\beta = 15^0$	$\beta = 20^0$	$\beta = 25^0$	$\beta = 30^0$
0	0	5,596	11,179	16,921	22,213	27,662	33,036
2,5	6,909	12,564	18,207	23,809	29,390	34,921	40,606
5	13,759	19,556	25,336	31,092	36,817	42,506	48,178
7,5	20,517	26,510	32,505	38,479	44,433	50,354	56,287
10	27,113	33,391	39,662	45,925	52,182	58,406	64,673
12,5	33,501	40,130	46,751	53,373	60,001	66,600	73,268
15	39,636	46,679	53,720	60,766	67,832	74,869	82,006
17,5	45,469	52,991	60,513	67,996	75,611	83,149	90,816
20	50,953	59,011	67,072	75,150	83,276	91,367	99,623

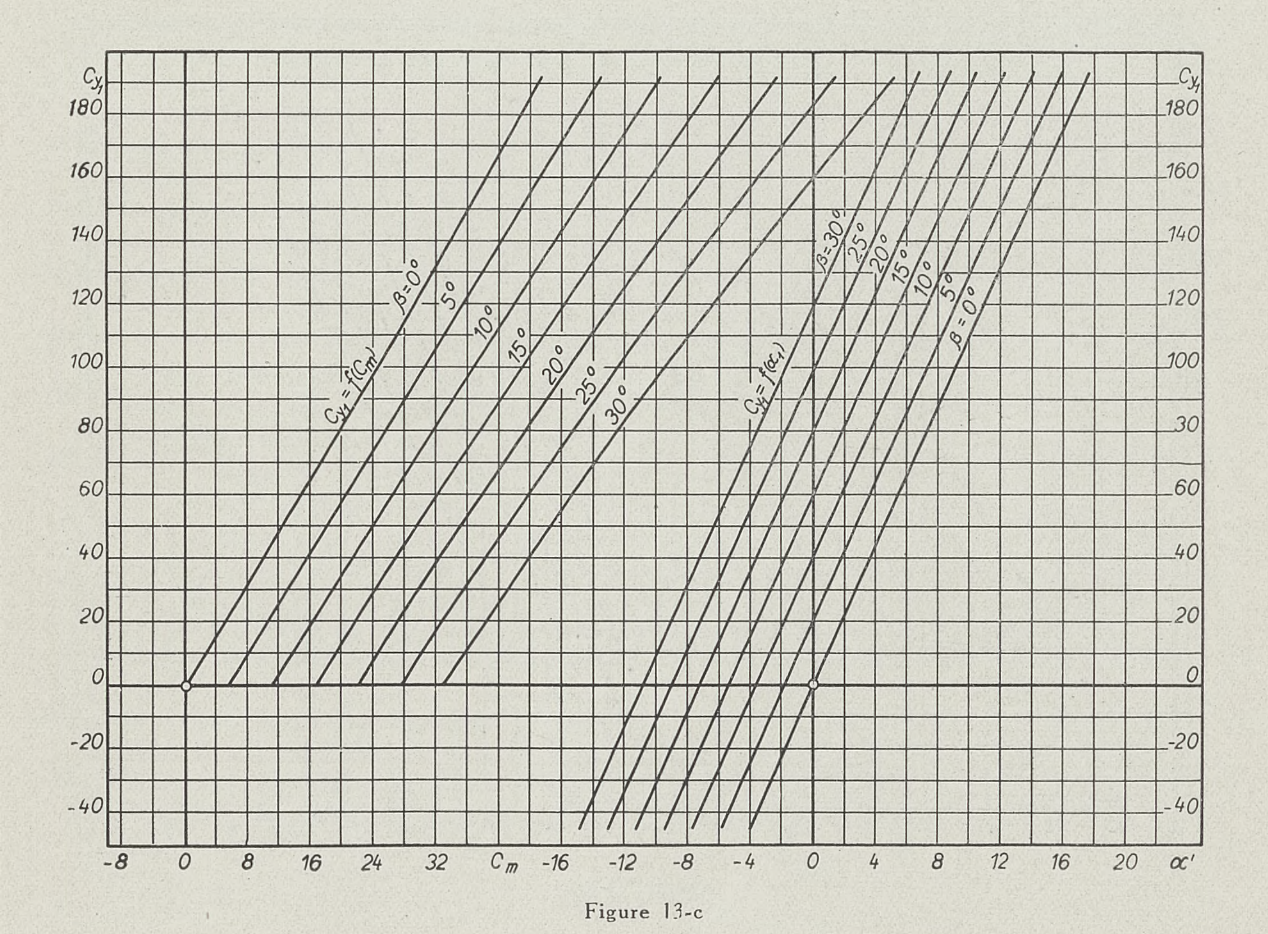


Figure 13-c

Characteristics of the Bi-Linear Profile, Joukovsky Potential.

$$\frac{l_2}{L} = 30\%$$

Table VIII-d

$\frac{l_2}{L} = 40\%$							
α	C_m						
	$\beta = 0^0$	$\beta = 5^0$	$\beta = 10^0$	$\beta = 15^0$	$\beta = 20^0$	$\beta = 25^0$	$\beta = 30^0$
0	0	5,129	10,252	15,367	20,461	25,499	30,512
2,5	6,909	12,083	17,279	22,441	27,600	32,700	37,826
5	13,759	19,060	24,384	29,688	34,987	40,266	45,506
7,5	20,517	26,005	31,506	37,047	42,514	48,008	53,538
10	27,113	32,864	38,591	44,465	50,263	55,994	61,846
12,5	33,501	39,585	45,587	51,882	58,035	64,120	70,363
15	39,636	46,118	52,439	59,243	65,818	72,322	79,022
17,5	45,469	52,693	59,096	66,489	73,547	80,533	87,755
20	50,953	58,417	65,500	74,874	81,159	88,686	96,484

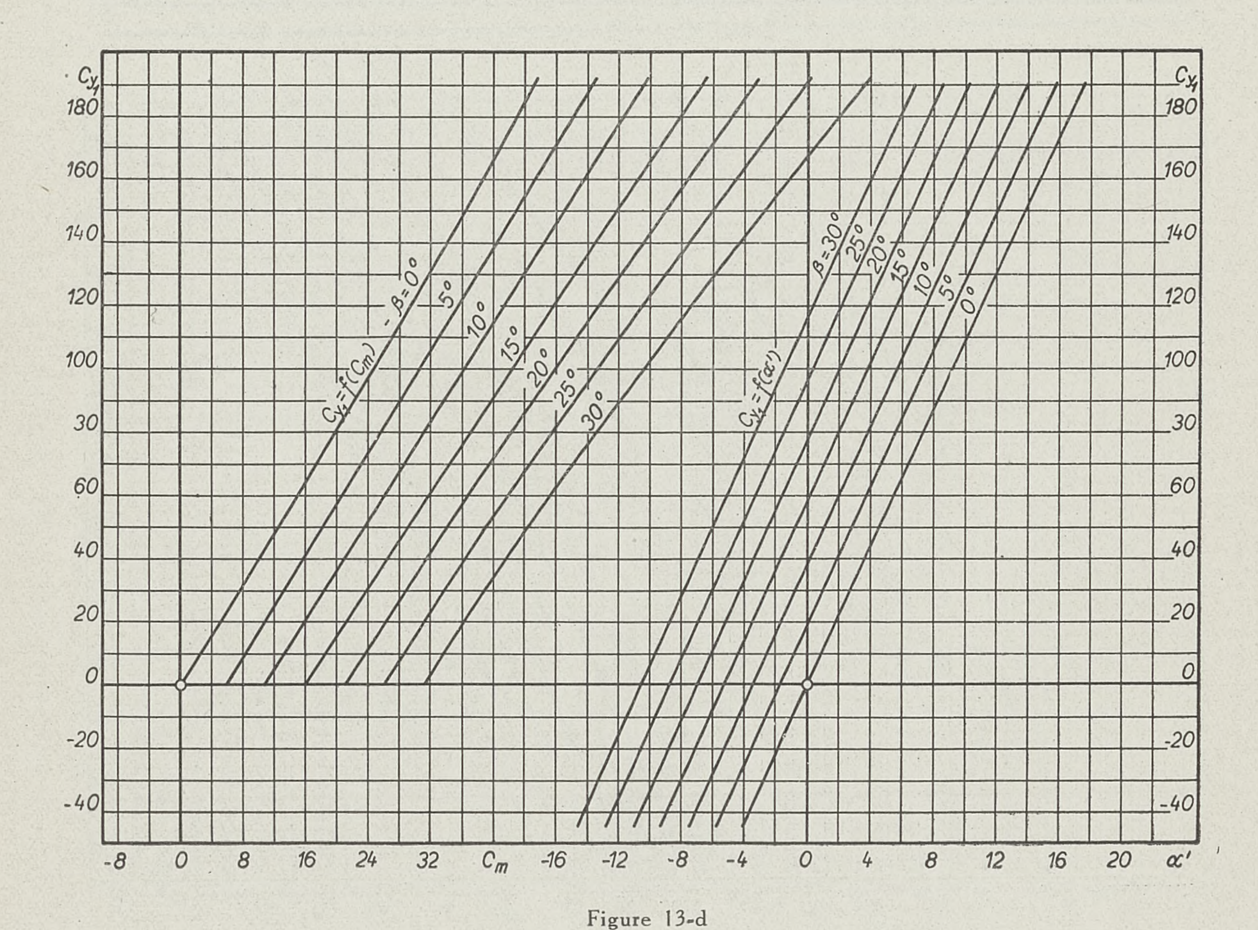


Figure 13-d

Characteristics of the Bi-Linear Profile, Joukovsky Potential.

$$\frac{l_2}{L} = 40\%$$

Table VIII-e

α	$\frac{l_2}{L} = 50\%$ C_m						
	β = 0°	β = 5°	β = 10°	β = 15°	β = 20°	β = 25°	β = 30°
0	0	4,365	8,723	13,098	17,510	21,855	26,275
2,5	6,909	11,319	15,794	20,140	24,593	28,991	33,489
5	13,759	18,267	22,818	27,337	31,903	36,426	41,074
7,5	20,517	25,188	29,939	34,759	39,382	44,098	48,969
10	27,113	32,017	37,036	41,973	46,971	51,950	57,114
12,5	33,501	38,706	44,055	49,300	54,613	59,920	65,446
15	39,636	45,195	50,943	56,557	62,247	67,947	73,898
17,5	45,469	51,452	57,644	63,827	69,815	75,967	82,400
20	50,953	57,410	64,106	70,632	77,253	83,911	90,884

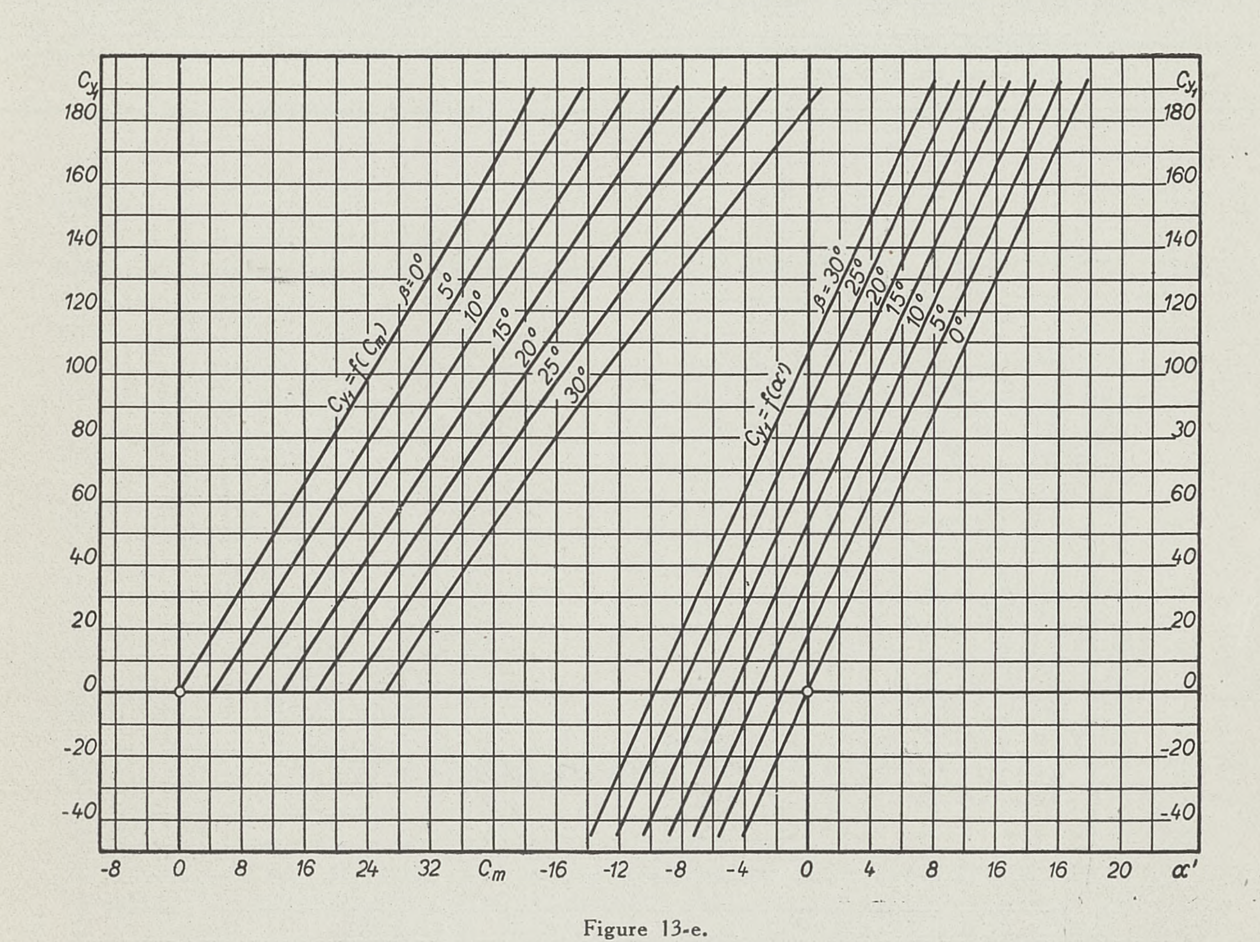


Figure 13-e.

Characteristics of the Bi-Linear Profile, Joukovsky Potential.

$$\frac{l_2}{L} = 50\%.$$

Table IX-a

$\frac{l_2}{L} = 10\%$																	
α			$\beta = 0^0$		$\beta = 5^0$		$\beta = 10^0$		$\beta = 15^0$		$\beta = 20^0$		$\beta = 25^0$		$\beta = 30^0$	
	C_{y_1}	C_{x_1}	C_m	C_{mf}	C_m	C_{mf}	C_m	C_{mf}	C_m	C_{mf}	C_m	C_{mf}	C_m	C_{mf}	C_m	C_{mf}
0	0	0	0	0	4,706	0,06478	9,384	0,12708	14,052	0,18855	18,678	0,24597	23,238	0,29772	27,718	0,33905
2,5	17,505	0,088	3,135	— 0,02275	7,861	0,04202	12,544	0,10429	17,240	0,16585	21,904	0,22333	26,504	0,27499	31,030	0,31432
5	34,977	0,352	6,253	— 0,04538	10,977	0,01926	15,683	0,08125	20,439	0,14276	25,084	0,19992	29,716	0,24999	34,276	0,28846
7,5	52,382	0,785	9,355	— 0,06763	14,055	— 0,00338	18,791	0,05809	23,507	0,11930	28,214	0,17615	32,866	0,22663	37,452	0,26208
10	69,686	1,380	12,414	— 0,08950	17,089	— 0,02589	21,867	0,03493	26,579	0,09550	31,292	0,15199	35,953	0,20113	40,552	0,23508
12,5	86,857	2,127	15,421	— 0,11050	20,076	— 0,04777	24,905	0,01214	29,601	0,07176	34,309	0,12758	38,971	0,17525	43,574	0,20782
15	103,864	3,009	18,362	— 0,13075	23,005	— 0,06903	27,898	— 0,01039	32,571	0,04817	37,267	0,10333	41,918	0,14899	46,514	0,18043
17,5	120,675	4,010	21,220	— 0,15000	25,869	— 0,08966	30,829	— 0,03230	35,478	0,02496	40,150	0,07927	44,784	0,12260	49,341	0,15304
20	137,252	5,111	23,978	— 0,16813	28,662	— 0,10929	33,707	— 0,05484	38,302	0,00226	42,951	0,05561	47,559	0,09646	51,859	0,12603

Note: C_{y_1} and C_{x_1} are the same for all profiles.

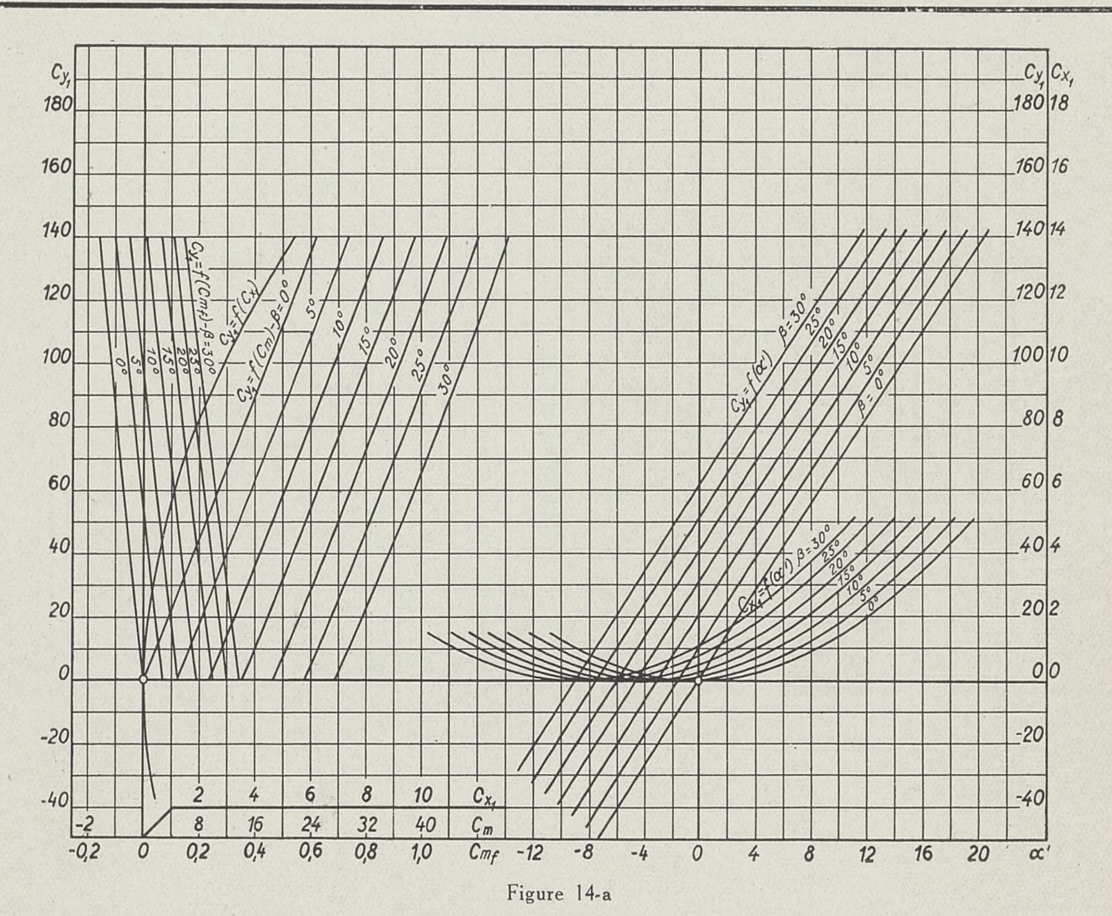


Figure 14-a

Characteristics of the Bi-Linear Profile, Discontinuous Potential.

$$\frac{l_2}{L} = 10\%$$

Table IX-b

α	$\frac{l_2}{L} = 20\%$													
	$\beta = 0^0$		$\beta = 5^0$		$\beta = 10^0$		$\beta = 15^0$		$\beta = 20^0$		$\beta = 25^0$		$\beta = 30^0$	
	C_m	C_{mf}	C_m	C_{mf}	C_m	C_{mf}	C_m	C_{mf}	C_m	C_{mf}	C_m	C_{mf}	C_m	C_{mf}
0	0	0	5,585	0,22568	11,035	0,44847	16,674	0,66242	22,148	0,86530	27,544	1,03780	32,855	1,21950
2,5	3,135	—0,06000	8,738	0,16576	14,320	0,38866	19,872	0,60266	25,412	0,80625	30,875	0,97690	36,273	1,16270
5	6,253	—0,11950	11,877	0,10533	17,464	0,32761	23,034	0,53510	27,649	0,74416	34,172	0,91629	39,622	1,10130
7,5	9,355	—0,17813	14,993	0,04516	20,575	0,26567	26,153	0,47760	31,792	0,67980	37,356	0,85250	42,897	1,03600
10	12,414	—0,23525	18,295	—0,01439	23,646	0,20348	29,223	0,41318	34,892	0,61341	40,492	0,78611	49,090	0,96712
12,5	15,421	—0,29075	21,131	—0,07293	26,672	0,14167	32,236	0,34813	37,932	0,54551	43,552	0,71750	49,194	0,89530
15	18,362	—0,34400	24,137	—0,12998	29,644	0,08024	35,187	0,28236	40,895	0,47659	46,517	0,64720	52,205	0,82104
17,5	21,220	—0,39463	27,084	—0,18515	32,551	0,01993	38,065	0,21817	43,776	0,40730	49,415	0,57580	54,950	0,74486
20	23,978	—0,44225	29,959	—0,23794	35,378	—0,03874	40,856	0,15425	46,563	0,33813	52,197	0,50370	57,928	0,66727

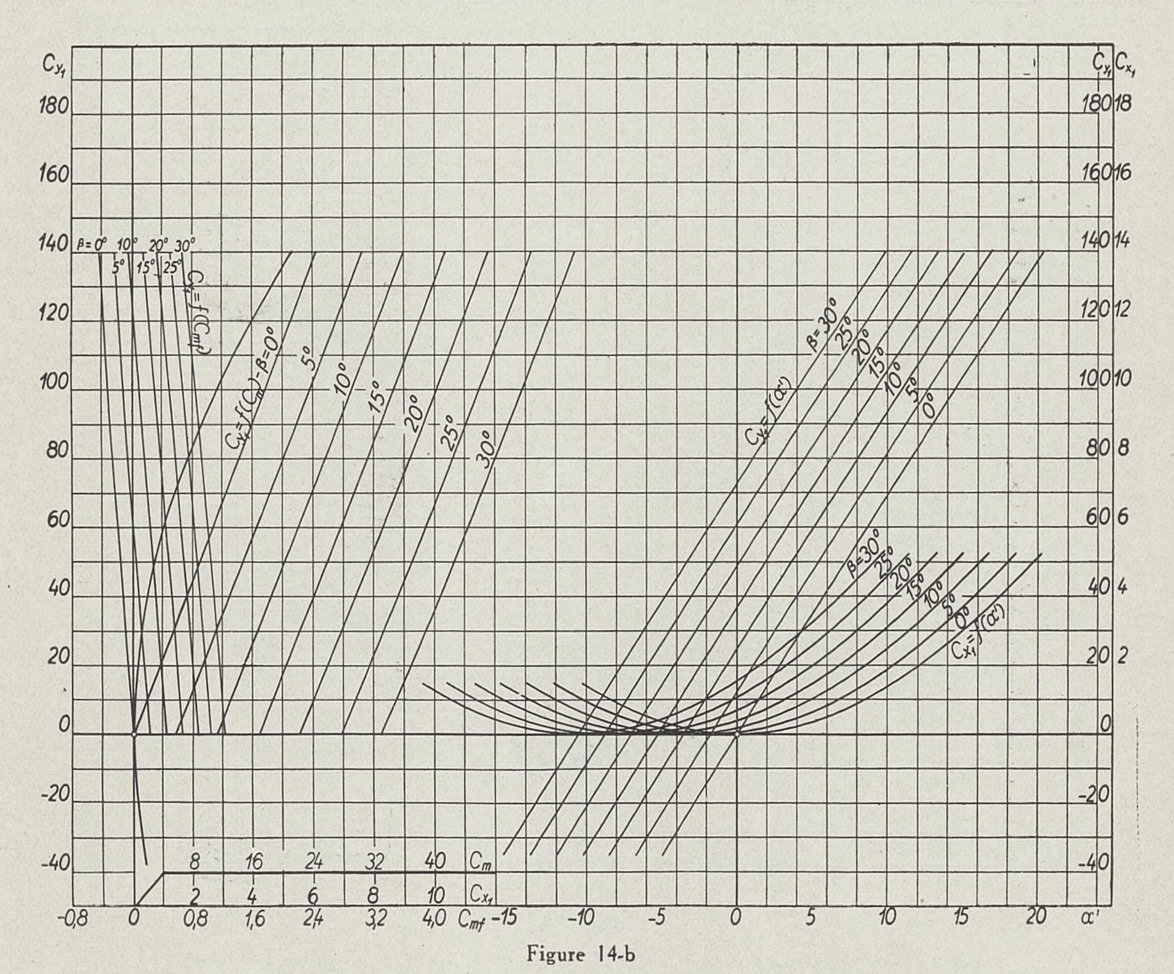


Figure 14-b

Characteristics of the Bi-Linear Profile, Discontinuous Potential.

$$\frac{l_2}{L} = 20\%$$

Table IX-c

$\frac{l_2}{L} = 30\%$														
α	$\beta = 0^0$		$\beta = 5^0$		$\beta = 10^0$		$\beta = 15^0$		$\beta = 20^0$		$\beta = 25^0$		$\beta = 30^0$	
	C_m	C_{mf}	C_m	C_{mf}	C_m	C_{mf}	C_m	C_{mf}	C_m	C_{mf}	C_m	C_{mf}	C_m	C_{mf}
0	0	0	5,598	0,43206	11,177	0,85889	16,726	1,27240	22,234	1,67200	27,679	2,0442	33,044	2,3896
2,5	3,135	—0,07650	8,745	0,35485	14,349	0,78172	19,939	1,20170	25,507	1,59620	31,252	1,9704	36,616	2,3162
5	6,253	—0,15238	11,874	0,27653	17,498	0,70192	23,121	1,12700	28,740	1,51580	34,717	1,8878	39,879	2,2333
7,5	9,355	—0,22700	14,979	0,19757	20,613	0,62035	26,261	1,04840	31,925	1,43170	38,064	1,7975	43,203	2,1419
10	12,414	—0,30000	18,053	0,11849	23,689	0,53716	29,354	0,96685	35,054	1,34400	41,283	1,6998	46,454	2,0423
12,5	15,421	—0,37075	21,084	0,04017	26,530	0,45335	32,390	0,88290	38,115	1,25360	44,365	1,5956	49,621	1,9357
15	18,362	—0,43863	24,061	—0,03704	29,682	0,36940	35,360	0,79718	41,105	1,16140	47,303	1,4860	51,971	1,8227
17,5	21,220	—0,50373	26,975	—0,11261	32,579	0,28609	38,253	0,71046	44,010	1,06800	50,087	1,3713	55,660	1,7040
20	23,978	—0,56388	29,805	—0,18569	35,389	0,20377	41,053	0,62297	46,820	0,97770	52,704	1,2528	58,339	1,5807

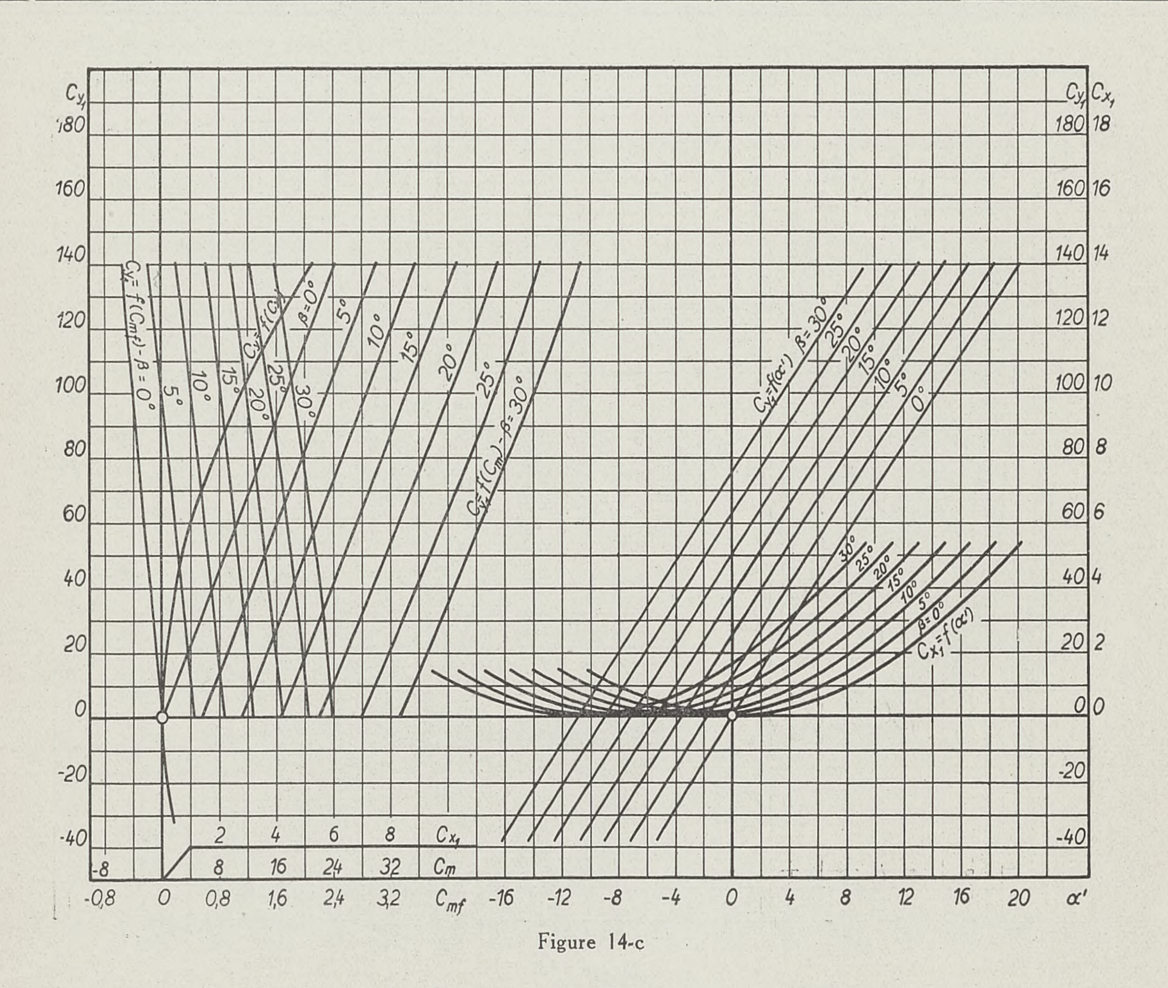


Figure 14-c

Characteristics of the Bi-Linear Profile, Discontinuous Potential.

$$\frac{l_2}{L} = 30\%$$

Table IX-d.

α	$\frac{l_2}{L} = 40\%$													
	β = 0°		β = 5°		β = 10°		β = 15°		β = 20°		β = 25°		β = 30°	
	C_m	C_{mf}	C_m	C_{mf}	C_m	C_{mf}	C_m	C_{mf}	C_m	C_{mf}	C_m	C_{mf}	C_m	C_{mf}
0	0	0	5,128	0,63589	10,251	1,26570	15,369	1,8798	20,453	2,4796	25,504	3,0413	30,512	3,5990
2,5	3,135	— 0,04650	8,268	0,58871	13,415	1,21770	18,573	1,8308	23,708	2,4309	28,818	2,9910	33,927	3,5525
5	6,253	— 0,09263	11,396	0,53539	16,561	1,16550	21,711	1,7755	26,936	2,3734	32,126	2,9296	37,284	3,4928
7,5	9,355	— 0,13813	14,498	0,48849	19,677	1,10950	24,902	1,7139	30,124	2,3077	35,337	2,8575	39,476	3,4202
10	12,414	— 0,18250	17,564	0,93631	22,721	1,05010	28,006	1,6470	33,263	2,2342	38,521	2,7756	43,863	3,3353
12,5	15,421	— 0,22550	20,584	0,38301	25,779	0,98774	31,053	1,5749	36,342	2,1534	41,639	2,6841	47,057	3,2387
15	18,362	— 0,26675	23,544	0,32920	28,743	0,92322	34,036	1,4984	39,353	2,0662	44,683	2,5841	50,162	3,1312
17,5	21,220	— 0,30600	26,432	0,27528	31,631	0,85643	36,983	1,4179	42,279	1,9729	47,627	2,4761	53,165	3,0135
20	23,978	— 0,34288	29,229	0,22185	34,428	0,78839	39,749	1,3342	45,111	1,8616	50,326	2,3610	56,025	2,8867

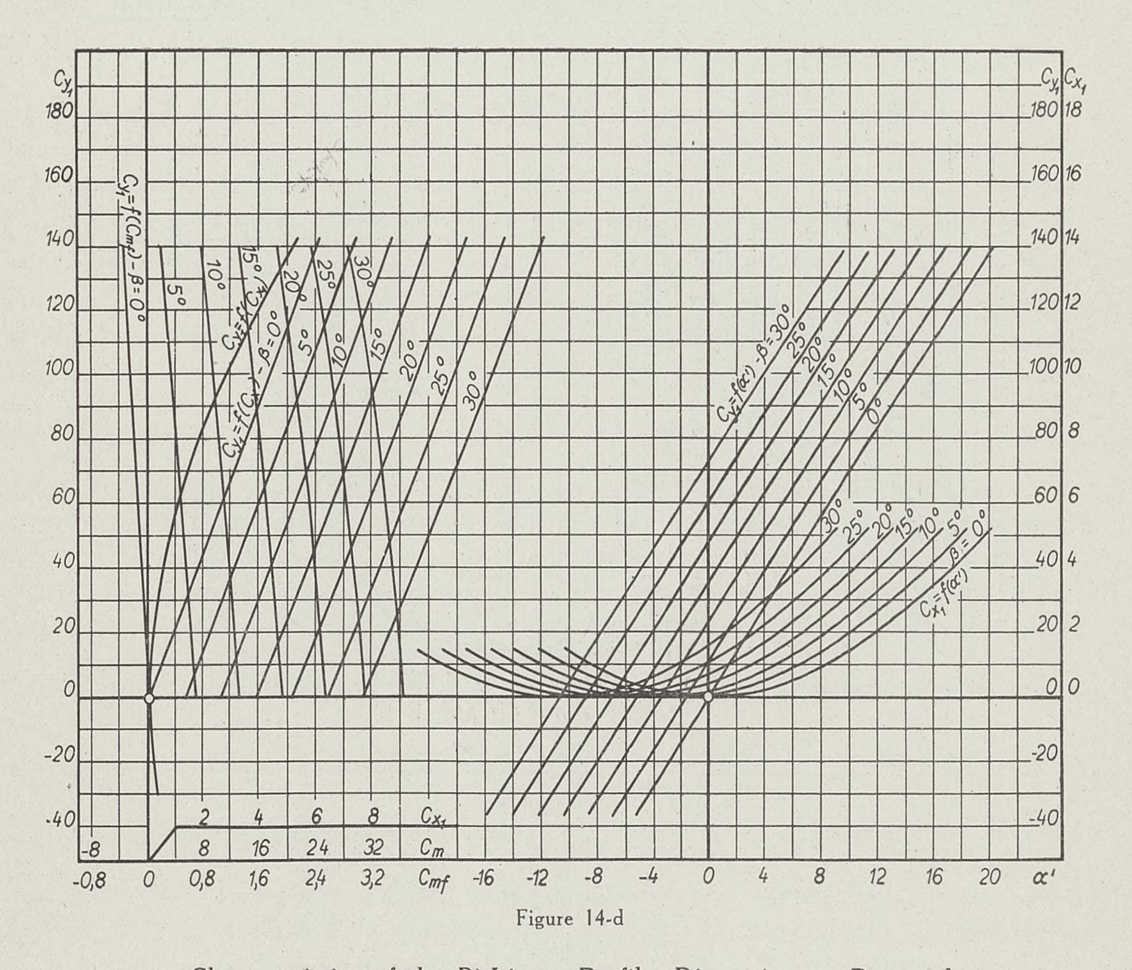


Figure 14-d

Characteristics of the Bi-Linear Profile, Discontinuous Potential.

$$\frac{l_2}{L} = 40\%$$

Table IX-e

	$\frac{l_2}{L} = 50\%$													
α	$\beta = 0^0$		$\beta = 5^0$		$\beta = 10^0$		$\beta = 15^0$		$\beta = 20^0$		$\beta = 25^0$		$\beta = 30^0$	
	C_m	C_{mf}	C_m	C_{mf}	C_m	C_{mf}	C_m	C_{mf}	C_m	C_{mf}	C_m	C_{mf}	C_m	C_{mf}
0	0	0	4,364	0,79125	8,723	1,5843	13,098	2,3619	17,483	3,1111	21,858	3,8799	26,273	4,6031
2,5	3,135	0,05688	7,497	0,84656	11,895	1,6389	16,287	2,4146	20,705	3,1617	25,128	3,9293	29,618	4,6504
5	6,253	0,11338	10,628	0,89861	15,044	1,6877	19,462	2,4589	23,912	3,2013	28,383	3,9647	32,964	4,6811
7,5	9,355	0,16900	13,727	0,94717	18,132	1,7304	22,610	2,4945	27,091	3,2298	31,610	3,9847	36,246	4,6949
10	12,414	0,22338	16,787	0,99159	21,262	1,7667	25,719	2,5209	30,231	3,2470	34,796	3,9931	39,503	4,6915
12,5	15,421	0,27600	19,796	1,03176	24,299	1,7963	28,776	2,5382	33,319	3,2524	37,928	3,9859	42,704	4,6713
15	18,362	0,32650	22,739	1,06730	27,273	1,8191	31,768	2,5462	36,340	3,2463	40,995	3,9643	45,839	4,6342
17,5	21,220	0,37450	25,662	1,09796	30,166	1,8348	34,735	2,5449	39,284	3,2288	43,969	3,9287	48,880	4,5805
20	23,978	0,41975	28,367	1,12349	32,962	1,8432	37,500	2,5342	42,133	3,1999	46,729	3,8791	51,702	4,5107

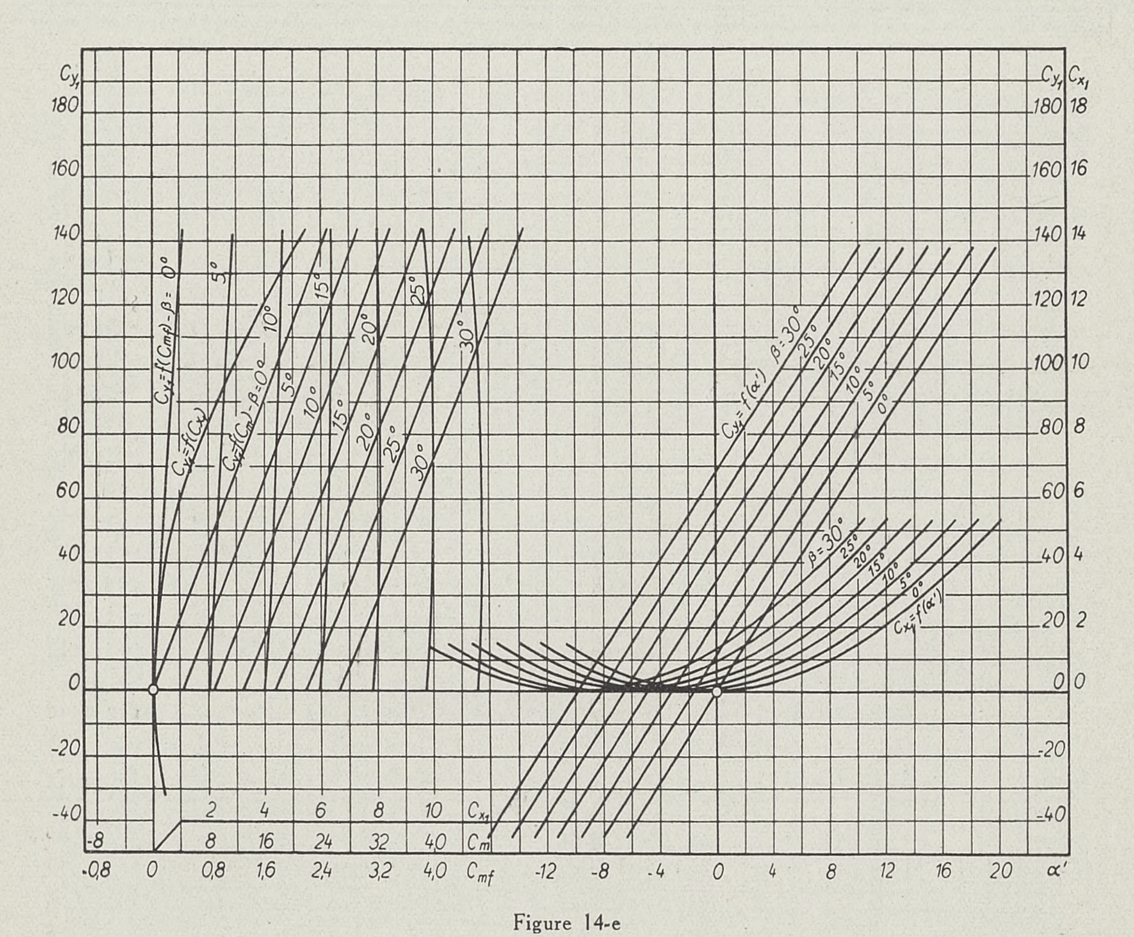


Figure 14-e

Characteristics of the Bi-Linear Profile, Discontinuous Potential.

$\frac{l_2}{L} = 50\%$

value of β are numerically the same as those for the same profile with the values of β and α' reversed in sign. The sign of C_{y_1} must also be changed but C_{x_1}, C_m, and C_{mf} remain the same as with the positive value of β. This means that in order to obtain the lift and drag curves for the new profile, it is simply necessary to change the sign of the angle of zero lift and displace the curves so that they remain parallel to their original positions. The curves of moment plotted against the lift are obtained by reflecting the original ones in the moment axis.

In case the flap-chord ratio is greater than 50%, the work is more difficult and the only satisfactory way to obtain the desired results is to calculate the various coefficients by using the original formulas. However, such values of this ratio are of little importance in practice so that it has not been considered worth while to make these computations at this time.

From the results shown in Figures 13 and 14, it is now possible to draw some conclusions concerning the behaviour of the characteristics of the bi-linear profile as the flap angle or flap-chord ratio is changed. It should be remembered, of course, that the theoretical results apply only in the range of values of the angle of attack below the burble point, where the lift curve is actually very close to a straight line. Since the coefficients, $\frac{K'_1}{L/2a}$ and $\frac{K'_3}{L/2a}$ in formulas (52) and (53) respectively, have been taken as constants, the curves representing the lift and drag coefficients as functions of the angle of attack, based on the discontinuous potential, are all parallel, the only quantity which changes with β and $\frac{l_2}{L}$ being the angle of zero lift. In the range where α is small, the lift curves are approximately straight lines while the drag curves are parabolas having their vertices on the α' axis at the point where the lift is zero. Thus from the standpoint of the lift and drag, the bi-linear profiles are all of equal merit with their polar curves all coinciding, the only difference between them being in their positions relative to the direction of the air stream.

A discussion of the moment coefficients obtained by means of the discontinuous potential is somewhat more difficult because of the greater complexity of the formulas (54) and (55). However the numerical results when plotted show that the curves of C_m plotted against C_{y_1} are very close to being straight lines of constant slope, $\frac{C_m}{C_{y_1}} = 0{,}1792$ (average value). Furthermore for a given value of the flap-chord ratio, the moment seems to increase uniformly with β for a given value of the lift. A somewhat similar situation exists in connection with the hinge moment calculated by the discontinuous potential, although the curves of C_{mf} plotted against C_{y_1} vary appreciably from straight lines and also are by no means all parallel. However a rough idea of the effect of the flap-chord ratio can be obtained by plotting the average values of $\frac{C_m}{\beta}$ and $\frac{C_{mf}}{\beta}$ for $C_{y_1} = 0$ as functions of $\frac{l_2}{L}$. Such curves are shown in Figure 15 with the corresponding numerical values in Table X. It thus appears that for the values of $\frac{l_2}{L}$ between 10% and 50%, the total moment varies but little. The hinge moment however mounts very rapidly with the flap-chord ratio and since it is desired to maintain this quantity at a minimum, it is advisable to use as small a value of $\frac{l_2}{L}$ as possible. Thus from this standpoint a flap-chord ratio of 10% would be better than one of 30% or 50% since it gives practically the same drag and total moment with a given lift and a considerably smaller hinge moment.

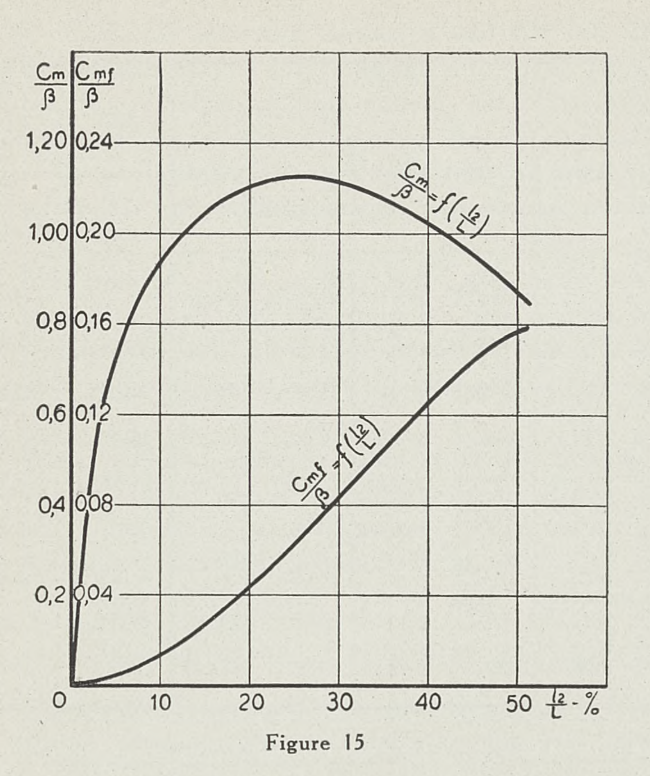


Figure 15

Table X

$\frac{l_2}{L}$ — %	$\frac{C_m}{\beta}$	$\frac{C_{mf}}{\beta}$
0	0	0
10	0,9345	0,01228
20	1,1062	0,04324
30	1,1122	0,08369
40	1,0226	0,12418
50	0,8738	0,15639

With the Joukovsky potential, the results obtained for the lift and total moment are qualitatively of the same nature as those obtained by means of the discontinuous potential. The slope of the lift curves is of course higher for the Joukovsky potential because of its larger circulation, but the angle of zero lift which depends only on the transformation function and not on the potential of the flow, is always the same for a given profile. The values of the total moment at the zero lift position are the same for both potentials, but the ratio of C_m to C_{y_1} in the case of the Joukovsky potential is somewhat higher than that obtained with the discontinuous potential, its average value being about 0,25.

It is interesting to compare the results based on the Joukovsky potential, obtained by what may be called an exact method, with those obtained by the approximate method employed by Glauert [1]). Using the notations and system of coefficients employed above, Glauert's formulas for the lift and total moment coefficients of the bi-linear profile may be written as follows:

$$C_{y_1} = 200a_1 \left(\alpha_s' + \frac{a_2}{a_1}\beta\right),$$

$$C_m = 0{,}25C_y + 200m\beta,$$

where a_1, a_2, and m are parameters which depend on the flap-chord ratio of the profile. If the lift coefficient is assumed to be a linear function of the angle of attack, and $\frac{C_m}{\beta}$ for $C_{y_1} = 0$ is taken as constant for a given flap-chord ratio, then the first of these expressions is correct in form, but the actual values of the parameters must be compared with those obtained by the exact method before a definite conclusion can be made as to their accuracy. Now the formula (52) may be written, with a very close approximation for small values of the angle of position α, in the form:

$$C_{y_1} = 100\frac{K_1}{L/2a}\alpha$$

[1]) *H. Glauert*: loc. cit. (reference 2, pg. 2).

or in terms of the angle of attack measured from the stationary part of the profile,

$$C_{y_1} = 100 \frac{K_1}{L/2a} (\alpha'_s - \alpha'_{s_0}) .$$

In the exact method the coefficient $100 \frac{K_1}{L/2a}$ was found to have an avarage value of $200{,}924\pi$ and since the value of a_1 obtained by Glauert (for infinite aspect ratio) is π, the values of the slope of the lift curves may be said to be in very good agreement. It has already been pointed out that the angle α'_{s_0} is practically a linear function of β for a given flap-chord ratio in the range here considered, so that it is permissible to write

$$\alpha'_{s_0} = -\frac{a_2}{a_1}\beta$$

from which

$$\frac{a_2}{a_1} = -\frac{\alpha'_{s_0}}{\beta}$$

The quantity $-\frac{\alpha'_{s_0}}{\beta}$ is approximately equal to the slope of the curves of α'_{s_0} plotted as a function of β in Figure 10. For the purpose of comparison with the values of $\frac{a_2}{a_1}$ obtained by Glauert, the value of $-\frac{\alpha'_{s_0}}{\beta}$ at $\beta = 15^0$ for the different flap-chord ratios was considered as the average. The values of this ratio as obtained by the two methods are given in Table XI. Here again the agreement is excellent and consequently it is permissable to conclude that in the case of the lift coefficient as calculated by the Joukovsky potential, Glauert's method is entirely satisfactory.

Table XI

$\frac{l_2}{L}$	$-\frac{\alpha'_{s_0}}{\beta}$ Exact	Glauert
0	0	0
10	0,393	0,396
20	0,548	0,550
30	0,658	0,660
40	0,745	0,746
50	0,817	0,818

A comparison of the exact and approximate formulas for the total moment coefficient is somewhat more difficult than in the case of the lift because of the more complicated expression obtained by the exact method and also because the calculated values given in Table VIII do not immediately justify the assumption that the moment coefficient may be written in the form employed by Glauert. For this reason the actual values of C_m were calculated by means of the approximate method for the families of profiles having flap-chord ratios of 30% and of 50% and are compared with the exact values in Table XII. It should be noted that for these values the angle of attack has been measured from the chord instead of the fixed part

Table XII

$\frac{l_2}{L} = 30\%$

α'	$\beta = 0^0$ C_{mG}	C_{mE}	ε	$\beta = 10^0$ C_{mG}	C_{mE}	ε	$\beta = 20^0$ C_{mG}	C_{mE}	ε	$\beta = 30^0$ C_{mG}	C_{mE}	ε
—10	—27,41	—27,11	—1,10	— 6,32	—	—	15,01	14,95	—0,40	36,78	35,90	—2,45
— 5	—13,71	—13,76	+0,36	+ 7,38	—	—	28,71	28,60	—0,39	50,48	51,10	+1,21
0	0	0	0	21,09	21,25	0,75	42,42	43,70	+0,64	64,19	67,70	5,18
+ 5	+13,71	+13,76	0,36	34,81	35,55	2,08	56,12	59,15	5,13	77,89	85,30	8,67
10	27,41	27,11	—1,10	48,52	49,75	2,47	69,83	74,85	6,72	91,60	—	—
15	41,10	39,64	—3,68	62,19	63,35	1,83	83,53	—	—	105,30	—	—
20	54,80	50,95	—5,59	75,90	—	—	97,24	—	—	119,01	—	—

Table XII (contd).

α'	$\frac{l_2}{L} = 50\%$											
	$\beta = 0^0$			$\beta = 10^0$			$\beta = 20^0$			$\beta = 30^0$		
	C_{mG}	C_{mE}	ε	C_{mG}	C_{mE}	ε	C_{mG}	C_{mE}	ε	C_{mG}	C_{mE}	ε
—10	—27,41	—27,11	—1,10	—10,45	—	—	—7,90	—	—	26,35	25,40	—3,74
—5	—13,71	—13,76	+0,36	+3,75	3,55	—5,63	21,60	21,30	—1,41	40,05	40,20	+0,37
0	0	0	0	18,50	17,65	—4,81	35,30	36,30	+2,76	53,75	56,25	4,44
+5	+13,71	+13,76	0,36	31,20	31,90	+2,20	49,00	51,30	4,49	67,45	73,10	7,73
10	27,41	27,11	—1,10	44,93	45,90	2,10	62,71	66,50	5,70	81,18	—	—
15	41,10	39,64	—3,68	58,65	59,40	1,26	66,42	—	—	94,90	—	—
20	54,80	50,95	—5,59	72,35	—	—	103,80	—	—	108,62	—	—

$C_{mG} = C_m$ calculated by Glauert's approximate method.
$C_{mE} = C_m$ calculated by exact method.
ε = error in per cent in value obtained by approximate method.

of the profile. It is thus seen that in some cases for a fairly small angle of attack, the error in the approximate method may be as high as 8% or 9% but since such values are obtained for fairly large flap angles, it is still possible to say that for practical purposes, this approximate method gives reasonably good results.

Inasmuch as the numerical values of the hinge moment have not been calculated by the exact method, no statement can be made at present concerning the accuracy of Glauert's formula for this quantity.

B. Comparison with Experimental Results.

The most satisfactory method for checking the theoretical results obtained above would of course be a comparison with a systematic series of tests on symmetric profiles having the flap-chord ratios and flap angles for which the theoretical results were calculated. Inasmuch as such experimental data of this kind as does exist is of a rather limited nature, a few experiments were made on a series of rectangular metal plates 10 cm. by 50 cm., of 2 millimeters thickness, and with a rounded leading edge and a sharp trailing edge. By bending the rear portion of such a plate along a line parallel to the trailing edge, a form resembling the bi-linear profile was obtained. Tests were made on these plates in the wind tunnel for flap-chord ratios of 15%, 30%, and 40%, and in each case for flap angles of 0°, 10°, 20°, and 30°, the lift, drag, and total moment coefficients being determined as functions of the angle of attack measured from the center line of the fixed part of the profile. The results of these tests are shown in Figure 16 and in Table XIII. These values have been corrected for wall interference of the wind tunnel by Prandtl's theory [1]).

[1]) See *E. Carafoli:* "Aérodynamique des Ailes d'Avion", (E. Chiron, Paris, 1928), Chap. IV, pgs. 103—04.

Table XIII

$\frac{l_2}{L} = 15\%$

β = 0°				β = 10°				β = 20°				β = 30°			
α'_s	C_{y_1}	C_{x_1}	C_m	α'_s	C_{y_1}	C_{x_1}	C_m	α'_s	C_{y_1}	C_{x_1}	C_m	α'_s	C_{y_1}	C_{x_1}	C_m
−4,8	−35,82	4,25	− 9,80	−9,8	−43,72	10,31	− 9,22	−9,8	−44,08	11,85	− 6,75	−9,8	−40,24	10,46	− 7,82
−2,4	−16,30	2,12	− 5,07	−7,4	−23,52	6,05	− 0,14	−7,4	−20,12	7,15	+ 5,24	−7,5	−10,96	6,37	+ 7,98
0	− 0,18	1,68	− 0,94	−5,0	− 2,42	3,36	+ 7,38	−5,0	+ 1,54	4,41	11,07	−5,1	+12,88	4,42	15,46
+2,4	+20,82	2,27	+ 4,69	−2,6	+19,00	2,40	10,68	−2,6	25,94	3,52	18,10	−2,7	37,32	4,28	24,27
4,8	36,82	4,57	8,13	−0,2	40,00	3,22	18,47	−0,2	44,26	4,50	21,46	−0,3	55,72	5,71	28,25
7,3	54,18	8,42	14,32	+2,2	56,40	5,06	23,98	+2,2	62,48	6,78	25,63	+2,1	75,56	8,51	33,19
9,7	64,02	12,69	20,28	4,7	72,56	8,44	26,87	4,6	78,84	10,44	28,36	4,6	91,92	12,58	37,87
12,2	67,86	16,75	23,60	7,1	85,10	12,97	32,41	7,1	91,46	15,10	33,61	7,0	102,99	17,69	42,62
14,7	70,28	20,62	25,44	9,6	89,82	17,99	36,96	9,6	94,98	20,28	36,88	9,5	103,66	22,98	45,68
17,2	71,86	24,99	26,99	12,1	89,72	22,65	38,23	12,1	94,30	25,28	39,05	12,1	99,80	27,29	47,06
19,7	70,18	27,68	28,36	14,6	88,24	26,74	38,24	14,6	91,18	29,15	40,24	14,6	97,76	31,62	45,25
22,2	69,80	29,96	27,93												

Note: The characteristics for β = 0° are the same for all flap-chord ratios.

$\frac{l_2}{L} = 30\%$

β = 10°				β = 20°				β = 30°			
α'_s	C_{y_1}	C_{x_1}	C_m	α'_s	C_{y_1}	C_{x_1}	C_m	α'_s	C_{y_1}	C_{x_1}	C_m
− 9,9	− 31,52	7,47	− 3,13	−14,9	− 18,80	9,43	2,10	−14,9	− 30,22	13,85	− 3,43
− 7,5	− 7,90	3,45	+ 6,92	−12,5	− 7,04	7,22	8,39	−12,4	− 17,00	11,63	+ 2,86
− 5,1	+ 12,34	1,86	11,38	−10,1	+ 14,60	4,55	19,35	−10,0	+ 5,64	9,27	13,60
− 2,6	28,04	1,92	15,48	− 7,7	37,52	2,86	26,98	− 7,7	35,92	7,69	25,61
− 0,2	43,88	2,87	18,81	− 5,2	51,50	3,44	29,45	− 5,3	64,60	8,03	30,07
+ 2,2	59,34	5,20	22,92	− 2,8	64,50	4,71	31,70	− 2,9	90,20	9,75	44,56
4,7	75,22	8,72	26,61	− 0,4	78,40	7,10	33,60	− 0,5	101,56	12,86	43,38
7,1	87,00	13,37	30,73	+ 2,1	91,84	10,47	35,65	+ 2,0	113,14	16,77	48,60
9,6	90,36	18,23	35,95	4,5	103,28	14,80	38,27	4,5	122,00	21,62	49,15
12,1	89,60	23,03	37,68	7,0	105,74	20,22	42,02	7,0	117,22	27,86	50,03
14,6	88,38	27,36	37,79	9,6	99,70	25,69	42,75	9,5	106,86	32,47	48,98
17,1	88,18	31,44	37,76	12,1	95,60	29,31	41,85	12,0	103,58	36,70	47,33
19,6	88,54	35,90	37,52					14,5	104,62	41,53	48,25
22,1	86,44	39,58	38,84					17,0	105,18	47,13	48,77
								19,5	103,16	51,03	50,10

$\frac{l_2}{L} = 40\%$

β = 10°				β = 20°				β = 30°			
α'_s	C_{y_1}	C_{x_1}	C_m	α'_s	C_{y_1}	C_{x_1}	C_m	α'_s	C_{y_1}	C_{x_1}	C_m
−12,4	−32,08	9,04	−5,54	−17,4	−15,88	9,86	1,34	−20,0	−4,26	9,94	7,55
−9,6	−16,94	6,21	+2,64	−15,0	−5,62	7,93	6,19	−17,5	+3,70	8,67	10,96
−7,5	+6,24	2,95	11,48	−12,5	+10,86	6,16	15,05	−15,1	19,84	7,30	18,71
−5,1	23,98	2,04	16,21	−10,2	34,92	4,40	27,30	−12,6	13,40	9,55	4,24
−2,7	39,00	2,60	18,34	−7,8	55,74	3,86	33,77	−10,2	40,40	8,23	27,83
−0,2	54,06	4,04	22,25	−5,3	69,28	4,82	36,28	−7,9	85,10	7,41	43,03
+2,2	69,00	6,57	25,26	−2,9	82,94	6,70	39,46	−5,4	95,00	9,48	44,70
4,6	83,62	10,24	29,70	−0,4	95,72	9,76	41,34	−3,0	104,92	12,44	45,70
7,1	92,34	15,38	33,80	+2,0	107,40	13,45	43,30	−0,5	114,60	16,07	46,90
9,6	93,36	20,68	37,14	4,5	115,30	18,36	45,08	+1,9	122,98	20,42	48,55
12,1	90,10	25,19	37,34	7,0	111,74	24,62	48,16	4,4	123,10	27,90	50,95
14,6	89,48	29,27	38,40	9,5	101,76	29,56	46,10	7,0	109,20	32,31	48,64

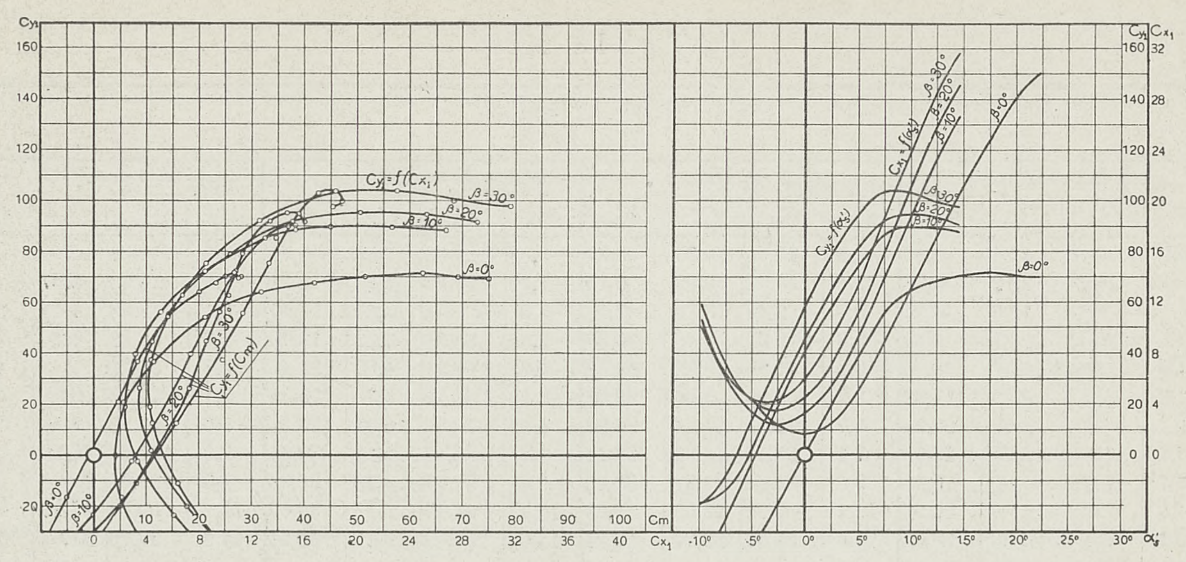


Figure 16-a, $\frac{l_2}{L} = 15\%$

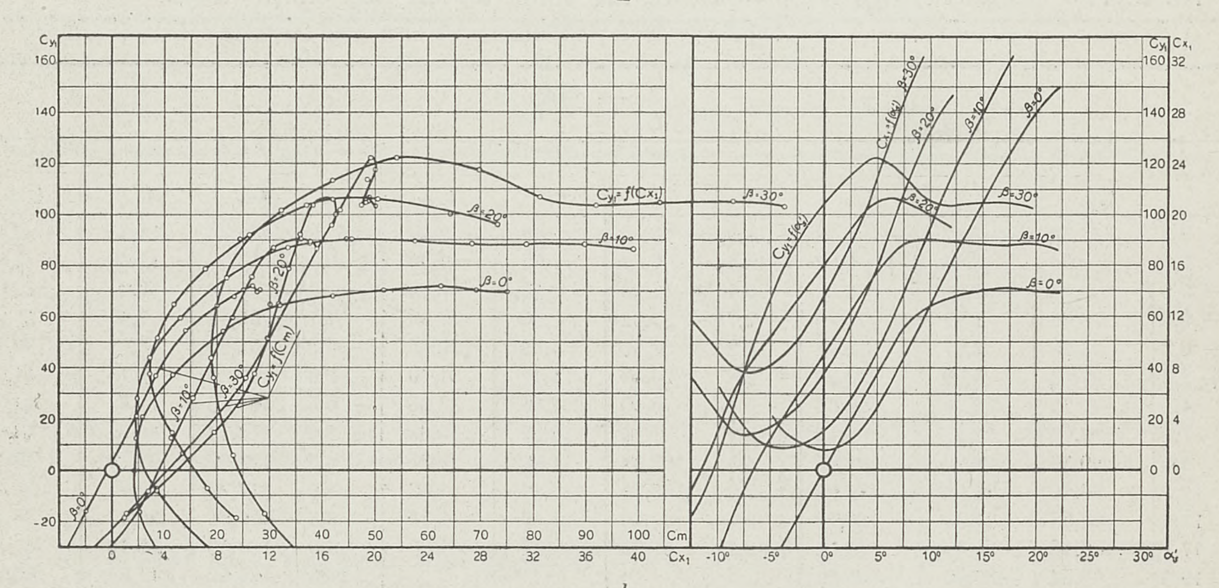


Figure 16-b, $\frac{l_2}{L} = 30\%$

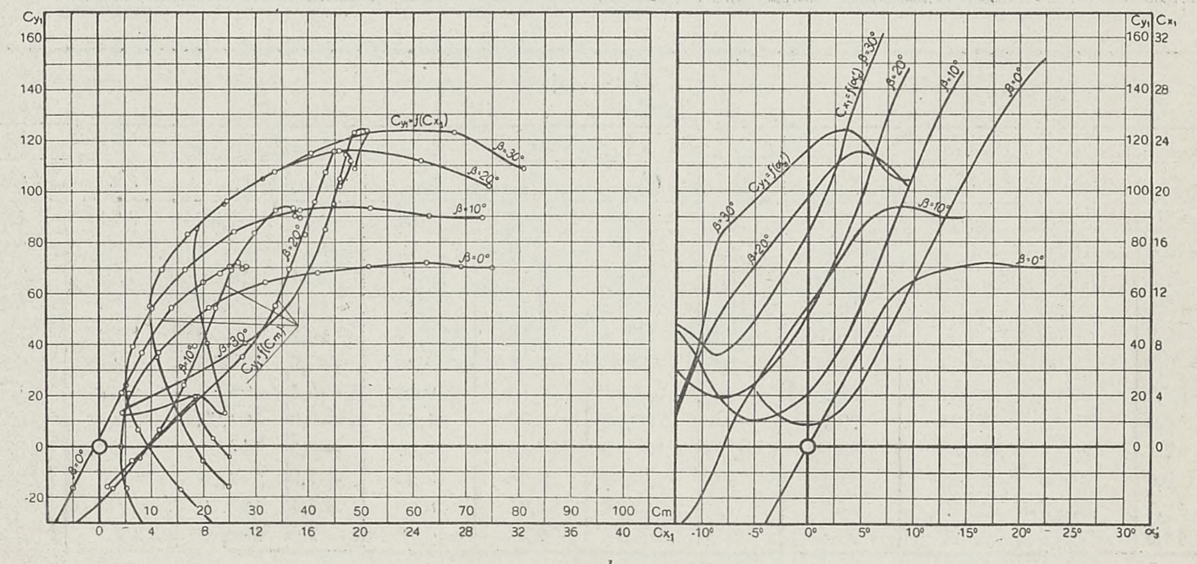


Figure 16-c, $\frac{l_2}{L} = 40\%$

Although these experimental results are for a finite aspect ratio, it is to be expected that the theoretical results for the lift and moment, which are for infinite aspect ratio, should at least be in qualitative agreement with the former values. It is seen at once that this is not the case for the range of flap angles studied. Except for small flap angles and flap-chord ratios, the lift curves are parallel straight lines for only a very limited range of values of the angle of attack. As the flap angle approaches 20^0, the slope of the lift curve experiences a sudden change at a small negative angle of attack, while for the larger flap-chord ratios, the curve beyond this point is quite irregular. A reasonable explanation of this strange behaviour of the lift coefficient seems to be that the phenomenon that takes place here is very similar to that which occurs when the maximum lift is reached. At certain high angles of attack the flow ceases to leave the rear of the wing smoothly at the trailing edge but breaks of at two points forming a wide turbulent wake behind the wing and causing irregular variations in its characteristics. With these bi-linear profiles a similar flow takes place at a small negative angle of attack, which is probably aggravated by the sharp change in contour at the hinge point. This phenomenon is what Witoszyński calls "double burbling" *(décollement double)* to distinguish it from the "single burbling" (*décollement simple*) represented by his potential function [1]). Furthermore at these negative angles of attack, it is possible that there may exist a region of "dead air" in the space directly under the hinge point which may cause an additional augmentation of these irregularities.

The moment coefficients when plotted as functions of the lift give curves which are even more irregular than those just discussed and although part of these irregularities may be due to inaccuracies in the shape of the model and to the lack of sufficient refinement in the running of the tests, it is believed that the curves above represent fairly accurately the profile characteristics under the different conditions. It is therefore necessary to conclude that expect for small flap angles, perhaps only as high as 15^0, the results of theory and experiment for the bi-linear profile are not even in good qualitative agreement.

Other experimenters have obtained similar results for profiles fitted with flaps and have explained the existing discrepancies between the theoretical and experimental values of the angle of zero lift in much the same way. For example Higgins and Jacobs [2]) in a series of tests on the N. A. C. A. M-6 airfoil, an asymmetric section fitted with a flap and ailerons, found that the theoretical values of this angle were quite different from those obtained by wind tunnel experiments, and in order to explain this difference, a photograph was made of the flow around this wing with the flap displaced and the wing set at the theoretical angle of zero lift. This photograph shows clearly that there is a "double burbling" in the rear of the wing instead of the potential flow assumed in the theory.

In the work of Glauert's referred to above [3]), he compares his theoretical results, based on the Joukovsky and Prandtl theories, with a series of experiments [4]) made by the British Advisory Committee for Aeronautics and concludes that the agreement between the two is quite good. These tests were made on both full scale and model airplanes, the R. E. 8, S. E. 5A, and S. E. 5C, fitted with tail planes of different flap-chord ratios and flap angles, but since the theoretical results are for the tail plane alone and no

---

[1]) C. *Witoszyński*: "La Mécanique des Profils d'Aviation", (E. Chiron, Paris, 1924). Chaps. 8 and 11

[2]) *George J. Higgins & Eastman N. Jacobs*: "The Effect of a Flap and Ailerons on the N. A. C. A. M-6 Airfoil Section", (U. S. National Advisory Committee for Aeronautics, Report No. 260, 1927).

[3]) *H. Glauert:* "Theoretical Relationships for an Airfoil with Hinged Flap", (Reports and Memoranda No. 1095, Aeronautical Research Committee, London, April, 1927).

[4]) *H. Glauert & I. L. Peatfield:* "Experimental Determination of Tailplane Characteristics", (British Advisory Committee for Aeronautics, Reports and Memoranda No. 761, 1921 — 22).

account is taken of the interference effect of the propeller slip stream and the rest of the airplane, it hardly seems justified to draw any conclusions concerning the accuracy of the latter from these experimental results.

If the above explanation of the discrepancy between the theoretical and experimental values of the angle of zero lift is a correct one, it seems reasonable to expect a better agreement for symmetric stream-lined profiles such as are used in practice. The basic hypothesis on which the theory then rests is that such profiles, when sufficiently thin, may be replaced by their mean camber lines. For profiles of this type, the upper surface will no longer present the abrupt change in contour at the hinge and part of the space underneath this point will be filled out, partially eliminating the dead air that was assumed to accumulate there with the bi-linear profile at small negative angles of attack. The limited experimental data which does exist for symmetric profiles of this type shows a much better agreement with the results obtained by theoretical methods, thus substantiating the above explanation. However this experimental data is not sufficient to enable a definite conclusion to be made at the present time concerning the merits of the theories that have been employed in this work.

No remarks have been made concerning the theoretical values obtained by the discontinuous potential for the drag coefficients, for all comparisons with experimental data would be meaningless until the effect of viscosity is completely taken into consideration. It seems quite probable that the introduction of viscosity in the problem would have little effect on the theoretical values of the lift and moment, and these values may therefore be checked by comparing them with experimental results. Although this comparison will not be taken up in detail in this paper, one remark may be made concerning the slope of the curves of the lift coefficient plotted as a function of the angle of attack. For infinite aspect ratio the Joukovsky theory gives 10,89 for this value, while the discontinuous potential gives a considerably smaller value, 6,93, and according to both theories, these are practically constant for all profiles. It thus seems that the value obtained by the discontinuous potential is too low, for experimental results on wings of aspect ratio 6 or thereabouts, give a slope of approximately the same magnitude. When the Prandtl induced drag theory is applied to the results given by the Joukovsky potential, a fairly good agreement is obtained with the experimental values of this slope, but at present a satisfactory modification of the discontinuous potential for the case of finite aspect ratio has not been achieved. Evidently the circulation around the infinitely long wing as given by the original discontinuous potential function is too small and it is possible that a better agreement could be obtained if this function were modified, perhaps along lines similar to those used on pages 24—29 above. But the mathematical difficulties in applying this function then become so involved, that before devoting a great deal of time and energy to this work, it might be well to ponder on the question as to whether it would not be more advantageous to abandon the basic method of assuming a potential of the flow around a profile "a priori", and instead to attempt to find by straight-forward, rational methods a solution to the fundamental dynamical equations representing such a fluid motion.

MILTON J. THOMPSON, M. S. E.

THE WIND TUNNEL OF THE AERODYNAMIC INSTITUTE OF WARSAW AND SOME NOTES ON THE STUDY OF LONGITUDINAL STABILITY.

In preparing this article the author has had a two-fold purpose in mind, the first being to give a description of the wind tunnel of the Aerodynamic Institute of Warsaw with a discussion of some of the problems encountered in its development, and second, to present briefly the method employed by this laboratory for the study of the longitudinal stability of an airplane. The first part of the paper, therefore, gives a description of the tunnel in its present state, followed by a short résumé of the study that was made in an effort to reduce the vibrations, turbulence, and irregularities of the air flow which existed in the tunnel built on the original plans, so as to improve the results of tests made therein. The second section is concerned with the procedure followed in the running of the usual tests required for the determination of the aerodynamic characteristics of an airfoil or airplane and the method used at the Aerodynamic Institute for applying this data to the study of the longitudinal stability of an airplane, in which several original features have been introduced. Except for the fact that the construction of the balance used in this tunnel makes it especially well adapted for the measuring of pitching moments, these two parts might have been treated as separate subjects, but because of this close relation, it has been considered more appropriate to present them together. With these preliminary remarks, we then proceed to the first section, the discussion of the wind tunnel and some of its problems.

I. The Wind Tunnel of the Aerodynamic Institute.

A. Introduction.

In the field of aerodynamic research the wind tunnel, first used extensively in this kind of work by Gustave Eiffel, still furnishes the most satisfactory means for the study and investigation of the various phenomena which occur in this branch of physics. In spite of the extremely valuable results which have been obtained by the application of mathematical methods to these problems, the theory cannot in its present state be considered as a practical tool for the use of the aeronautical engineer, and even though it be greatly enlarged and improved upon, it is doubtful if the analytical methods will ever completely displace the experimental in the solution of many of the problems encountered in the design and construction of airplanes and lighter-than-air craft.

The wind tunnel, however, possesses several inherent disadvantages which have hindered its development, chief among these being the extremely high cost of the equipment, and second, the fact that due to scale effect and irregularities in the flow, the results of laboratory experiments are not always a sufficiently close approximation to the actual conditions existing in flight, nor do the existing theories which correct for the phenomenon of scale effect and the like, always give satisfactory results. These last conditions can be improved only by increasing the size of the tunnel, the velocity of the air stream, or the density of the air as in the variable density tunnel of the United States National Advisory Committee for Aeronautics, and by the introduction of various devices for the elimination of the irregularities in the flow, all of which mean an increase in the cost. Furthermore the flow in different tunnels is seldom the same so that it is never safe to compare directly the results of tests made in different laboratories even though the Reynolds' number be the same for both. This last fault is perhaps the one for which a remedy may most easily be found, the obvious solution being the adoption of some sort of international standards on which all aeronautical laboratories will operate so that their results will present a sufficient degree of uniformity for practical purposes. Finally the existence of oscillatory motions and turbulence in the air flow caused by the vibrations of the structure forming the tunnel and of the air-propelling mechanism is another problem, the seriousness of which is gradually becoming recognized although at present there is very little information available on the subject.

Because of the existence of these difficulties in the design and construction of a wind tunnel and the lack of information as to just what is the most satisfactory type, this branch of aeronautical engineering can hardly be considered as having passed far beyond the elementary stages of its development, yet on it is dependent to a very high degree, the scientific evolution of a really safe form of aerial transportation. Consequently any new types of tunnels or equipment should be of considerable interest and for this reason the writer has felt that it would be worth while to prepare a description of the the laboratory now in operation at the Aerodynamic Institute of Warsaw, and a discussion of some of the problems met with in its construction.

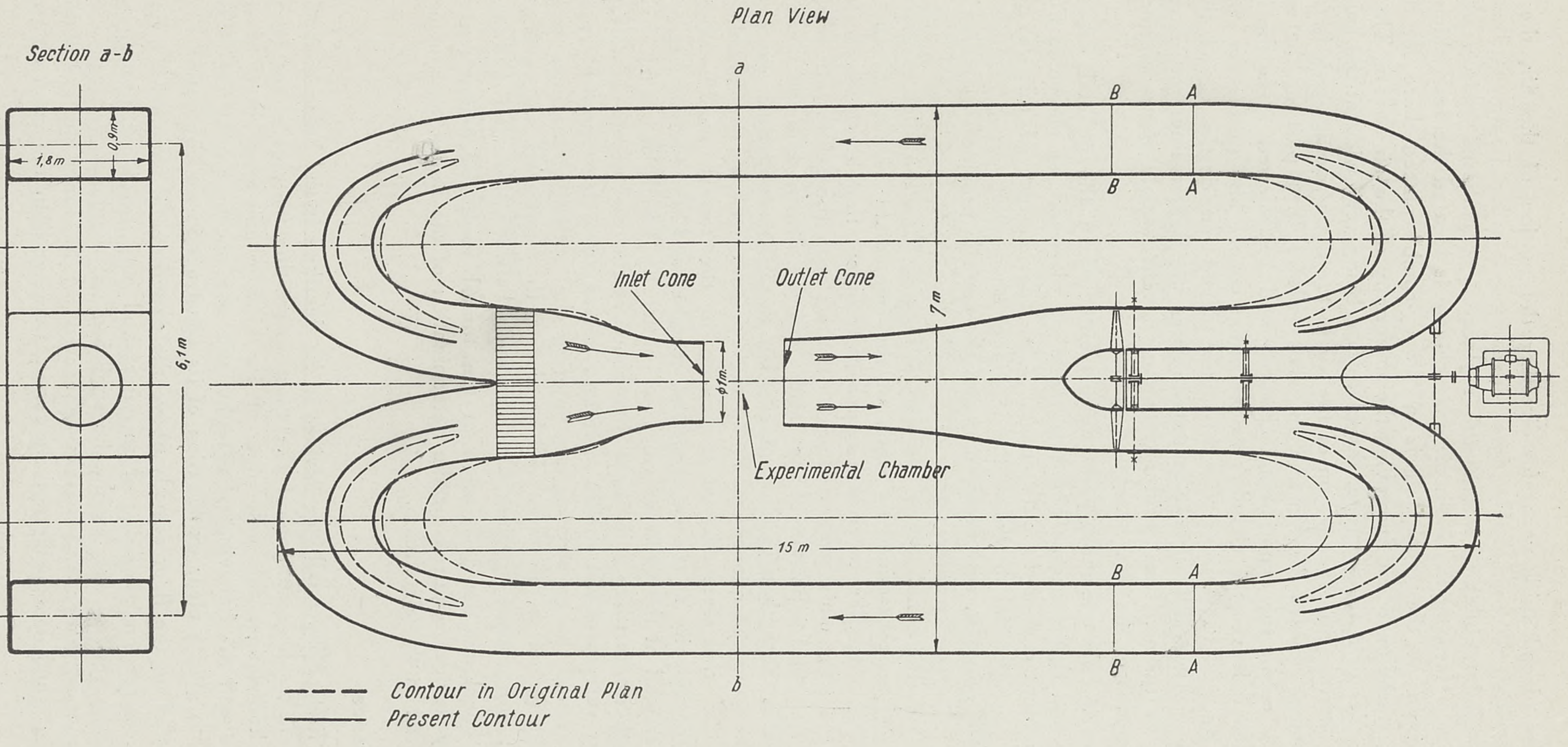
B. Description of the Tunnel.

1. The Structure.

The wind tunnel of the Aerodynamic Institute is of the so-called double return type, a form now considered to be the most satisfactory by many authorities on the subject. The tunnel itself is circular in cross-section throughout the main passage-way which passes through the experimental chamber, and rectangular thrroughout the return passage-ways. It is built of reinforced concrete and is located on the first floor of the building which houses it. The placing of the tunnel directly on the foundation of the building would be the most advantageous from the standpoint of reducing to the greatest extent, the possibility of the existence of vibrations due to lack of rigidity of the structure, but because of lack of space this location was not employed here, although a larger tunnel, the balance for which is not yet completed, has been built directly on the ground. The main air passage-way is built in the shape of a venturi tube and at its throat, which is one meter in diameter, a break is made in which the models to be tested are suspended. The space surrounding this portion of the tunnel, known as the experimental chamber, is open to the atmosphere. The details of the construction are shown schematically in Figure 1.

The contour of the walls in plan view is especially interesting, the curves at the turns being obtained by a mathematical treatment of the fluid motion[1]). At these turns

[1]) *J. Bonder*: "Zmiana kierunku prądu jednostajnego o 180°", Przegląd Techniczny, t. LXIII, 1925 r. Translated into English as "Change of 180° in the Direction of a Uniform Current of Air", U. S. National Advisory Committee for Aeronautics, Technical Memorandum No. 350.



The Wind Tunnel of the Aerodynamic Institute of Warsaw
Plan View
Section a-b
0,9m
1,8m
6,1 m
a
b
B
A
Inlet Cone
Outlet Cone
7 m
φ1m
Experimental Chamber
15 m
Contour in Original Plan
Present Contour

Figure 1.

there are also placed guide vanes for directing the motion of the air, the contours and positions of which were originally determined by a similar treatment but for practical reasons, as will be explained later, were replaced by cambered plates. At one end of the venturi tube forming the main air passage-way is located the fan which sets the air in motion, while at the other end is a "honey-comb" placed there for the purpose of reducing the turbulence and improving the uniformity of the air stream. The fan is a two-bladed propeller of a special type, the plan-form being very wide at the hub and tapering rapidly to a narrow tip. The motion of the air in the main passage-way is from the experimental chamber toward the fan and in what follows that part of the venturi tube by which the air enters the experimental chamber will be referred to as the inlet cone and that by which it leaves the chamber as the outlet cone. The power for driving the fan is supplied by a 50 H. P. direct current motor placed outside the tunnel, the shaft which connects the motor and fan being mounted along the center line and extending through the wall of the tunnel. The local alternating current supply is transformed into direct current by means of the Ward-Leonard system.

There is only one other point to be mentioned in the general description of the tunnel itself and that concerns a device made of ply-wood, as shown in Figure 2, which fits over the blunt end of the outlet cone. The inner surface of this device or sheath is parallel to that of the inside of the outlet cone, extends a short way into it, and between it and the cone is provided a small clearance. The outer portion tapers off rapidly to a point just beyond the outer wall of the cone. Since the air in flowing from the inlet to the outlet cone is unconstrained by walls in the immediate vicinity of the experimental chamber, there is a region of turbulent flow along the surface on which the main stream comes in contact with the quieter air outside the tunnel and a portion of the latter may be drawn into the outlet cone along with that which originally left the inlet cone, thus causing an increase in the quantity of air in the circuit formed by the tunnel. This increase, if it were allowed to remain in the tunnel, would mean a continual increase in the velocity at the experimental chamber and the opening between the sheath and the inner wall of the cone provides an outlet by which any such excess air may escape. Furthermore there is a slight divergence of the air stream at this point and the tapered outer surface of the sheath therefore serves to at least partially prevent this turbulent flow around the air stream from entering the outlet cone. Such turbulent air as does enter the tunnel at this point will be close to the inner wall, and setting up a reversal of the flow, will escape through the clearance between this wall and the sheath.

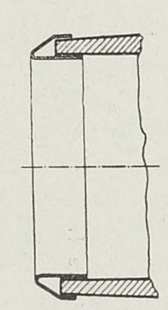


Figure 2

This concludes the description of the tunnel itself and it now remains to discuss the auxilliary devices required for the determination of the forces and moments acting on a model placed in the air stream.

2. The Balance.

The first of the auxilliary devices to be decribed is the balance used in connection with this tunnel, which is one of the most interesting features of the laboratory and to this writer's knowledge, the only one of its kind in existence. It is of an exceedingly simple nature and the following paragraphs and the accompanying sketch (Figure 3) will be sufficient to give a clear explanation of its construction and operation.

Mounted on the floor directly above the experimental chamber is a vertical pedestal of circular cross-section consisting of an outer shell and an inner portion which may be rotated about its vertical axis within the shell but not displaced vertically. Suspended in the experimental chamber and rigidly connected to the inner portion of the pedestal is a circular ring which is considerably larger in diameter than the main air passage at this

point and has its center on the longitudinal axis of the tunnel. The ring and pedestal are mounted so that they may be rotated about any one of three mutually perpendicular axes which for reasons that will soon appear, we shall call the lift, drag, and moment

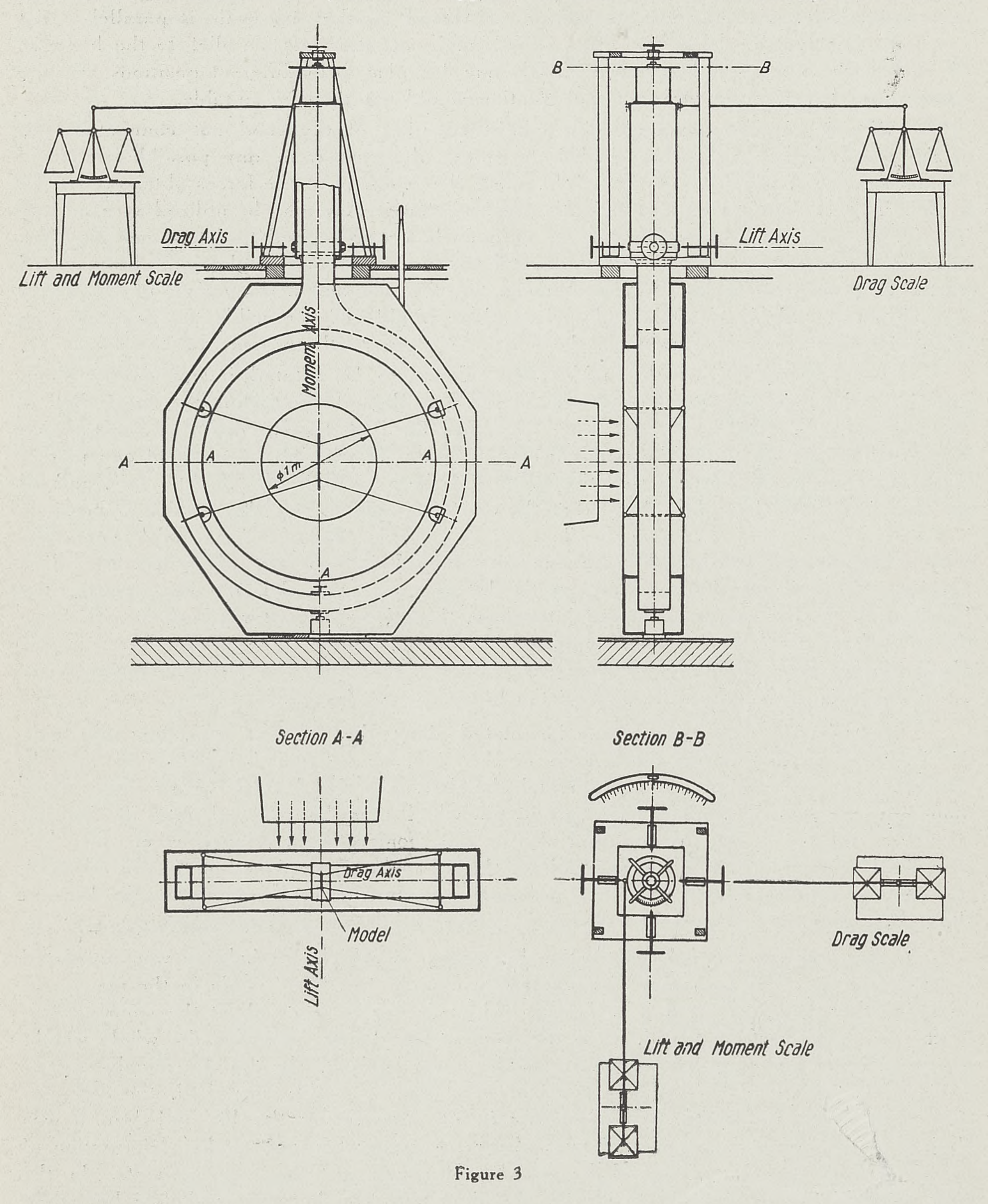


Figure 3

axes. The lift and drag axes lie in a plane parallel to and slightly above the the plane of the floor on which the pedestal is mounted, the former being parallel to the longitudinal axis of the tunnel, while the moment axis coincides with the vertical axis of the pedestal and passes through the intersection of the first two. In the usual tests of a model airfoil

or airplane, the model is mounted in the center of the ring by means of fine wires connected to the latter, so that the lift, drag, and pitching moment which act due to the motion of the air will cause the ring and pedestal to rotate about the lift, drag, or moment axis respectively. For example, an airfoil is placed so that its span is parallel to the vertical or moment axis and its chord at 0^0 angle of attack is parallel to the lift axis. Of course for some special tests the model may be placed in different positions and the names used here for the three axes of rotation would not then be suitable.

The ring is also surrounded by a light covering of ply-wood not connected to it or the pedestal, the purpose of which is to protect the ring from any possible motion of the air against it, which of course would affect the readings of the forces obtained for the model. This covering is built sufficiently rigid so that it may also be utilized as a mounting for the placing of objects in the air stream when it is desired to determine only their influence on some other model. A horizontal tail surface, for example, may be mounted on the ring and the wing of an airplane on the covering and a comparison of the results of such a test with those of the tail surface alone would make possible the determination of the deflection of the air stream at the empennage due to the presence of the wing.

The construction which enables the balance to be rotated independently about anyone of the three aforementioned axes is easily explained. Encircling the outer shell of the pedestal is a metal band containing two pairs of diametrically opposite holes which serve as bearings by which the apparatus may be supported. The centers of one pair of these holes lie on the lift axis and the centers of the other pair on the drag axis, and all are fitted with ball bearings. Now directly opposite each one of these holes or bearings is a steel pin mounted firmly on the floor surrounding the base of the pedestal but provided with a hand-screw so that the pin may be moved into or out of its corresponding bearing. When it is desired to measure the lift acting on a model, the pins opposite the bearings on the lift axis are screwed into place, the other pair is turned so that it is free of the pedestal, and the balance, supported by the first pair of pins, is now free to rotate about the lift axis. Similarly for the measurement of the drag, the pins on the drag axis are screwed into place and the pair on the lift axis are released.

In order that the balance may be rotated about the moment axis, an adjustable pin is placed on this axis at the bottom of the ring, its bearing being located directly beneath it on the floor of the experimental chamber. On the floor above a frame-work is built over the pedestal supporting a second pin which may be screwed into its bearing placed on the top of the pedestal and also on the moment axis. Hence when this last pair of pins is screwed into place and both the other pairs mentioned above are released, the balance may be rotated about the moment axis. In the measurement of the lift and drag these pins on the moment axis are of course withdrawn from their bearings.

This was the original construction by means of which the balance was supported but because of a very apparent disadvantage a change has been made in the manner of retaining the apparatus when it is desired to have it free to rotate about the moment axis. With the system just described, when the moment was being measured the whole weight of the pedestal and ring was supported by the lower bearing, the top one merely serving as a guide, and since the ring was made of wood and was not very rigid, the deformations in it were considerable. Consequently if after measuring the lift and drag, it was desired to determine the moment, it was always necessary because of this deformation of the ring to readjust the postion of the model before making these measurements. In the new construction the supports on the lift and drag axes are the same as before but when the balance is free to rotate about the moment axis, the upper bearing carries all the weight while the lower one serves as a guide. Thus the only possible change in the position of the model when changing from the lift or drag axis to the moment axis is a vertical deflection resulting from the extension of the pedestal due to the weight of the ring

which it supports, and since the position of the model with respect to the moment axis is not changed, all three quantities, lift, drag, and moment, may be measured without any readjustment.

With the discussion of the mode of supporting the ring and pedestal completed, it now remains to show how the actual magnitude of the forces and moment acting on the model may be determined. In order to measure the lift an arm is pinned to the pedestal near its top at a point directly above the lift axis, this arm in turn being connected to a two-pan balance of the usual type placed on a table at one side of the pedestal. The tendency of the pedestal to rotate about the lift axis due to the lift acting on the model is thus transmitted by this arm to the balance causing one of its pans to rise. The various lever arms of the apparatus are so proportioned that the weight which must be placed on the higher pan to bring them both to the same level is exactly equal to the gross lift of the model, that is, the actual lift of the model plus any influence of the supporting wires and the weight of the ring and pedestal. Because of the way in which the arm leading from the pedestal to the balance is connected, this same balance may be used for measuring the moment, but in this case the gross moment about the moment axis equals the distance from this axis to the point of connection of the transmiting arm multiplied by 1,5 times the weight necessary to bring the balance to a position of equilibrium. The drag is measured in a similar way, another arm being connected to the pedestal at a point also directly above the lift axis but diametrically opposite the point of connection of the first one This arm is connected to another balance of the same type as that serving to measure the lift and moment, and the weight required to bring it to a position of equilibrium is exactly equal to the gross drag of the model.

The angle of attack of the model is changed by rotating the inner portion of the pedestal and the attached ring, which carries the model, within the outer shell which is held in a fixed position, the axis of rotation being the vertical axis of the pedestal which coincides with the moment axis. In order that this may be done conveniently a hand-screw and calibrated quadrant are fastened to the outer shell and a pointer placed on the inner portion which indicates the angle of attack in any given postion. A hand-lever is also attached to the covering of the ring and extends through the floor above the experimental chamber so that the covering may be rotated simultaneously with the ring. In the case of the lift and drag measurements, the outer shell of the pedestal is held fixed by its supporting pins, but when the moment is being measured it is necessary to first screw into position one of the supporting pins on either the lift or drag axis, then change the angle of attack, and after releasing this pin, determine the moment.

3. The Velocity Indicator.

In the running of a test only one other measurement is required in addition to those discussed above and that is the velocity of the air stream in the experimental chamber, and the device by means of which this value is obtained will now be discussed. Through the top of the inlet cone, some distance back of its entrance into the experimental chamber, there extends a short way into the air stream a small tube, the projecting end of which is closed. Near this end of the tube there is drilled a small hole in its lateral surface facing the air stream, while the other end is connected to a manometer outside the tunnel. Since the pressure at the hole in the tube is purely static and atmospheric in the experimental chamber, the velocity in the latter is equivalent to the reading of the manometer which gives the head in millimeters of water. A calibration of the tunnel, however, showed that a slight correction must be introduced here and that the average velocity head throughout the region of uniform velocity in the experimental chamber is equal to 1,015 times the reading of the manometer. It might also be mentioned here that

the diameter of this region of uniformity is about 0,95 m., slightly less than the diameter of the tunnel at this point.

This concludes the description of the tunnel and its equipment. The greatest advantage which is obtained with the type of balance used is that in measuring the lift, drag, and moment, it is necessary to read the load on only one scale for each of these items. This is of special value in the case of the moments for the loads produced thereby are usually relatively small and if they are divided between two or more scales, as in many other existing types of balances which permit the measurements of moments, the errors of observation are quite liable to increase. Furthermore in making a reading on any scale it is necessary to synchronize as nearly as possible the fluctuations of the manometer giving the velocity head with those of the scale which measures the load, and make the reading when both are steady at the same instant. It is quite evident that this is considerably facilitated when only one scale reading is required. Only one disadvantage is evident in this construction and that is that the values of the angle of attack at which a model may ordinarily be set are limited to approximately $\pm 30^0$ since the supporting ring strikes the walls of the inlet and outler cones when turned this far. This however is not a very serious handicap because it is only in certain special tests that it is necessary to go beyond the limits of this range and if required, the range may be extended by mounting the model in two or more different positions.

It is expected in the near future to replace the balance, which is built largely of wood, by one constructed entirely of metal which of course will be a considerable improvement but the design of the apparatus will be fundamentally the same as that described above. As mentioned previously there is also in the process of construction at the present time a balance for another larger tunnel in which it is intended to duplicate the various features of the smaller one, employing a metal construction wherever possible. The tunnel itself is already completed and has a diameter of 2,5 meters at the experimental chamber.

C. Study and Improvement of Flow Conditions.

In the above paragraphs the description given is of the laboratory at present and in what is considered by its designers as a satisfactory state. Many changes have been made in the original plans in an attempt to improve the conditions of operation and the writer has felt that a review of this work would be of considerable value since very little information on it exists in the literature of aeronautics. However, since the writer was not intimately connected with this development, the following should be considered as a general survey of the work that was done rather than a detailed discussion.

When the tunnel was first put into operation, the construction being according to the original plans, the vibrations of the building housing it were found to be very disagreeable to the occupants, although the magnitude was not considered great enough to be dangerous. While the results of tests made under these conditons differed somewhat from those obtained in other laboratories, this difference was not very large, and being to a certain extent expected, the designers were inclined to considered that from an aerodynamic standpoint, the tunnel was satisfactory. However, when various changes were actually made in an effort to lessen the vibrations, it was found that as these decreased, the pulsations of the air flow decreased, and the results of tests were improved. For this reason the study of the vibrations originally begun principally for the sake of comfort, was carried considerably further than might have otherwise been the case and an appreciable improvement in the operating conditions was obtained. No attempt has been made in what follows to discuss the changes which were introduced in any sort of chronological order. In the actual work that was done, these changes were made one by one and what has been noted here is simply their effect on the vibrations, pulsations of the air flow, and operating conditions in the tunnel.

In the original design of the tunnel, the width of the return passage-ways at the turns was somewhat larger than at present and at each turn there was one guide vane of concrete construction built into tunnel. It was found that by extending the internal walls at the turns so as to decrease the width of the sections at these points, an improvement was obtained in both the vibrations and aerodynamic characteristics. A complete study of this effect, however, necessitated the removal of the original guide vanes and vanes built of wood were put in their places in order that the experimenting done in this connection might be easily carried out. The original vanes had crescent-shaped cross-sections while the new ones are simply cambered plates. The extensions built on the internal wall were also made of wood and the distances to the outer wall measured parallel to the axis of the tunnel at each point on the turn were decreased so as to remain in approximately constant ratio with the original dimensions. The internal walls and guide vanes at each turn were set in different positions until the most satisfactory conditions were obtained and it is these positions that are shown in Figure 1, the dotted lines representing the original positions. A further decrease of the area of the sections at the turns nearest the fan was also made by raising the floor and lowering the ceiling of the passage-ways at these points and was found to be of advantage. The lines $A-A$ and $B-B$ in Figure 1 represent the beginning and end of the inclined portion of the floor which leads from the portion of the passage whose height was decreased to that of full height.

One of the commonest devices used in wind tunnels for the reduction of turbulence and improvement of the air flow is the so-called "honey-comb", an arrangement of mutually orthogonal planes intersecting at regular intervals or of cylindrical tubes placed with their axes parallel to the direction of flow. In the tunnel of the Aerodynamic Institute the honey-combs of the first type are employed and the results of the experiments are of a very interesting nature. It was found in general that the effect of the honey-comb was to keep the air moving in a direction parallel to the axis of the tunnel, but as far as the reduction of turbulence was concerned, the device simply acted so as to more firmly establish the the conditions already existing in the flow. If the motion of the air was fairly steady and smooth before the honey-comb was put in place, then its presence was an improvement, but if the air flow was not very good to begin with, the honey-comb only made matters worse. Furthermore one honey-comb was found to be sufficient to obtain the desired effect, the presence of any additional ones only causing a loss of energy. The most advantageous position for this honey-comb was found to be in the inlet cone just before the turns at the point in this neighborhood where the velocity was the lowest so as to reduce the energy loss as much as possible.

A good deal of experimenting was also done with the shape of the inlet and outlet cones before the types now in use were developed. Some of the types which were used in the outlet cone are shown in Figure 4 but it is hardly nesessary to go into the details of what it was hoped accomplish with these. The device described on page 74 was finally developed as the most satisfactory in that in addition to fulfilling the requirement

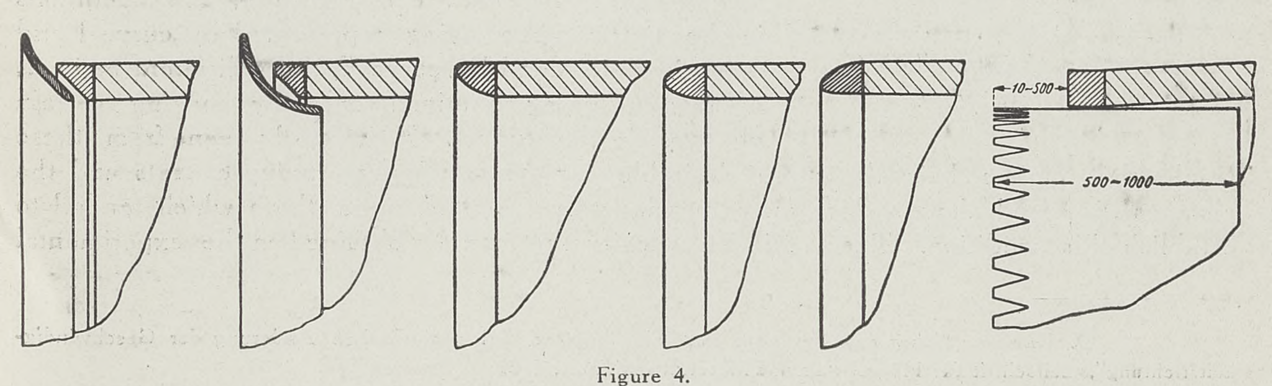


Figure 4.

of providing an opening for the escape of any excess air which the air stream might acquire as it passed the experimental chamber, it also gave the most uniform distribution of velocity across the working section of the chamber. It might be mentioned in this connection that the flaring shaped opening shown above was one of the poorest types used.

The only change made in the inlet cone was a decrease of its diameter for a short distance back of the opening as shown by the solid lines in Figure 1. A few other minor changes were experimented with but as no beneficial results were obtained, they were not made permanent and it is not deemed worth while to bring them into this discussion.

As these various changes were made in the construction of the tunnel, those which were beneficial caused a decrease of the vibrations and at the same time a diminution of the turbulence of the air stream with, as mentioned above, a corresponding improvement in the results of the test of models, and it now remains to discuss some of the relations which were observed between these quantities. It was observed during this study of the characteristics of the tunnel that the vibrations and turbulence which it was desired to eliminate were closely connected with the existence of an oscillating movement of the direction of the air stream. Furthermore when the amplitude of this oscillation was large, the values of the lift and drag coefficients for a model airfoil tested under these conditions were found to be too large and too small respectively when compared with other existing data. This phenomenon is of a nature similar to the so-called "Katzmayr effect"[1]), Katzmayr having obtained similar results by mechanically inducing an oscilation of the direction of his air stream. In addition to this effect, the turbulence of the air undoubtedly had some influence on the results of model tests. To obtain quantitative relations between the characteristics of a model and these factors was rather difficult, but the magnitude of the oscillations of the direction of the velocity, and to a certain extent the degree of turbulence as well may be said to be more or less closely represented by the magnitude of the pulsations of the water column in the manometer which measures the velocity head in the experimental chamber. Not only was the pressure distribution in the experimental chamber investigated after each change in the tunnel but tests were made in every case on a model airfoil, and it was found that the aerodynamic characteristics, that is the lift and drag coefficients, C_y and C_x, of this wing at a given angle of attack varied qualitatively with the pulsations of the manometer somewhat as shown in Figure 5. From this data it is seen that there exist two regimes, the first for which the pulsations are relatively small and for which C_y and C_x are practically constant, and the second for greater pulsations accompanied an increase of C_y and a decrease of C_x. The values of the characteristics obtained in the first regime are considered to be the best on the basis of comparison with other existing data. Now the variation of the pulsations as a function of the velocity in the experimental chamber is shown in Figure 6, the conditions in the first regime being represented by curve I and those in the second by curve II, these different regimes, of course, being obtained only by making certain changes in the tunnel. It is easily seen from these results that regime I is the more desirable for the satisfactory runing of tests and the changes discussed above which were permanently adopted were those which tended to establish this condition. The maximum velocity that can be obtained in the experimental

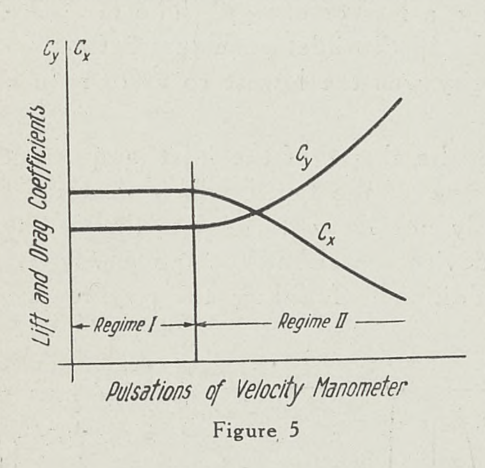


Figure 5

[1]) *R. Katzmayr:* "Über das Verhalten von Flügelflächen bei periodischen Änderung der Geschwindigkeitsrichtung", Zeitschrift für Flügtechnik und Motorluftschiffahrt, 1922.

chamber under these conditions is equivalent to a velocity head of about 160 mm. of water, that is about 180 km. per hour (112 miles per hour). The so-called efficiency of the tunnel, that is, the kinetic energy of the air passing through the experimental chamber in one second divided by the energy supplied to the motor in the same time, lies between 3,6 and 3,7.

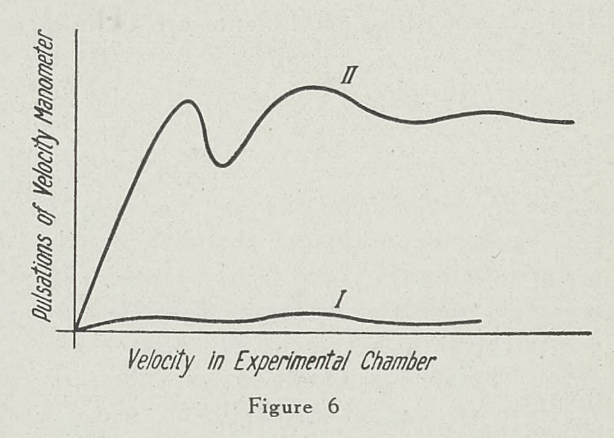


Figure 6

While the discussion of this work of improving the operating conditions of the wind tunnel is of a very brief and sketchy nature, it is hoped that it will be of value in the solution of other similar problems. The staff of the Aerodynamic Institute are now working with an experimental wind tunnel constructed of wood with walls of rubberized fabric in which the phenomena of vibrations, turbulence, and their effects on the results of tests will be studied more exhaustively. The purpose in building this experimental tunnel is also to determine whether or not the flexible material used for the walls will have a dampening effect on any vibrations that may exist. In the small tunnel discussed in the preceding pages, a by-pass of a similar nature was introduced in one of the return passage-ways and although found to be of some benefit, was later removed. When the equipment of the larger tunnel is completed, it is intended to reproduce therein many of these experiments which were made in the smaller one.

The value of any research of this kind certainly cannot be overestimated for on it is dependent to a very large extent the improvement of existing tunnels and the development of new ones, nor can the standardization of all laboratories suggested in the introduction be accomplished without a considerable increase in the knowledge of the various phenomena which are encountered in their construction and operation.

II. Some Notes on the Study of Longitudinal Stability.

Having completed the first part of this paper dealing with the development of the wind tunnel of the Aerodynamic Institute, it is now proposed to discuss the method used in this laboratory for the study of the longitudinal stability of an airplane based on data obtained from wind tunnel experiments. Strictly speaking this study is an approximation to that of dynamic longitudinal stability since in what follows the airplane will be cosidered only in statical conditions and any moment about its center of gravity due to the thrust of the propeller will be neglected. There is nothing unusually complicated about this treatment of the problem and the fact that it has not been more extensively used in other laboratories may quite possibly be due to the greater difficulties encountered therein in the determination of pitching moments, which here are very easily and accurately measured with the type of balance used in the wind tunnel. Several of the points mentioned here have been discussed in detail in a bulletin of the *Service Technique de l'Aéronautique* of Belgium [1]). Because of the simplicity of this method, it has been deemed unnecessary to describe the procedure in great detail; the various steps will be outlined briefly and as an example, the results obtained by the author for a particular model airplane will be given.

---

[1]) *Fr. Haus:* "Introduction a l'Étude de la Stabilité Dynamique des Avions", Bulletin du Service Technique de l'Aéronautique, (Belgique), Nr. 5, Juin, 1927.

Before proceeding to the actual study of longitudinal stability, it will be necessary to give the various formulas required for the calculation of the usual coefficients, C_y, C_x, and C_m, and the position of the center of pressure, from the data observed during a test. The lift and drag coefficients are defined as follows:

$$C'_y = \frac{100 P_y}{q S}, \qquad C'_x = \frac{100 P_x}{q S}$$

where P_y and P_x are the net loads on the lift and drag balances, q is the dynamic pressure in the experimental chamber, equal to 1,015 times the reading of the velocity manometer (see pg. 77), and S is the area of the model being tested. The value of q is maintained as nearly constant as possible throughout a test, usually at 100 mm. of water which is equivalent to a velocity of about 144 km. per hour (90 miles per hour). The net load on any balance is obtained by subtracting from the actual readings made during a test, the zero reading of the balance, which changes with the angle of attack of the model, and the effect of the wires supporting the model. These last values are obtained by replacing the model by a wire which holds the other wires in their original positions and then determining the lift, drag, and moment of this system of wires, from which must be subtracted the calculated effect of the wire replacing the model. Most of the models tested in this laboratory are constructed so that the supporting wires are of certain standard lengths, making it unnecessary to repeat this process for every new model.

Because of the fact that the air stream is not exactly parallel to the lift axis of the balance, the above formulas for C_y and C_x are not quite correct. If δ is the angle of deflection and is positive when it decreases the angle of attack, then the true values of C_y and C_x are:

$$C_y = C'_y \cos \delta + C'_x \sin \delta, \qquad C_x = C'_x \cos \delta - C'_y \sin \delta.$$

But since δ is very small, in this case $0{,}5^0$, these values are given approximately by the formulas

$$C_y = C'_y = \frac{100 P_y}{q S}, \qquad C_x = C'_x - C'_y \sin \delta = \frac{100 P_x}{q S} - C'_y \sin \delta \quad . \;. \;. \quad (1)$$

This deflection δ has been taken into consideration in the setting of the device which measures the angle of attack so that the latter measures directly the true value of this angle and no correction is required.

To calculate the moment coefficient C_m, a point of reference must be chosen and this is usually taken on the leading edge in the case of a wing, or on what corresponds to the leading edge for other models. As explained on page 77, the moment about the moment axis of the balance is $1{,}5\, r\, P_m$, where P_m is the net load on the moment scale and r is the distance from the moment axis to the point of connection with the pedestal of the arm leading from the pedestal to the scale. Then if K is the distance from the point of reference to the moment axis, which is assumed to intersect the chord of the model, l the length of this chord, and i the angle of attack as shown in Figure 7, the moment coefficients is

$$C_m = \frac{1{,}5\, r\, P_m \cdot 100}{q S l} - \frac{K}{l}\left[C_y \cos i + C_x \sin i\right] \quad . \;. \;. \;. \;. \;. \quad (2)$$

A positive value of C_m indicates that the moment is acting so as to decrease the angle of attack.

The distance to the center of pressure from the point of reference in per cent of the chord, l, is given by the formula

$$c.\ p. = \left[\frac{1{,}5\ r\ P_m \cdot 100}{qSl\ (C_y \cos i + C_x \sin i)} - \frac{K}{l} \right] 100 \quad \ldots\ldots \quad (3)$$

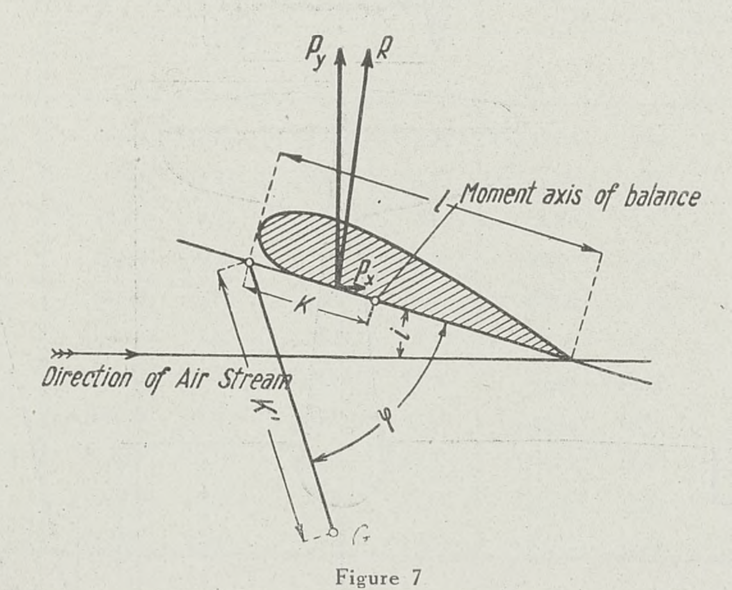


Figure 7

In case it is desired to calculate the moment coefficient about some other point such as G in Figure 7, the following expression may be used:

$$C_{mG} = C_m - \frac{K'}{l} \left[C_y \cos (i + \varphi) + C_x \sin (i + \varphi) \right] \quad \ldots\ldots \quad (4)$$

where K' and φ are defined as shown in Figure 7. Here C_{mG} is positive when the moment about the center of gravity is acting in the same direction as a positive moment about the leading edge. The angle φ is positive when G is below the wing chord and negative when above.

The development of these formulas is simply a matter of elementary trigonometry and mechanics and it has not been considered necessary to present the details here.

In order to obtain the necessary data for the study of the longitudinal stability of an airplane, the values of C_y, C_x, and C_{mG}, where G is the center of gravity, must be determined for different angles of attack and for different settings of the elevators. The model which was tested by the author is shown with its principal dimensions in Figure 8. A test was first made on this model complete except for the horizontal tail surface, and its characteristics obtained as shown in Figure 9 and Table I, the coefficients being based on the area and chord of the wing. The moment about the center of gravity, taken at point G in Figure 8, was then computed by means of formula (4). The curves in Figure 9 drawn with broken lines represent the same data obtained by adding together the separate effects of the wing, fuselage, and structure, although the curve of $C_m = f\,(i)$ has been omitted since the moment was calculated directly about the center of gravity. The characteristics of the first two items were determined experimentally and the effect of the structure, drag and moment alone being considered, was calculated using the resistance coefficients given in Table II. These values are defined

Figure 8

——— Experimental Values
- - - - Calculated Values
Note: C_m is referred to leading edge of wing.

——— Experimental Values
- - - - Calculated Values

Figure 9

in the same way as the coefficients for the wing except that the area on which they are based is the projected area in the direction of motion of the airplane. It was assumed that these coefficients did not change with the angle of attack, and the effect of strut No. 8, which supports the horizontal tail surface, was omitted. The curve of moment

Table I

i^0	Experimental Values[1]				Calculated Values		
	C_y	C_x	C_m	C_{mG}	C_y	C_x	C_{mG}
— 7,5	— 14,72	12,06	4,03	2,22	— 16,06	12,84	1,14
— 5	— 0,99	8,12	8,93	4,61	— 2,46	8,95	4,66
— 2,5	+ 14,38	6,35	12,60	4,85	+ 14,36	6,50	6,01
0	30,90	6,13	17,00	5,46	32,27	6,51	5,95
+ 2,5	49,00	6,63	21,75	6,50	50,09	7,28	7,21
5	67,00	7,95	26,30	7,77	68,39	8,67	8,70
7,5	84,90	9,46	31,00	10,15	86,34	10,30	10,68
10	100,90	11,27	35,40	13,30	102,44	12,21	13,14
12,5	116,40	13,58	39,32	16,62	118,24	14,67	16,24
15	127,00	16,64	39,53	17,03	132,38	17,51	19,78
17,5	126,00	20,20	36,71	15,41	132,61	21,22	19,92

Table II

Unit	Member	C_x
Landing Chassis	Strut No. 1	20,0
	Strut No. 2	20,0
	Axle	80,0
	Wheel	46,5
Inter-Plane Structure	Strut No. 3	30,0
	Strut No. 4	30,0
	Strut No. 5	30,0
	Strut No. 6	45,0
	Strut No. 7	45,0
Motor	Cylinder	80,0
	Exhaust Pipe	80,0
Empennage	Vertical Fin	1,0
	Strut No. 8	30,0

about the center of gravity plotted against angle of attack, $C_{mG} = f(i)$, shows that the airplane without its horizontal tail surface is never in equilibrium within the flying range, and it is now necessary to determine the characteristics of the plane with this surface attached.

The characteristics of the horizontal tail surface with the elevators set at different angles are shown in Figure 10 and in Table III, β being the flap angle or braquage. These values were not obtained by the author.

[1]) In all experimental work in this paper, the correction factor 1,015 on the reading of the velocity manometer, was ignored.

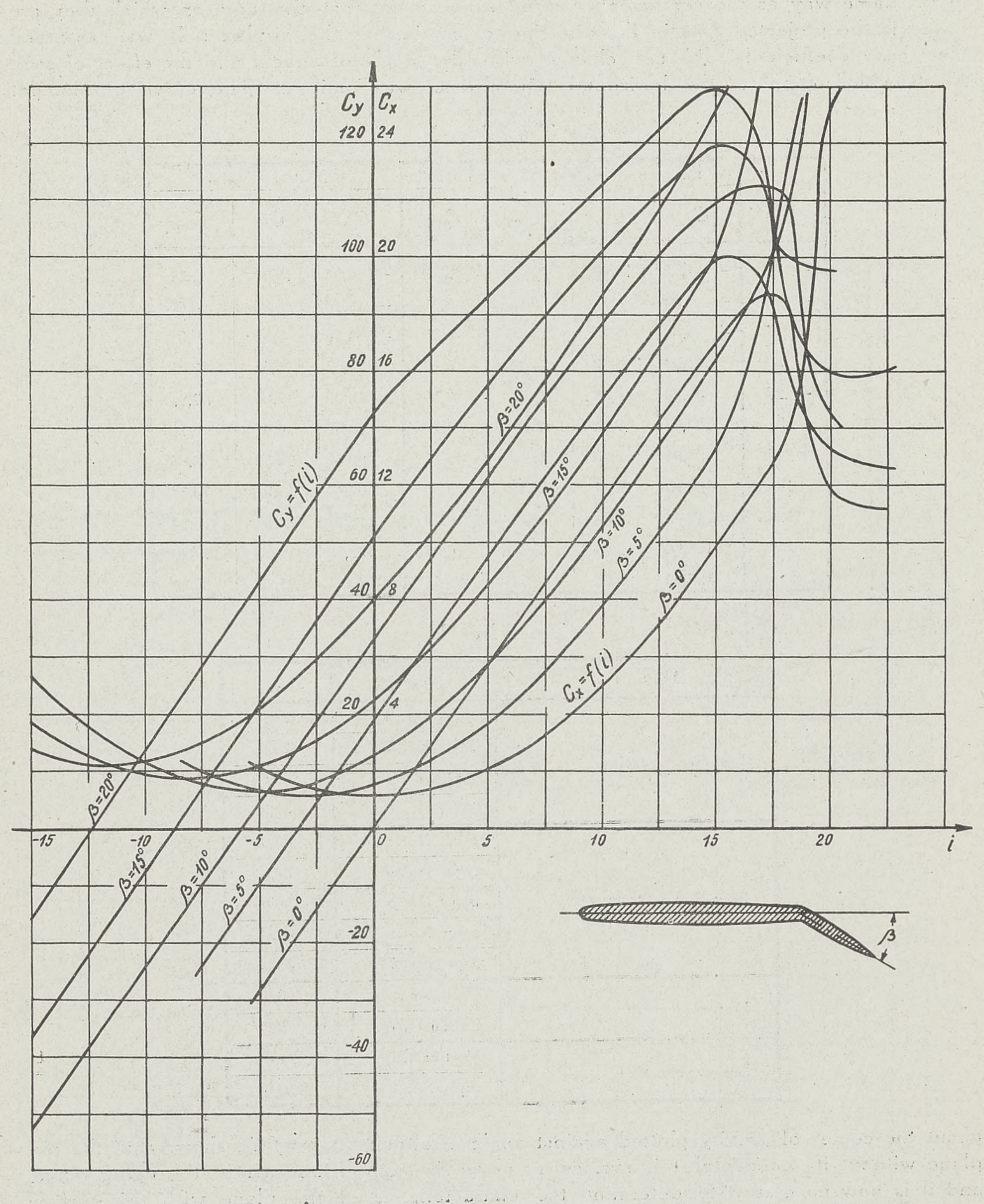
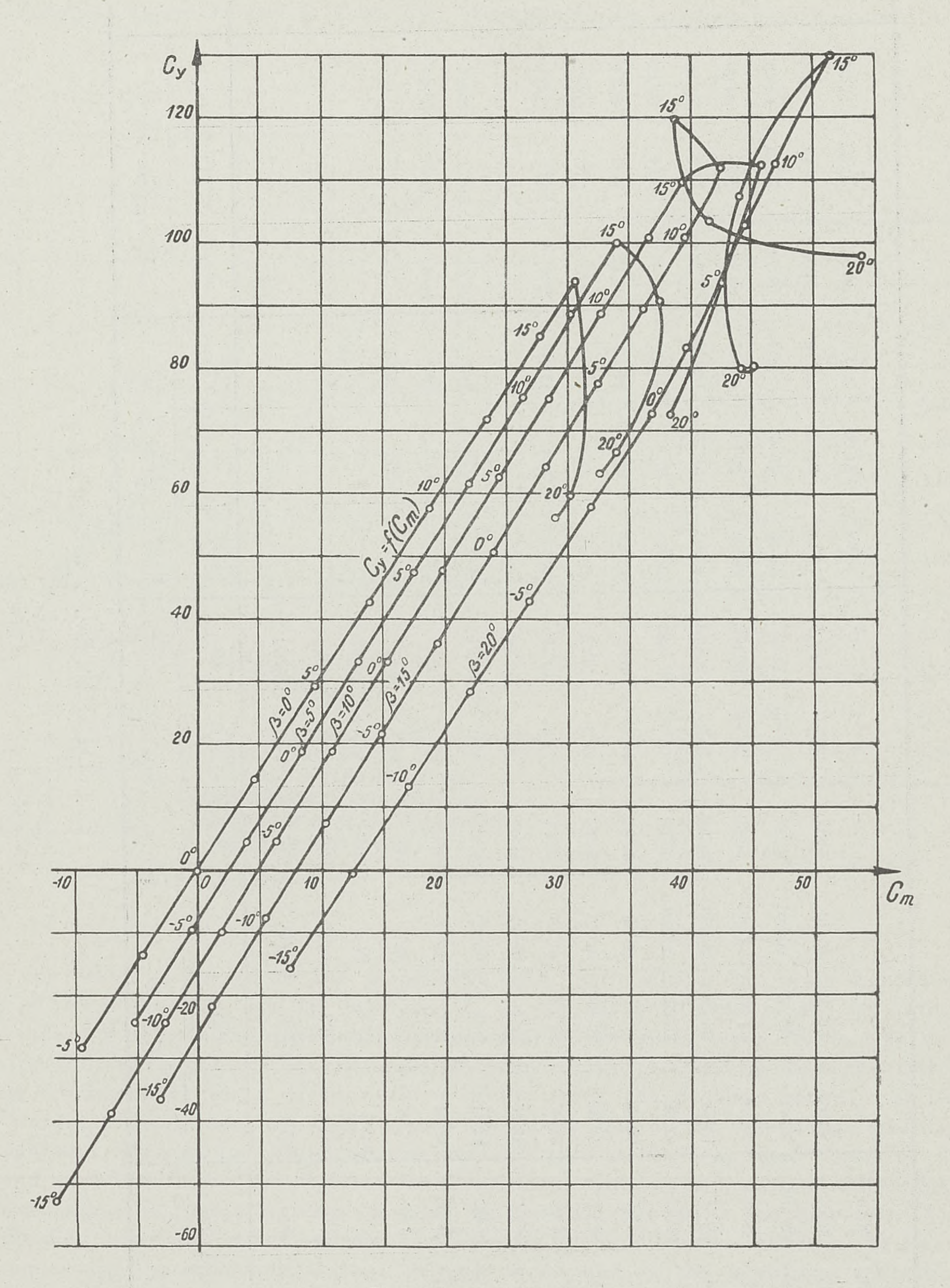

Cy Cx
120 24
100 20
80 16
60 12
40 8
20 4
-20
-40
-60
-15
-10
-5
0
5
10
15
20
i
Cy=f(i)
Cx=f(i)
β=20°
β=15°
β=10°
β=5°
β=0°
β

Figure 10-a



C_y
C_m
120
100
80
60
40
20
-20
-40
-60
-10
0
10
20
30
40
50
$C_y = f(C_m)$
$\beta = 0°$
$\beta = 5°$
$\beta = 10°$
$\beta = 15°$
$\beta = 20°$

Figure 10-b

Table III

i^0	$\beta = 0^0$			$\beta = 5^0$			$\beta = 10^0$			$\beta = 15^0$			$\beta = 20^0$		
	C_y	C_x	C_m	C_y	C_x	C_m	C_y	C_x	C_m	C_y	C_x	C_m	C_y	C_x	C_m
—15	—	—	—	—	—	—	— 52,85	5,21	—11,67	— 36,60	3,72	— 3,20	— 15,81	2,69	7,39
—12,5	—	—	—	—	—	—	— 38,92	3,45	— 7,30	— 21,67	2,52	+ 1,00	— 0,76	2,21	12,70
—10	—	—	—	—	—	—	— 24,20	2,27	— 3,00	— 7,78	1,89	5,45	+ 13,42	2,30	16,90
— 7,5	—	—	—	—24,10	2,00	— 5,36	— 9,80	1,58	+ 1,94	+ 7,36	1,77	10,27	28,36	3,03	22,00
— 5	—28,32	2,13	— 9,67	— 9,84	1,34	— 0,52	+ 4,36	1,39	6,32	21,65	2,11	14,91	43,00	4,18	26,90
— 2,5	—13,64	1,36	— 4,50	+ 4,55	1,16	+ 3,89	18,96	1,66	10,92	36,06	3,05	19,34	57,90	5,91	31,85
0	0,00	1,14	0,00	18,73	1,59	8,30	33,18	2,50	15,48	50,40	4,42	23,95	72,92	7,89	36,89
+ 2,5	+14,62	1,38	+ 4,40	33,11	2,38	12,88	47,42	3,87	19,82	64,15	6,32	28,20	83,33	10,20	39,60
5	29,08	2,07	9,50	47,33	3,72	17,45	61,57	5,63	24,32	77,70	8,53	32,57	93,40	12,76	42,50
7,5	42,95	3,22	14,00	61,24	5,48	21,90	75,16	7,84	28,52	89,90	11,03	36,35	102,77	15,66	44,34
10	57,65	4,96	18,71	75,18	7,70	26,30	88,73	10,51	32,90	101,00	13,92	39,73	112,50	18,50	46,86
12,5	71,94	7,16	23,40	88,50	10,39	30,36	100,76	13,44	36,76	111,05	16,96	42,58	122,50	21,64	49,54
15	85,08	9,87	27,80	99,76	13,37	33,88	109,65	16,47	39,29	119,85	20,13	38,74	129,85	25,14	51,28
17,5	93,84	12,80	31,26	90,50	20,13	37,60	112,15	20,33	45,72	103,50	27,50	41,66	107,30	32,38	43,93
20	59,52	25,31	30,07	66,65	28,32	33,81	72,57	32,28	38,34	97,79	35,22	53,88	79,75	39,84	44,09
22,5	56,04	26,73	28,93	63,05	30,72	32,66	—	—	—	—	—	—	80,05	43,64	45,11

The deflection of the air stream at the empennage due to the presence of the wing was next determined by the method suggested in Part I (pg. 76), the results being shown in Figure 11 and in Table IV. An approximate method has been used here

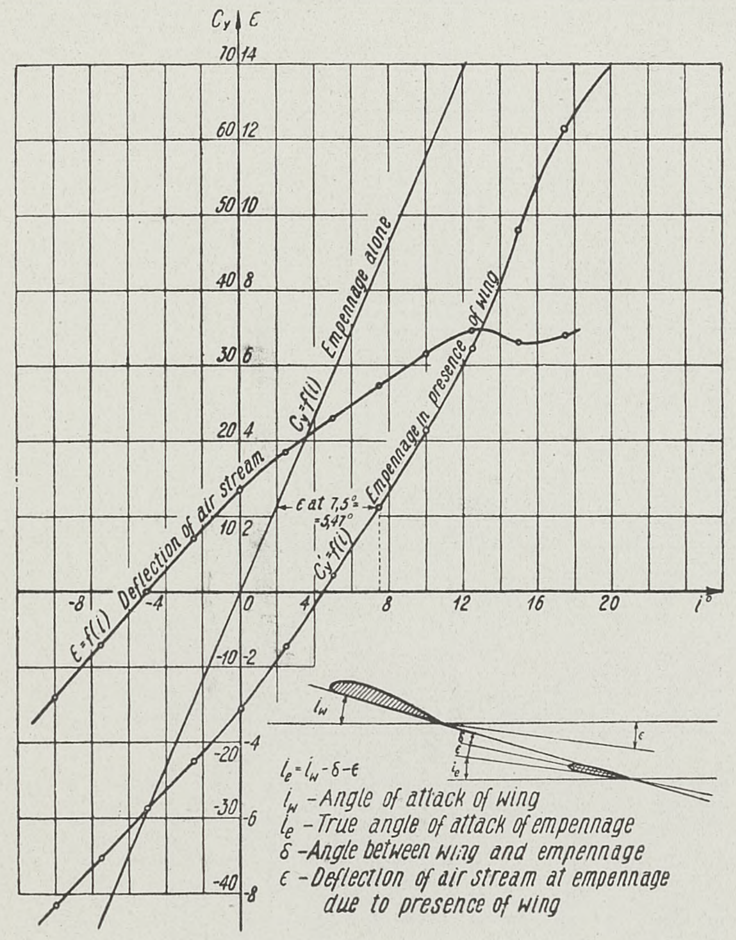


Figure 11

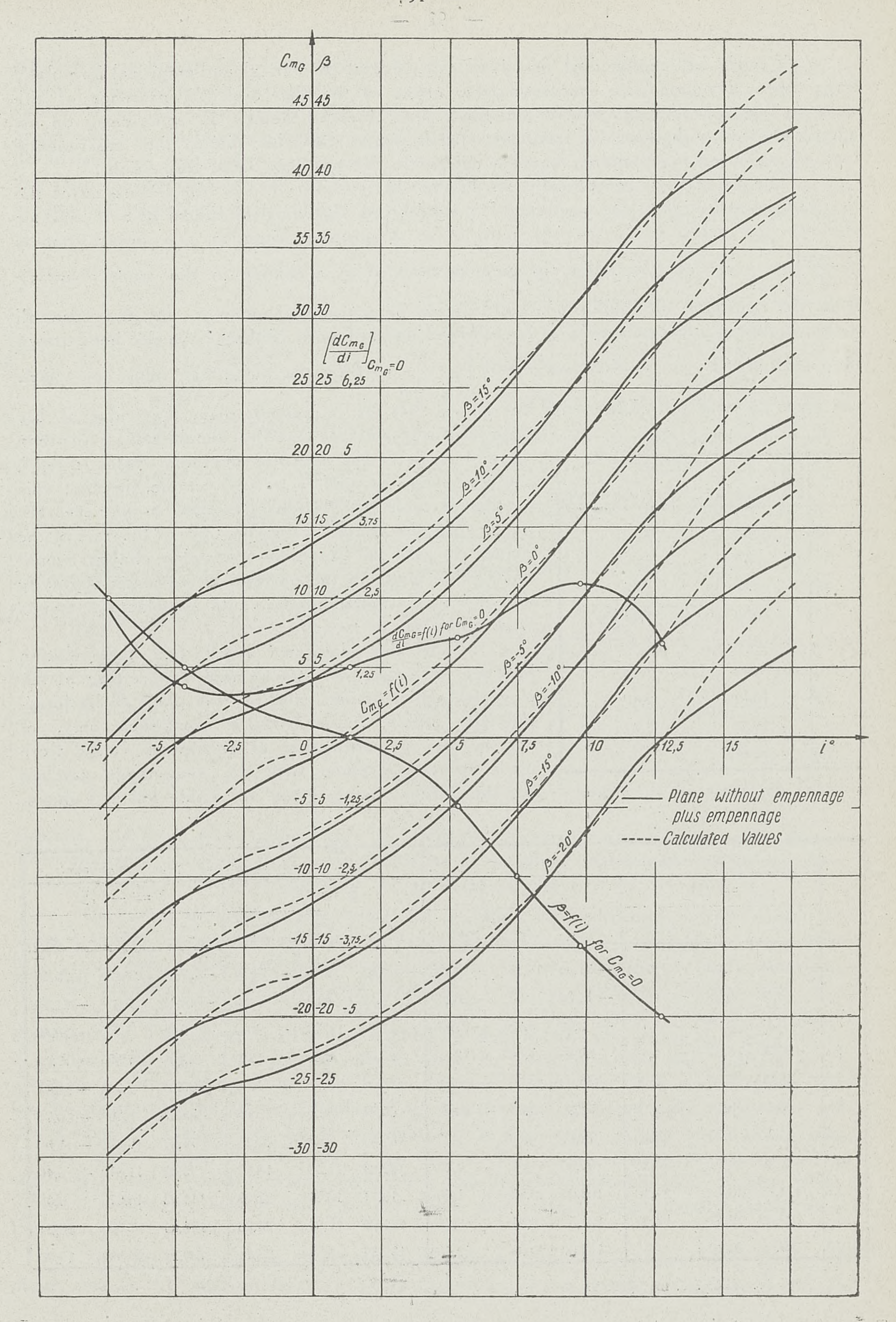
Table IV

i^0	C_y	C'_y	ε
—10	— 57,65	— 41,60	— 2,80
— 7,5	— 42,95	— 35,30	— 1,42
— 5	— 28,32	— 28,60	0,00
— 2,5	— 13,64	— 22,50	+ 1,40
0	0,00	— 15,60	2,70
+ 2,5	+ 14,62	— 7,26	3,72
5	29,08	+ 2,13	4,60
7,5	42,95	11,26	5,47
10	57,65	21,40	6,30
12,5	71,94	32,30	6,94
15	85,08	48,00	6,60
17,5	93,84	61,40	6,80

in that the values of the lift of the empennage with and without the wing have been compared rather than the total air reaction. C_y is the lift coefficient of the tail surface alone while C'_y is the same quantity in the presence of the main wing. From this data it was possible to determine the true angle of attack of the empennage and the corresponding characteristics for a given position of the wing, the decalage between the two being known. The moment about the center of gravity due to the empennage was then calculated and when all its characteristics were referred to the area and chord of the wing and added to the values obtained for the airplane without its horizontal tail surface, the curves shown in Figure 12 were obtained for various settings of the elevators. The corresponding numerical values are given in Table V. The difference between the calculated curves and the experimental ones is quite small and in the remaining discussion only the latter will be considered. Strictly speaking these last curves are not entirely experimental ones since the characteristics of the horizontal surface of the empennage were added algebraically to those of the plane without this member, and only the influence of the wing on the tail surface was taken into consideration. The values of C_y and C_x will be given later on. In Table V C_{mG} is the moment coefficient for the plane without empennage plus empennage, and C'_{mG} the calculated value for the complete plane.

Table V

i^0	$\beta = 0^0$		$\beta = 5^0$		$\beta = 10^0$		$\beta = 15^0$		$\beta = -5^0$		$\beta = -10^0$		$\beta = -15^0$		$\beta = -20^0$	
	C_{mG}	C'_{mG}	C_{mG}	C'_{mG}	C_{mG}	C'_{mG}	C_{mG}	C'_{mG}	C_{mG}	C'_{mG}	C_{mG}	C'_{mG}	C_{mG}	C'_{mG}	C_{mG}	C'_{mG}
—7,5	— 10,50	— 11,58	— 4,63	— 5,71	— 0,33	— 1,41	4,91	3,83	— 16,12	— 17,20	— 20,68	— 21,76	— 25,43	— 26,51	— 29,83	— 30,91
—5	— 7,13	— 7,34	— 0,46	— 0,67	+ 3,93	+ 3,72	9,20	8,99	— 11,86	— 12,07	— 16,53	— 16,74	— 21,43	— 21,64	— 26,23	— 26,44
—2,5	— 4,05	— 2,89	+ 1,63	+ 2,79	6,05	7,17	11,34	12,50	— 9,76	— 8,60	— 14,38	— 13,22	— 19,48	— 18,32	— 24,68	— 23,52
0	— 1,58	— 1,09	4,11	4,60	8,55	9,04	13,88	14,37	— 7,29	— 6,80	— 11,86	— 11,37	— 17,16	— 16,67	— 22,86	— 22,37
+2,5	+ 1,35	+ 2,06	7,05	7,76	11,46	12,17	16,81	17,52	— 4,37	— 3,66	— 8,91	— 8,20	— 14,41	— 13,70	— 20,41	— 19,70
5	5,06	5,99	10,77	11,70	15,23	16,16	20,67	21,60	— 0,63	+ 0,30	— 5,15	— 4,22	— 10,73	— 9,80	— 17,38	— 16,45
7,5	10,28	10,81	15,91	16,44	20,36	20,89	26,03	26,56	+ 4,58	5,11	+ 0,06	+ 0,59	— 5,56	— 5,03	— 12,74	— 12,21
10	16,17	16,01	21,88	21,72	26,44	26,28	31,94	31,78	10,36	10,20	5,97	5,81	+ 0,40	+ 0,24	— 6,78	— 6,94
12,5	22,38	22,00	28,00	27,70	32,56	32,18	37,95	37,57	16,26	15,88	12,15	11,77	6,65	6,27	— 0,49	— 0,87
15	25,90	28,65	31,57	34,32	36,17	38,93	41,37	44,12	20,16	22,91	15,67	18,42	10,24	12,99	+ 3,17	+ 5,92
17,5	28,74	33,25	34,26	38,77	39,06	43,57	43,66	48,17	22,93	27,44	18,42	22,93	13,08	17,59	6,29	10,80



C_{m_G} β
45 45
40 40
35 35
30 30
$\left[\frac{dC_{m_G}}{di}\right]_{C_{m_G}=0}$
25 25 6,25
20 20 5
15 15 3,75
10 10 2,5
5 5 1,25
-5 -5 -1,25
-10 -10 -2,5
-15 -15 -3,75
-20 -20 -5
-25 -25
-30 -30
-7,5
-5
-2,5
0
2,5
5
7,5
10
12,5
15
i°
β=15°
β=10°
β=5°
β=0°
β=-5°
β=-10°
β=-15°
β=-20°
$\frac{dC_{m_G}}{di}=f(i)$ for $C_{m_G}=0$
$C_{m_G}=f(i)$
β=f(i) for $C_{m_G}=0$
Plane without empennage plus empennage
Calculated Values

Figure 12

It might be mentoned at this point that several theoretical and empirical formulas[1]) have been developed for calculating the effect of the flap and the presence of the wing on the horizontal tail surface but the results obtained thereby in some cases do not agree very well with those of laboratory experiments. For this reason the experimental method was used in obtaining the data needed in the problem under discussion.

The data shown graphically in Figure 12 is sufficient for the discussion of the longitudinal stability of this airplane. For equilibrium C_{mG} must of course be zero, and for stability the curve of $C_{mG} = f(i)$ must have a positive slope at this point, that is $\left[\frac{d\,C_{mG}}{di}\right]_{C_{mG}=0} > 0$, in order that the moment induced by a change in the angle of attack from the position of equilibrium will always be a restoring moment. In this case all these conditions are easily seen to be fulfillied and in Figure 12 there have also been drawn the curves of $\left[\beta\right]_{C_{mG}=0} = f(i)$ and $\left[\frac{d\,C_{mG}}{di}\right]_{C_{mG}=0} = f(i)$, the numerical values of which are given in table VI. Experience has shown that for a transport plane the value of this slope or "coefficient of stability" should not be less than 0,6 and since in this case the minimum value is 0,75, the plane may be said to be very stable, in fact this coefficient could be decreased somewhat if necessary by moving the center of gravity toward the rear of the plane. In case the plane were unstable, changes would have to be made in the position of the center of gravity and the other characteristics until satisfactory results were obtained.

Table VI

i^0	$\left[\beta\right]_{C_{mG}=0}$	$\left[\frac{d\,C_{mG}}{di}\right]_{C_{mG}=0}$
— 7,5	10,25	2,40
— 5	5,70	1,00
— 2,5	2,40	0,77
0	0,75	1,00
+ 2,5	— 0,90	1,45
5	— 4,30	1,75
7,5	—10,10	2,37
10	—15,35	2,73
12,5	—19,60	1,92

From this data we have then the relation between the angle of attack and the setting of the elevators which must exist for the plane to be longitudinally stable, under statical conditions only, of course. As a verification of this work, tests were made on the airplane with the empennage attached and the elevators set at 0° and — 15°, the results being given in Table VII and shown

Table VII

i^0	Plane with empennage attached.						Plane without empennage plus empennage.					
	β = 0°			β = — 15°			β = 0°			β = — 15°		
	C_y	C_x	C_{mG}	C_y	C_x	C_{mG}	C_y	C_x	C_{mG}	C_y	C_x	C_{mG}
—7,5	— 22,50	12,93	— 13,02	— 27,30	14,16	— 24,04	— 20,87	12,63	— 10,50	— 27,72	13,65	— 25,43
—5	— 8,08	8,99	— 10,60	— 14,30	10,21	— 23,28	— 6,22	8,61	— 7,13	— 13,19	9,64	— 21,43
—2,5	+ 8,11	6,96	— 7,73	+ 2,32	8,28	— 21,66	+ 10,07	6,77	— 4,05	+ 2,98	7,71	— 19,48
0	26,30	6,62	— 4,87	20,00	7,80	— 19,45	27,52	6,50	— 1,58	20,30	7,35	— 17,16
+2,5	45,00	7,03	— 1,60	38,00	8,00	— 16,88	46,53	6,95	+ 1,35	39,27	7,71	— 14,41
5	63,10	8,18	+ 2,18	56,20	8,85	— 13,70	65,71	8,23	5,06	58,40	8,86	— 10,73
7,5	81,50	9,55	6,80	74,70	10,13	— 9,37	84,97	9,73	10,28	77,67	10,20	— 5,56
10	98,10	11,47	12,20	92,50	11,68	— 4,15	102,29	11,55	16,17	95,02	11,87	+ 0,40
12,5	114,70	13,79	17,10	108,00	13,85	+ 1,50	119,17	13,91	22,38	111,92	14,07	6,65
15	129,50	16,67	23,65	121,50	16,91	6,70	131,27	17,06	25,90	124,04	17,05	10,24
17.5	129,10	20,20	—	121,00	20,60	12,40	132,39	20,80	28,74	125,19	20,56	13,08

[1]) *Fr. Haus:* loc. cit. § 8, 9.

graphically in Figure 13. The curves obtained previously by adding the separate effects of the plane without its empennage and the empennage are also shown for the same cases. While the polars agree quite well, the curves of moment plotted against angle of attack show a considerable difference so that if accurate results were desired, it would be advisable to continue these last tests for other settings of the elevators. However in this case the principal object of the experiments was to provide an illustration of the method of procedure rather than to discuss in detail the properties of this particular

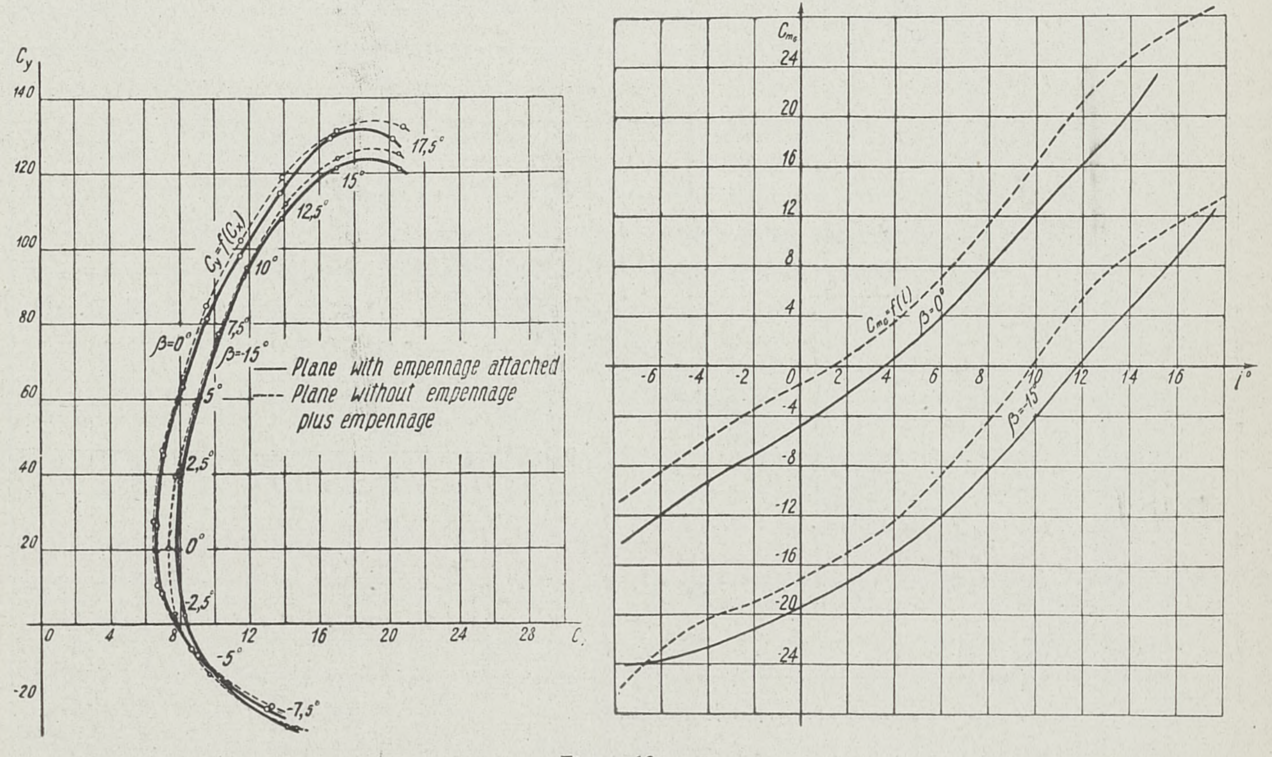


Figure 13

airplane, and so in what follows only the first set of curves will be discussed, that is, those obtained by adding to the characteristics of the plane without its empennage, those of the empennage when corrected for the effect of the presence of the wing.

One other experiment was made which might be mentioned at this point, this being a test of the airplane with the elevators set at 0^0 and the wing ailerons set at $\pm 20^0$. It is known that a plane which is longitudinally stable with the ailerons in the zero position will sometimes lose this property when the latter are displaced as in a turn, especially if the center of gravity is relatively close to the chord of the wing in the case of a monoplane. The characteristics of the plane in this position are shown in Figure 14 and in Table VIII; the data for the plane with the ailerons in the zero position is also given, these values being taken from Figure 13 and Table VII. The values given here for the plane with the ailerons displaced are not the true characteristics under this condition since the resultant air force no longer acts in the center of the span of the wing, but the error in assuming that such is the case is of an inappreciable magnitude and its effect here may be considered as negligible. The difference between the moment curves shows that it may safely be said that the plane will remain longitudinally stable when the ailerons are displaced.

The last point in this discussion is the determination of the true polar of the airplane, that is, the curve of $C_y = f(C_x)$ for $C_{mG} = 0$. In the accompanying figure (No. 15)

and in Table IX are shown the polars and lift curves for different settings of the elevators, while the curve of $\beta = f(i)$ for $C_{mG} = 0$ in Figure 12 gives the angle of attack at which the plane must fly when the elevators are set at a given angle. Thus with $\beta = 5^0$, the

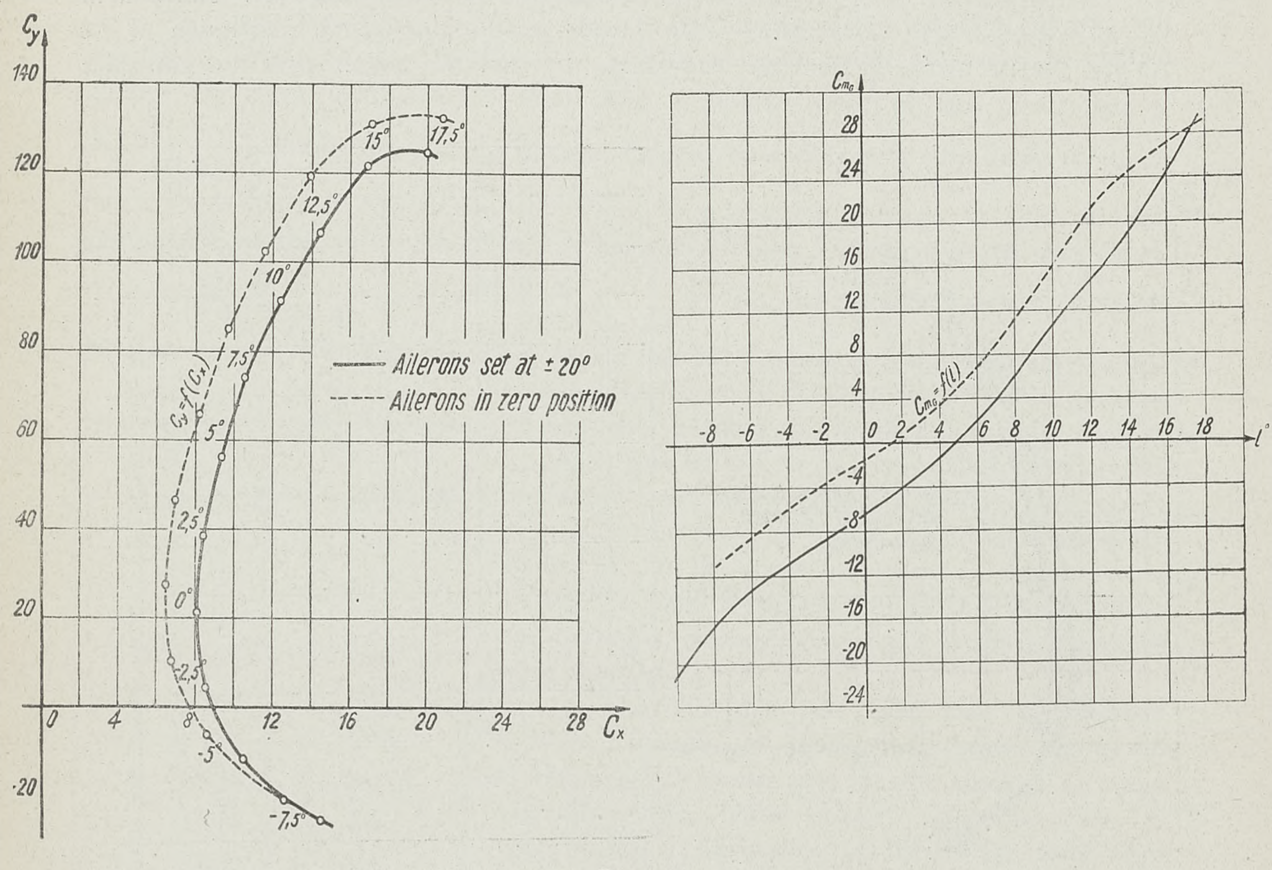


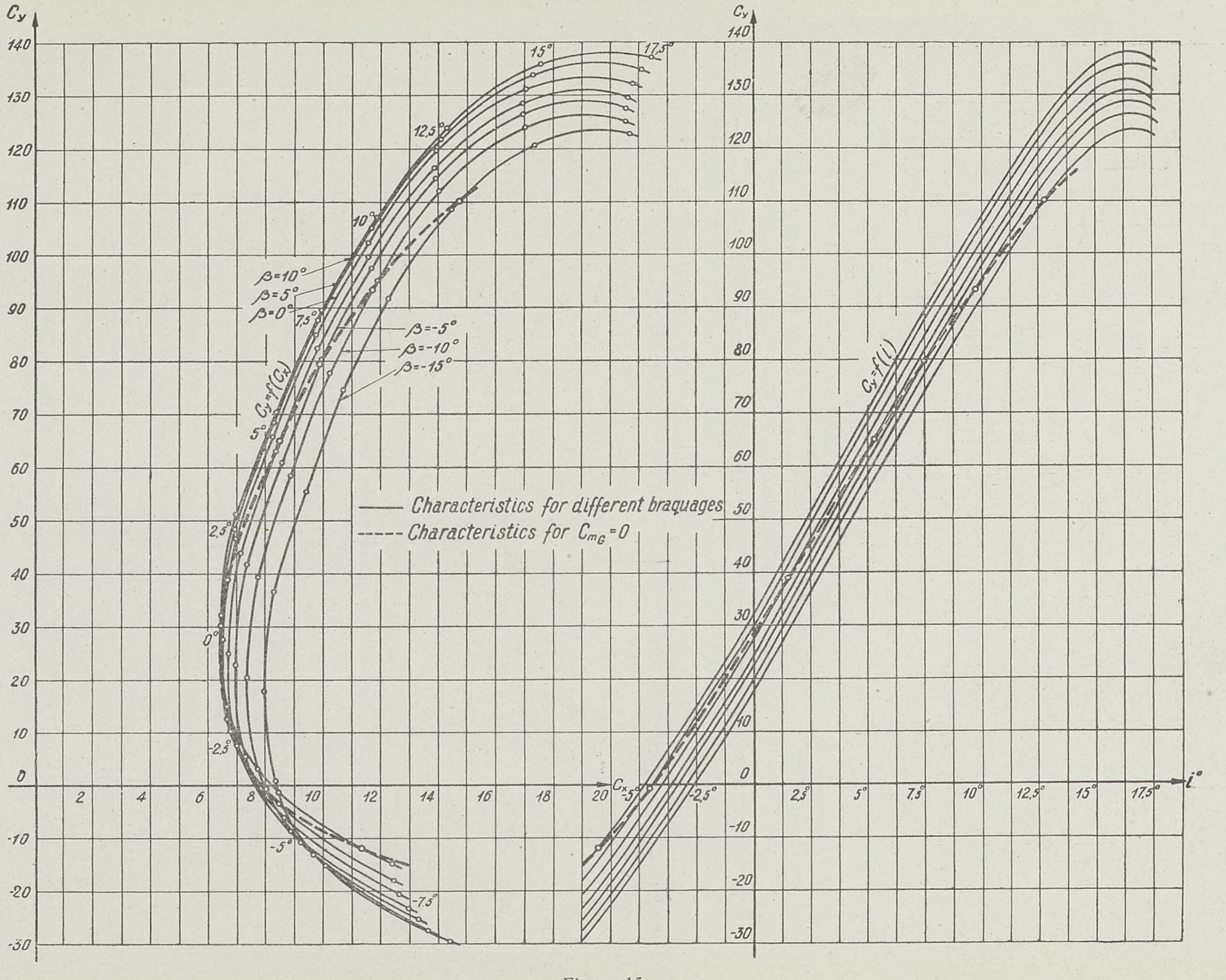
Figure 14

Table VIII

i^0	C_y	C_x	C_{mG}
—10	— 32,6	19,44	—21,03
— 7,5	— 25,3	14,54	—15,58
— 5	— 11,8	10,57	—12,01
— 2,5	+ 4,0	8,55	— 9,22
0	21,2	8,08	— 6,43
+ 2,5	38,5	8,44	— 3,40
5	56,0	9,37	+ 0,26
7,5	74,0	10,59	4,87
10	91,2	12,40	9,80
12,5	106,7	14,46	15,70
15	121,8	16,89	21,80
17,5	124,5	20,05	29,20

the angle of attack for $C_{mG} = 0$ is found to be $5{,}30^0$ and the lift coefficient at this angle of attack and position of the elevators is seen to be 65,6 while C_x is 8,43. In this way a point on each of the polars corresponding to the different settings of the elevators is obtained and joining these points gives the true polar of the airplane under the conditions of statical longitudinal stability. It is this curve that should be used in calculating the perfomance of the plane instead of the usual one for $\beta = 0^0$, for the difference is easily seen to be of an appreciable magnitude, especially in the region of maximum lift. The numerical values for the points on this true polar are given in Table X.

In conclusion let us outline briefly the procedure that has been given here. The first step is to obtain the characteristics of lift, drag and pitching moment about the center of gravity of the airplane with the elevators set in different positions. The best method is



Characteristics for different braquages
Characteristics for $C_{m_G}=0$
$C_y=f(i)$
$C_y=f(C_x)$
$\beta=10°$
$\beta=5°$
$\beta=0°$
$\beta=-5°$
$\beta=-10°$
$\beta=-15°$
C_y
C_x
$i°$

Figure 15

Table IX

i^0	$\beta = 0^0$		$\beta = 5^0$		$\beta = 10^0$		$\beta = -5^0$		$\beta = -10^0$		$\beta = -15^0$		$\beta = -20^0$	
	C_y	C_x	C_y	C_x	C_y	C_x	C_y	C_x	C_y	C_x	C_y	C_x	C_y	C_x
—7,5	—20,87	12,63	—18,17	12,45	—15,13	12,40	—23,49	12,94	—25,62	13,30	—27,72	13,65	—29,60	14,41
—5	—6,22	8,61	—3,53	8,46	—1,48	8,44	—8,85	8,88	—10,99	9,21	—13,19	9,64	—15,24	10,28
—2,5	+10,07	6,77	+12,74	6,65	+14,80	6,66	+7,43	7,00	+5,30	7,29	+2,98	7,71	+0,76	8,34
0	27,52	6,50	30,18	6,41	32,24	6,44	24,85	6,70	22,75	6,96	20,30	7,35	17,89	7,95
+2,5	46,53	6,95	49,19	6,90	51,25	6,96	43,87	7,11	41,75	7,34	39,27	7,71	36,62	8,28
5	65,71	8,23	68,38	8,24	70,46	8,33	63,06	8,35	60,97	8,54	58,40	8,86	55,47	9,40
7,5	84,97	9,73	87,62	9,80	89,69	9,93	82,32	9,79	80,25	9,92	77,67	10,20	74,46	10,69
10	102,29	11,55	104,96	11,67	107,07	11,86	99,64	11,56	97,56	11,65	95,02	11,87	91,80	12,32
12,5	119,17	13,91	121,83	14,09	123,91	14,32	116,49	13,86	114,44	13,90	111,92	14,07	108,72	14,45
15	131,27	17,06	133,90	17,29	136,05	17,58	128,60	16,94	126,53	16,95	124,04	17,05	120,88	17,34
17,5	132,39	20,80	135,03	21,12	137,17	21,48	129,70	20,61	127,64	20,55	125,19	20,56	122,88	20,68

to test a model of the complete plane, although calculated values will give a good indication of the results to be expected and should be made as a preliminary step.

Table X

β	C_y	C_x
—20	110,0	15,50
—15	93,1	11,72
—10	79,7	9,90
— 5	65,6	8,43
0	+ 38,7	6,70
+ 5	— 0,7	8,01
10	— 11,9	11,31

If the plane is longitudinally stable, that is there exist points in the flying range of the angle of attack for which $C_{mG} = 0$ and $\left[\frac{d\,C_{mG}}{di}\right]_{C_{mG}=0} > 0$, then the data thus obtained makes it posible to determine the relation which must exist between the angle of attack and the braquage or flap angle of the elevators under these conditions. A test should also be made with the ailerons displaced, one up and the other down, to make sure that the stability will be preserved in such maneuvers as a turn. Finally by the method described above, the true polar of the airplane is obtained, which should be used as a basis for the determination of the performance.

